Control of gene expression in E. coli BL21 (DE3) population upon long-term continuous cultivation.

Auteur : Sloodts, Alizée
Promoteur(s) : Delvigne, Frank
Faculté : Gembloux Agro-Bio Tech (GxABT)
Diplôme : Master en bioingénieur : chimie et bioindustries, à finalité spécialisée
Année académique : 2024-2025
URI/URL : http://hdl.handle.net/2268.2/24317

LIÈGE université
Gembloux
Agro-Bio Tech

CONTROL OF GENE EXPRESSION IN *E. COLI* BL21 (DE3) POPULATION UPON LONG-TERM CONTINUOUS CULTIVATION

ALIZEE SLOODTS

**MASTER'S THESIS SUBMITTED IN PARTIAL FULFILLMENT
OF THE REQUIREMENTS FOR THE DEGREE OF MASTER IN BIOENGINEERING,
SPECIALIZATION IN CHEMISTRY AND BIO-INDUSTRIES**

ACADEMIC YEAR 2024-2025

SUPERVISOR: FRANK DELVIGNE

LIÈGE université
Gembloux
Agro-Bio Tech

CONTROL OF GENE EXPRESSION IN *E. COLI* BL21 (DE3) POPULATION UPON LONG-TERM CONTINUOUS CULTIVATION

ALIZEE SLOODTS

**MASTER'S THESIS SUBMITTED IN PARTIAL FULFILLMENT
OF THE REQUIREMENTS FOR THE DEGREE OF MASTER IN BIOENGINEERING,
SPECIALIZATION IN CHEMISTRY AND BIO-INDUSTRIES**

ACADEMIC YEAR 2024-2025

SUPERVISOR: FRANK DELVIGNE

The master's thesis presented below was conducted in the Microbial Processes and Interactions department of Gembloux Agro-Bio Tech (University of Liege, Belgium).

Acknowledgements

This work is the result of many hours of reflection, hands-on experimentation, and intense writing. I would like to sincerely thank all those who made it possible, helped, or supported me over the past six months.

This master's thesis marks the achievement of five years of study at Gembloux Agro-Bio Tech. I am deeply grateful to all the professors who shaped my knowledge, and to my friends and family whose unfailing support and encouragement helped me persevere through doubts and challenges.

I would like to express my gratitude to my supervisor, Professor Frank Delvigne. I sincerely thank him for giving me the opportunity to work on this project. Thank you for your guidance, availability, and constructive feedback throughout this journey.

My sincere thanks also go to Tiphaine, for her help throughout the experiments and the many cups of coffee we shared while I talked about my worries and little victories.

I am especially grateful to Laurie for the time she generously gave me, and for her continuous support. She was always present, attentive, and concerned about how I was doing. I am also deeply thankful for her careful proofreading, insightful feedback, and guidance throughout the writing process.

I would also like to thank Andrés for his encouragement and helpful comments during the review of this master's thesis. A special thank you to Vincent for our long and enriching discussions, his valuable advice, IT help, and support throughout this journey.

I would like to warmly thank Samuel for his clear and patient training on the bioreactors, which was essential for my data collection. His guidance made a real difference in my ability to operate them with confidence. I am also grateful to Andrew for always being available when technical issues came up, and for his kind encouragement.

I would also like to thank the entire FD team for the great working atmosphere and all the shared moments, both professional and friendly.

To my friends, Léa, Constance, Zoé, and Amelie, thank you for being there, for sharing your stories and listening to mine. Your support has been truly invaluable. Thank you for the after-work hangouts that helped me decompress, and special thanks to Constance for the many much-needed coffee breaks.

Finally, I want to express my heartfelt thanks to my family. To my little sister, who supported me and sat by my side during long study sessions throughout my studies; and to my mom and dad, thank you for your constant support, your listening ear, and your wise advice all along the way.

A very special thank you to my partner, Nicola, who supported me with patience, despite the countless hours I dedicated to this work and all the conversations that revolved around it. Thank you for always being there.

Abstract (EN)

Continuous cultivation in bioreactors offers several advantages for recombinant protein production, including higher volumetric productivity, consistent product quality, and maximized equipment uptime. However, its industrial deployment remains limited due to the emergence of population heterogeneity, especially when using microorganisms engineered with burdensome gene circuits.

In this study, we investigated the population dynamics of *Escherichia coli* BL21 (DE3) carrying a burdensome gene circuit, the T7-based GFP expression system, during long-term chemostat cultivation (>100 hours). An automated flow cytometry setup enabled single-cell fluorescence monitoring and the assessment of population heterogeneity, using entropy as a metric, under different environmental conditions. As expected, the experiments have shown that population heterogeneity appears over time in continuous culture. To mitigate this diversification, we tested two strategies: modifying the carbon source (glucose vs. xylose) and reducing the cultivation temperature. The assumption was that lowering the strain's maximal growth rate would reduce the switching cost and promote population homogenization, reflected by lower entropy. However, both strategies had limited impact on homogenizing GFP expression within the population, indicating that reducing switching cost alone is insufficient to control population diversification in continuous cultures.

Finally, this work highlights key factors influencing population stability, including the importance of switching cost, the critical role of culture history before and during continuous culture, and the phenomenon of environmental escape. This latter mechanism allows part of the population to evade unfit phenotypic states and may also be connected to mutational escape. Controlling it could therefore help limit the emergence of mutants in continuous bioreactors. Overall, this work provides evidence that effective control of population dynamics in continuous recombinant protein production requires a multifactorial approach integrating host population traits, genetic circuit design, and environmental parameters.

Résumé (FR)

La culture continue en bioréacteur présente plusieurs avantages pour la production de protéines recombinantes, notamment une productivité volumique accrue, une qualité de produit constante et une utilisation optimale des équipements. Cependant, son déploiement industriel reste limité en raison de l'émergence d'une hétérogénéité au sein des populations, en particulier lors de l'utilisation de micro-organismes modifiés avec des circuits génétiques à forte charge métabolique (*burdensome*).

Dans cette étude, nous avons examiné la dynamique de population d'*Escherichia coli* BL21 (DE3) portant un circuit génétique à forte charge métabolique, le système d'expression de la GFP basé sur le promoteur T7, au cours de cultures en chemostat de longue durée (> 100 heures). Un dispositif de cytométrie en flux automatisée a permis de suivre la fluorescence à l'échelle unicellulaire, et d'évaluer l'hétérogénéité de la population en utilisant l'entropie comme indicateur, dans différentes conditions environnementales. Comme attendu, les expériences ont montré que l'hétérogénéité de population apparait au cours du temps en culture continue. Afin de limiter cette diversification, nous avons testé deux stratégies : la modification de la source de carbone (glucose vs. xylose) et la réduction de la température de culture. L'hypothèse était qu'une diminution du taux de croissance maximal de la souche réduirait le coût de transition d'état phénotypique (*switching cost*) et favoriserait l'homogénéisation de la population, traduite par une entropie faible. Cependant, les deux stratégies ont eu un impact limité sur l'homogénéisation de l'expression de la GFP au sein de la population, indiquant que la réduction du *switching cost* à elle seule est insuffisante pour contrôler la diversification en culture continue.

Enfin, ce travail met en évidence des facteurs clés influençant la stabilité des populations, notamment l'importance du *switching cost*, le rôle déterminant de l'historique de la culture avant et pendant la culture continue, ainsi que le phénomène d'échappement des contraintes environnementales (*environmental escape*). Ce dernier mécanisme permet à une partie de la population d'échapper à un état phénotypique défavorable et pourrait également être lié à l'échappement mutationnel (*mutational escape*). Son contrôle pourrait ainsi contribuer à limiter l'émergence de mutants dans les bioréacteurs en continu. Dans l'ensemble, cette étude fournit des éléments montrant que le contrôle efficace de la dynamique des populations dans la production en continu de protéines recombinantes nécessite une approche multifactorielle intégrant les caractéristiques de la population hôte, la conception du circuit génétique et les paramètres environnementaux.

Contents

List of Figures

List of tables

List of abbreviations

ALE	Adaptive laboratory evolution
ART-FCM	Automated real-time flow cytometry
ATP	Adenosine triphosphate
CA	California
cAMP	Cyclic adenosine monophosphate
CAP	Catabolite activator protein
DNA	Deoxyribonucleic acid
DO	Dissolved oxygen
E. coli	*Escherichia coli*
$EIIA^{Glc}$	Glucose-specific Enzyme IIA
FC	Flow cytometry
FSC	Forward scatter
GDA	Gene duplication and amplification
GFP	Green Fluorescent protein
g	gram
H	Entropy
HDB	History-dependent behaviour
HPLC	High-performance liquid chromatography
h^{-1}	Per hour
IPTG	Isopropyl β-D-1-thiogalactopyranoside
IS	Insertion sequences
kb	Kilobase (1000 base pairs of nucleic acid)
L	Litre
LB	Lysogeny Broth
LGT	Lateral gene transfer
mL	Millilitre
mg	Milligram
MMR	Mismatch repair
mRNA	Messenger ribonucleic acid
μ_b	Mutation rate per base pair per generation
µm	Micrometre
μ_{max}	Maximal growth rate

NADH	Nicotinamide adenine dinucleotide
nm	Nanometre
OD600	Optical density at 600 nm
P. pastoris	*Pichia pastoris*
P. putida	*Pseudomonas putida*
PBS	Phosphate-buffered saline
PCR	Polymerase chain reaction
P_{T7}	T7 promoter
PTFE	Polytetrafluoroethylene
rpm	Revolutions per minute
RFC	Reactive flow cytometer
RNA	Ribonucleic acid
S. cerevisiae	*Saccharomyces cerevisiae*
SIM	Stress-induced mutagenesis
SSC	Side scatter
TAE	Tris-acetate-EDTA buffer
tRNA	Transfer ribonucleic acid
TMG	Methyl-β-D-thiogalactopyranoside
T7 RNAP	T7 RNA polymerase
USA	United States of America
USD	United States dollars
v/v	Volume per volume
VVM	Vessel volume per minute

State of the art

1. Current production process in the biopharmaceutical industry

In recent decades, the development of biotechnology has revolutionized industrial production systems. Advances in genetic engineering have opened a new era in bioindustries, enabling natural microorganisms to be genetically engineered to produce a wide range of products, including recombinant proteins[1,2]. This breakthrough allows the production of almost any protein in both prokaryotic and eukaryotic hosts, as long as the gene sequence is provided. Specifically, the gene encoding the desired product, often carried on a plasmid under the control of a constitutive or inducible promoter[3], is introduced into a host cell. The host's internal machinery then translates the sequence and synthesizes the corresponding protein[1].

Among the various branches of biotechnology, the pharmaceutical industry was the first to identify this opportunity and invest significantly in the production of recombinant products[4]. The earliest achievement in this field was Humulin, a recombinant form of human insulin developed by Eli Lilly and Company, which became the first biopharmaceutical approved by the FDA in 1982[4,5]. This was quickly followed by the commercialization of other recombinant therapeutic proteins, such as hormones, cytokines, and antibodies, produced using diverse biological host systems[4]. Today, most biopharmaceuticals are recombinant proteins produced using genetically modified microorganisms[6], with *Escherichia coli* (*E. coli*) and *Saccharomyces cerevisiae* (*S. cerevisiae*) being the most widely used microbial hosts for this purpose[7]. For example, recombinant human growth hormone developed by Genentech (San Francisco, CA, USA) is produced using *E. coli,* whereas Sargramostim, a recombinant granulocyte-macrophage colony-stimulating factor developed by Bayer HealthCare Pharmaceuticals (Stockholm, Sweden), is manufactured using *S. cerevisiae*[4,8].

A central step in the production of these proteins is the propagation of microbial cells, which constitutes the core of the upstream process[3,9]. In industrial settings, recombinant microorganisms are typically cultivated at several cubic meters scale in stirred-tank bioreactors[10,11]. These systems operate under controlled conditions and follow one of the three main operational modes: batch, fed-batch, and continuous[7,9].

Since the 1950s, batch and fed-batch operations have remained the standard in industrial biomanufacturing[3,12]. Currently, the majority of biopharmaceutical processes, including recombinant protein production, are still performed in fed-batch mode[12–14], such as the industrial manufacture of recombinant human insulin in *E. coli*[15]. Fed-batch cultivation is preferred over batch because it offers several advantages, including biomass intensification, increased product yields, and reduced by-product formation, owing to the metabolic control enabled by various available feeding strategies[10,15]. Indeed, in batch mode, nutrients are only supplied at the start of the process, whereas in fed-batch mode, they are intermittently added during the culture[7,9]. Importantly, the ability to temporally separate the biomass accumulation from the product expression helps maintain cell viability over extended periods. This supports higher overall product yields.

2. Emerging trends towards continuous bioprocessing

Following its commercial introduction in the 1980s, the scale and diversity of biopharmaceutical products have grown considerably, with the pharmaceutical sector reaching global sales of USD 336 billion in 2021[11,16]. As demand increases, the industry faces growing pressure to produce larger volumes at lower costs. In this context, continuous manufacturing emerges as a promising alternative to batch and fed-batch systems[14,16].

In batch production, each step begins only after the previous one is completed, resulting in multiple holding periods that extend overall process time[16]. Similarly, fed-batch systems require a complete harvest at the end of cultivation, followed by sterilization, cleaning, and biomass regeneration. These steps represent the most time-consuming phase of the process and result in frequent downtime[17,18]. Moreover, the inability to maintain optimal production rates throughout the fed-batch cycle leads to increased operating costs and limits productivity[3]. To overcome these limitations and improve overall space-time yield, the biopharmaceutical industry is gradually moving towards continuous processing[4,14].

In a continuous bioprocess, culture medium or nutrients are continuously supplied as an input stream to the bioreactor system, while the product-containing harvest is simultaneously removed as the output stream. The chemostat represents the earliest and most basic model of this operational mode. It maintains a constant bioreactor volume by continuously supplying fresh medium, generally containing a single limiting nutrient, while simultaneously removing culture at the same volumetric rate[11,19]. Under these conditions, only cells capable of growing at a rate equal to the dilution rate can be maintained in the system, otherwise, they are progressively washed out[19]. A comparison between batch, fed-batch, and continuous systems, is presented in Table 1. It provides a concise, though not exhaustive, summary of their main operational features.

TABLE 1: COMPARATIVE OVERVIEW OF OPERATIONAL FEATURES IN BATCH, FED-BATCH, AND CONTINUOUS (CHEMOSTAT) CULTIVATION MODES[7,9,19].

Criterion	Batch	Fed-batch	Continuous (chemostat)
Medium feeding strategy	All nutrients added at the beginning	Nutrients added intermittently during cultivation	Continuous supply of fresh medium
Harvest strategy	At the end of the culture	At the end of the culture	Continuous removal of culture
Process duration	Short, ends after nutrient depletion	Longer than batch, ends after final feeding	Theoretically indefinite
Growth control	Uncontrolled after inoculation	Partially controlled via feeding	Growth rate tightly controlled by the dilution rate
Culture volume	Fixed volume	Volume increases over time with feeding	Constant volume maintained by balanced inflow/outflow
Process interruption	Requires downtime between batches (cleaning, sterilization, setup)	Requires downtime between cycles	Minimal downtime, fewer interruptions
Productivity	Limited, often lower due to nutrient depletion	Higher productivity due to high cell density	High space-time yield

Continuous processes are steady-state modes of production that offer multiple advantages, including reduced cleaning and setup frequency, lower manual labour requirements, greater productivity consistency (less batch-to-batch variation), more stable product quality, and a smaller facility footprint[9,11,16,17,20]. Because it operates without interruptions between steps, continuous production enhance process efficiency[16]. Thus, transitioning from batch or fed-batch to continuous production systems could significantly reduce product costs and address many of the challenges facing the biopharmaceutical industry[3,11]. Specifically, it could meet the need for robust and highly efficient processes for the manufacture of specialised proteins and molecules at lower cost[21].

Continuous processing is already well established in other industrial sectors, such as petrochemicals and white biotechnology. The latter refers to industries that employ biological systems for the production of industrial molecules used in the commodity chemicals, electronics, and energy sectors [7,14,22–24]. In biopharmaceuticals manufacturing, however, continuous systems remain only partially implemented, and mostly for monoclonal antibody production using mammalian cells[3,14,25]. Their application with bacteria and yeast is still uncommon[14]. Interest in this operating mode is growing because of the many potential benefits outlined above, but several challenges still hinder its widespread adoption[3,11]. One of the main issues is genetic and phenotypic instability during long-term cultivation, which leads to time-dependent variations in productivity and reduces process robustness[3,17].

3. Population dynamics: genotypic and phenotypic instability in continuous culture

One of the main challenges in implementing continuous bioprocesses with microbial hosts is their long-term biological instability[3]. Among the primary causes, the metabolic burden associated with the expression of heterologous (i.e. non-native) proteins is particularly critical[26]. Long-term cultivation also exposes cells to constant selective pressure, which can trigger genetic variability such as plasmid loss and spontaneous mutations, leading to faster-growing but less productive cells[3,17,27]. In addition, the inherent heterogeneity of microbial populations makes it difficult to maintain phenotypic stability over time[28]. To overcome these challenges, a better understanding of the internal cellular mechanisms that drive such instabilities is needed.

3.1. Metabolic burden: a key driver of instability

When a bacterial strain is engineered to produce a specific compound, part of its metabolism is redirected towards product formation. This rewiring can significantly destabilise the biochemistry and physiology of the host cell, triggering several stress responses, especially through what is known as metabolic burden[26,29]. Although this concept remains partly unexplored, metabolic burden generally refers to the fraction of a host cell's resources, such as energy carriers (e.g., ATP, NADH) and carbon precursors, allocated to heterologous gene expression and the maintenance of engineered pathways[29,30]. As a result, it often causes a decline in growth rate, genetic instability and impaired protein synthesis (Figure 1), ultimately reducing the overall productivity of the desired product[26,30,31].

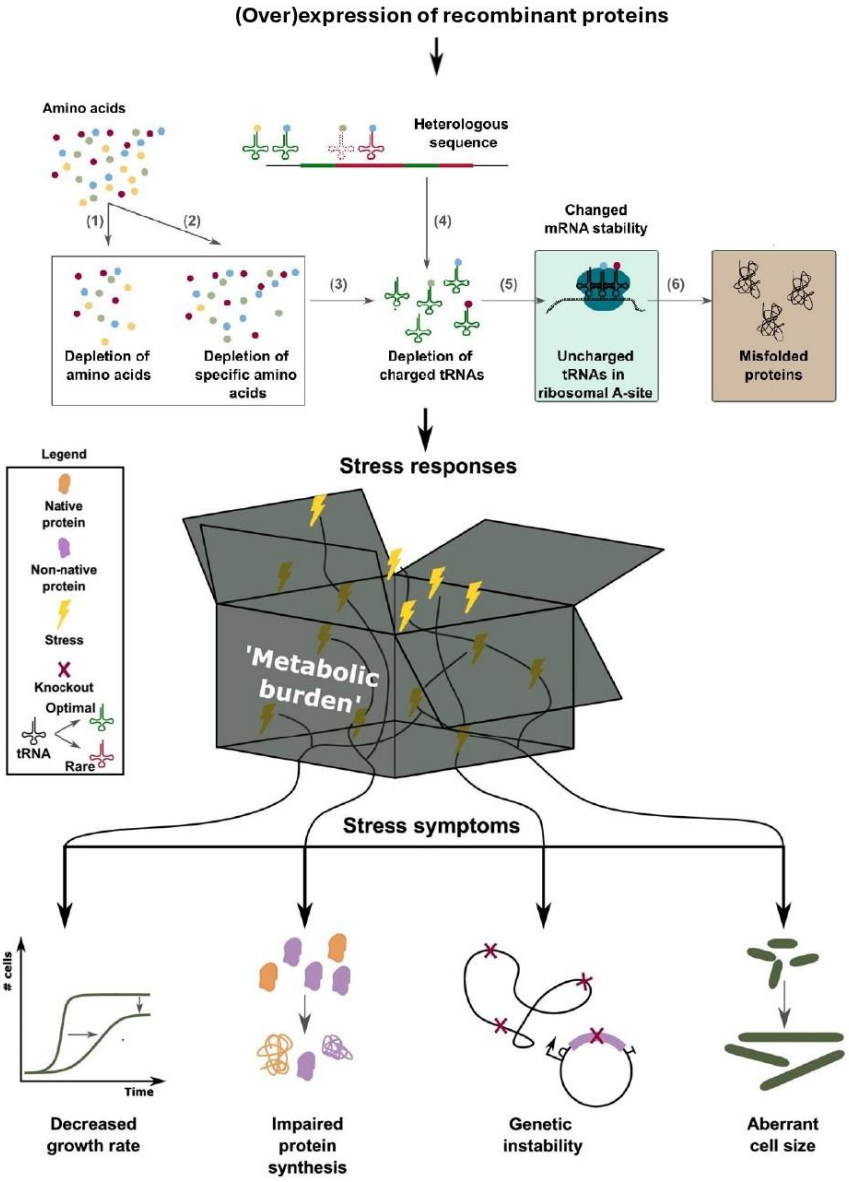

FIGURE 1: SCHEMATIC OVERVIEW OF THE EFFECTS OF METABOLIC BURDEN IN ENGINEERED MICROBIAL CELLS DUE TO RECOMBINANT PROTEIN PRODUCTION.

Metabolic burden resulting from recombinant gene expression triggers cellular stress responses, leading to decreased growth, impaired protein synthesis, genetic instability, and morphological changes such as filamentation. Combination of figures from Snoeck et al. (2024)[26].

At the molecular level, the expression of heterologous proteins can disrupt the cell's natural codon usage balance. In microbial systems, rare codons are associated with transfer ribonucleic acids (tRNAs) that are present at low abundance and therefore take longer to reach the ribosome. The synthesis of heterologous proteins containing such codons can thus slow down translation, leading to the accumulation of uncharged tRNAs at the ribosomal A-site[26,32]. Moreover, recombinant protein production creates a constant competition between native and heterologous genes, resulting in tRNA and amino acid depletion, translation errors, and even amino acid deletions[26,33]. Consequently, the accumulation of misfolded proteins increases, putting pressure on chaperones and proteases, which eventually become saturated and ineffective. This leads to the activation of global stress responses such as the stringent response and the heat-shock response (for a detailed description of the underlying

mechanisms, see Snoeck et al., 2024[26]). These responses downregulate genes related to translation, DNA replication and energy production, further reducing productivity and growth[26,34].

At the genetic level, metabolic burden creates a strong selective pressure on microbial populations. Under stress conditions, cells rely more heavily on error-prone DNA repair pathways, especially during double-strand break repair, a phenomenon known as stress-induced mutagenesis (SIM). This increases the likelihood of mutations, and as a result, engineered cells often lose their ability to produce the target protein[26]. Cells that acquire beneficial mutations, such as those that reduce or eliminate the expression of the recombinant gene, gain a survival or growth advantage. Therefore, the genetic sequence encoding the heterologous protein, which often represents a burden for the cell, may be lost over time. This can occur through mutations in the expression system, plasmid loss, or even alterations in regulatory circuits[26,27,31].

Metabolic burden can also alter cell morphology. A common phenotype is the formation of filamentous cells, which continue to grow but fail to divide. This may serve as a protective mechanism, preventing the transmission of damaged DNA to daughter cells[26]. The filamentation phenotype has been observed in *E. coli* upon overexpression of membrane-associated proteins, further illustrating how excessive expression can disrupt cell division[35].

This burden is particularly critical in continuous bioprocesses, where engineered strains are exposed to stress and selective pressure over extended periods. Over time, this phenomenon becomes a major factor in the loss of stability and productivity, and represents one of the main biological challenges limiting the industrial application of continuous microbial processes[26,31]. As an example, a study demonstrated that in chemostat cultures of *E. coli* expressing green fluorescent protein (GFP), productivity dropped below the detection limit after approximately three days of cultivation, a phenomenon often attributed to metabolic burden and genetic instability[36,37].

A well-known system for recombinant protein production is the T7 expression system in *E. coli* BL21 (DE3). While it is highly effective for achieving high levels of recombinant protein expression, it also clearly illustrates the challenges that can arise from excessive metabolic burden, particularly under stressful conditions or during long-term cultivations.

3.1.1 The T7 expression system in E. coli as a model of metabolic burden

E. coli is the most widely used microbial host for recombinant protein production due to its rapid growth, well-characterised genetics, and low-cost cultivation requirements[38]. It has been employed in the production of various therapeutic proteins, including Insulin[4]. Among the many engineered strains, *E. coli* BL21 (DE3) carrying a pET plasmid is one of the most commonly used, both in research and in industrial applications. Its popularity is mainly due to its low acetate production and high replication rate[36,38,39]. In this system, the gene of interest is located on the pET plasmid under the control of a T7 promoter (P_{T7}), and its transcription is driven by the bacteriophage T7 RNA polymerase (T7 RNAP), which is encoded chromosomally in the DE3 lysogenic region of *E. coli* BL21 (Figure 2)[40,41].

The T7 RNAP is under the control of the isopropyl β-D-1-thiogalactopyranoside (IPTG)-inducible lacUV5 promoter, a strong variant of the native lac promoter[40,42]. Upon IPTG induction, T7 RNAP is produced and initiates transcription at the T7 promoter with high specificity and efficiency, without requiring any

auxiliary transcription factors[41]. However, although IPTG is widely used for its tight control and high induction efficiency, it has been associated with increased cellular stress and reduced viability during long induction periods[17,43,44]. This is partly due to its toxicity at elevated concentrations and because it increases the metabolic burden already imposed on the cells[45]. Moreover, its relatively high cost (9.39€/g) makes it less desirable for large-scale applications. As an alternative, lactose offers a non-toxic and cost-effective inducer (0.02€/g) that enables tuneable expression through endogenous metabolic regulation. It is therefore frequently used to reduce metabolic burden and improve process economics in long-term cultivations[14,17,46].

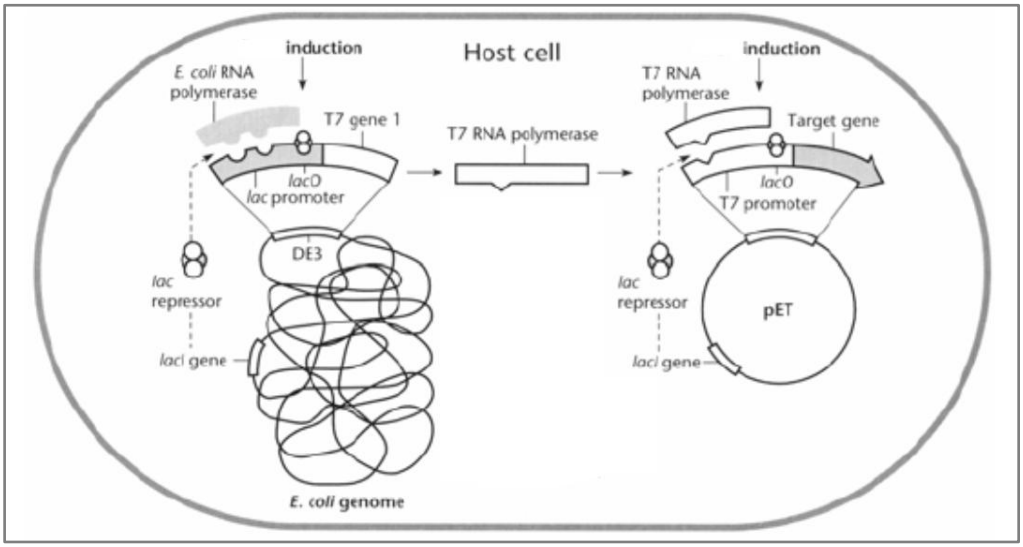

FIGURE 2: SCHEMATIC REPRESENTATION OF THE T7 EXPRESSION SYSTEM IN E. COLI BL21 (DE3).
In this system, the gene encoding T7 RNAP is integrated into the bacterial chromosome under control of the lacUV5 promoter, which is repressed by the LacI repressor in the absence of an inducer. Upon addition of IPTG or lactose, LacI is inactivated, allowing T7 RNAP expression. The polymerase then binds to the T7 promoter on the pET expression plasmid and initiates transcription of the gene of interest. As seen in the figure, many pET vectors also include a lac operator downstream of the T7 promoter, providing additional layer of repression directly at the plasmid level. This dual control enables tight regulation and strong induction of recombinant protein expression[40,47]. Extracted from Beselin A. (2005)[48].

This system is of particular interest because T7 RNAP transcribes approximately eight times faster than the native *E. coli* RNA polymerase, enabling high-level expression of recombinant proteins[40,49]. However, this high transcriptional activity comes at a cost. Even low levels of T7 RNAP can drive excessive production of the target mRNA, leading to competition for ribosomes, amino acids, and energy. This results in strong metabolic burden, growth inhibition, and often activation of stress responses[38,41,50].

Furthermore, the system is prone to leaky expression: basal levels of T7 RNAP can be produced even in the absence of the inducer, which can be problematic when expressing toxic proteins. The overexpression pressure also promotes instability: cells often accumulate mutations in the expression cassette, decreasing the expression of the T7 RNAP, or they may lose the plasmid altogether as survival strategies[50,51]. Despite the high expression potential, the assumption that more mRNA leads to more protein does not always hold, especially when cellular resources are limiting, often resulting in lower yields than expected[39,49,50].

The genetic instability observed with the T7 expression system illustrates how expression demands can disrupt microbial cell factories. When cells are placed under such pressure, particularly during long-term or continuous cultivation, they often develop mechanisms to relieve the burden. These include mutations or regulatory changes that ultimately lead to genotypic diversification. The next section explores these adaptive responses and the resulting heterogeneity in microbial populations.

3.2. Genotypic heterogeneity in continuous microbial cultures

During long-term continuous cultures, microbial populations are exposed to persistent environmental pressures and stresses, which often drive the emergence of genotypic heterogeneity. Genetic variation occurs primarily through mutational events, each with distinct mechanisms and frequencies[52]. An overview of the main genetic diversification mechanisms in bacteria is presented in Figure 3.

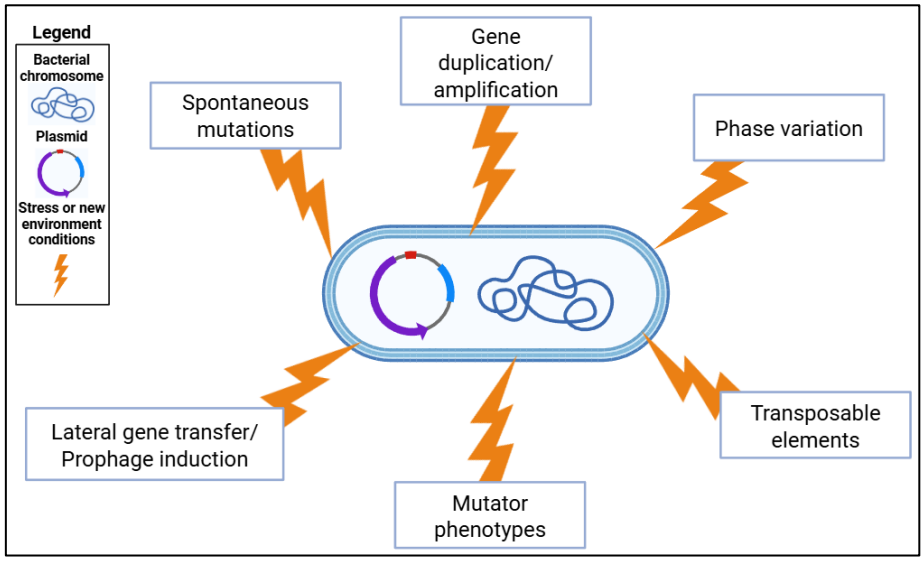

FIGURE 3: MAIN DIVERSIFICATION MECHANISMS IN BACTERIAL POPULATIONS ENHANCED UNDER STRESS CONDITIONS. Created with BioRender.com.

3.2.1 Spontaneous mutations

Spontaneous mutations arise during DNA replication due to polymerase errors[52]. Although the mutation rate per base pair per generation (μ_b) is typically very low (estimated around 10^{-10} in *E. coli*[53]), their impact is significant in large populations. Beneficial mutations are rare, with rates around 10^{-9} to 10^{-8} per genome[54], while deleterious or neutral mutations are far more common[52,55]. Therefore, bacteria must constantly balance their ability to adapt to environmental change with the need to preserve genomic integrity. To manage this trade-off, they rely on regulatory mechanisms that maintain high-fidelity replication under stable conditions but allow increased genome variability when stress or selection pressures arise[52]. Under such conditions, elevated mutation rates can enhance adaptability by generating greater genetic diversity from which beneficial variants may be selected[52].

3.2.2 Gene duplication and amplification (GDA)

One of the most common mechanisms of genomic variation is gene duplication and amplification (GDA). This process involves the duplication of specific genes, sometimes up to 40 copies, and occurs at frequencies ranging from 10^{-2} to 10^{-4} per genome. In non-selective environments, up to 10% of a bacterial population may harbour such duplications[52]. This frequency is influenced by the history of the culture, particularly prior exposure to stress[56]. GDAs commonly arise via RecA-dependent homologous

recombination between repeated sequences in the genome, RecA-independent mechanisms, or rolling-circle amplification, where a DNA segment is repeatedly copied in a loop-like manner[52]. In selective conditions, GDAs can improve fitness by boosting the expression of beneficial genes. For example, gene amplification has been shown to promote antibiotic resistance by increasing the production of antibiotic-modifying enzymes and target molecules[57]. Conversely, in non-selective environments, GDAs are usually lost through recombination[52,57]. Importantly, they allow beneficial mutations to arise in one gene copy while preserving the wild-type version in another. Once a favourable mutation is acquired, the extra gene copies are often lost, stabilizing the genomic change[52].

3.2.3 Phase variation and contingency loci

Genome variation at contingency loci enables bacteria to modulate gene expression rapidly and reversibly through high-frequency changes in specific DNA regions. These hypermutable regions promote frequent and reversible switching of gene expression, referred to as phase variation. This mechanism introduces genetic diversity in genes where phenotypic variation is advantageous (e.g., stress responses), while minimising the risk of deleterious mutations elsewhere[52]. Mutation rates at contingency loci can exceed those of spontaneous mutation, ranging from 10^{-2} to 10^{-5} per genome per generation[58]. Phase variation is driven by mechanisms such as slipped-strand mispairing, DNA inversions, or epigenetic modifications (e.g., DNA methylation). These mechanisms allow the population to explore alternative phenotypes in fluctuating environments[52]. In some cases, phase variation even targets DNA repair genes, increasing overall mutation rates and promoting adaptive evolution[59]. As with other mechanisms of genomic instability, prior stress exposure can influence the frequency of these events[52].

3.2.4 Transposable elements

Transposable elements, particularly insertion sequences (IS), are mobile genetic elements widespread in bacterial genomes[60]. These elements move via transposition and can cause mutations that disrupt or alter gene expression. Experimental evolution studies on *E. coli* have shown frequent IS-mediated transposition events under selective conditions experienced in chemostats, such as nutrient limitation or antibiotic exposure, often leading to beneficial mutations[61,62]. Additionally, IS elements promote genomic deletions through recombination between homologous sequences, leading to the loss of DNA regions. This process can result in mutator phenotypes and increase adaptive potential[52,61]. The frequency of transposition and deletion events is also influenced by the culture history and stress, such as DNA damage or prolonged starvation[52].

3.2.5 Mutator subpopulations

Another strategy to increase genetic variation involves the emergence of mutator subpopulations, which carry mutations in DNA repair genes, especially those involved in the mismatch repair (MMR) pathway (e.g., *mutS, mutL, mutH, uvrD*). These subpopulations exhibit constitutively high mutation rates, sometimes over 100-fold above the usual rate[52]. They arise spontaneously during population growth and are often selected because they enhance the chance of acquiring beneficial traits such as antibiotic resistance or improved nutrient utilisation[52,63,64]. Moreover, MMR-deficient strains display elevated rates of homologous recombination and uptake of foreign DNA, thereby accelerating genome evolution[65].

3.2.6 Stochasticity and Stress-induced mutagenesis (SIM)

Bacteria can also modulate their mutation rate temporarily through stochastic events and SIM. Stochastic variation arises from transcriptional or translation errors, or from cell divisions with insufficient MMR elements[52]. In contrast, SIM involves the regulated activation of stress-response pathways that increase the mutation rate in response to environmental cues[66]. This mechanism is well documented in *E. coli*, where up to 80% of long-term cultured colonies exhibit SIM phenotypes[67]. The degree of mutation rate increase is strain-specific and varies with selection pressure, ranging from a few-fold to over 1000-fold[52,67]. This strategy allows cells to preserve genome stability under optimal conditions, while promoting genetic diversity when adaptation is needed[52].

3.2.7 Other sources of genotypic variation

Additional mechanisms may also contribute to genetic heterogeneity. Lateral gene transfer (LGT) allows the integration of foreign DNA into the genome[68]. Stress can also affect plasmid stability, leading to intra-population variability[69]. Furthermore, stress can induce prophage activation, introducing additional genetic changes[70].

3.2.8 Population dynamics and selection

Ultimately, selection and competition between subpopulations play a central role in the evolution of microbial populations. When beneficial mutations arise under changing conditions, affected subpopulations may gain a fitness advantage and alter population structure by changing the ratio of subpopulations within the entire population. In some cases, a highly advantageous mutation may sweep through the population and replace the original genotype. However, in more complex scenarios, particularly in large populations, multiple beneficial mutations may coexist[52]. For example, in environments with several carbon sources, different subpopulations may specialise in metabolising one substrate while others adapt to a different one[52,71]. In *E. coli* chemostat cultures, population diversification is often driven by trade-offs[52]. A classic example is the coexistence of one subpopulation with higher stress resistance but slower growth and another with faster growth but lower stress resistance[52,72].

These mechanisms demonstrate how environmental stress and culture history shape genomic variability. As a result, chemostat systems, particularly those involving high metabolic burden, are especially prone to genetic drift and diversification over time.

3.3. Phenotypic heterogeneity in continuous microbial cultivations

Beyond genotypic heterogeneity, biological diversity also exists among genetically identical cells exposed to the same environment, a phenomenon known as phenotypic heterogeneity[28,73]. In such populations, individual cells can differ in terms of growth, respiration, and metabolic activity, often following bimodal or multi-modal distributions[73–75]. These subpopulations may exhibit lower fitness in a given environment but can become advantageous when environmental conditions change[52]. Therefore, phenotypic heterogeneity enables microbial populations to adapt to changing environments and promotes the survival of the genotype[28]. However, such heterogeneity is a major challenge in industrial bioprocessing[75,76]. Indeed, significant heterogeneity in both production and cell viability has been observed among populations engineered for the biosynthesis of recombinant molecules, thereby impacting the expected yield[77,78].

Phenotypic heterogeneity can be classified as either qualitative, in which clearly distinct phenotypic states exists within the population, or quantitative, where phenotypic traits show a continuous variation among cells[28,73]. Several mechanisms are at the origin of this phenotypic diversity, as illustrated in Figure 4, and described below[28].

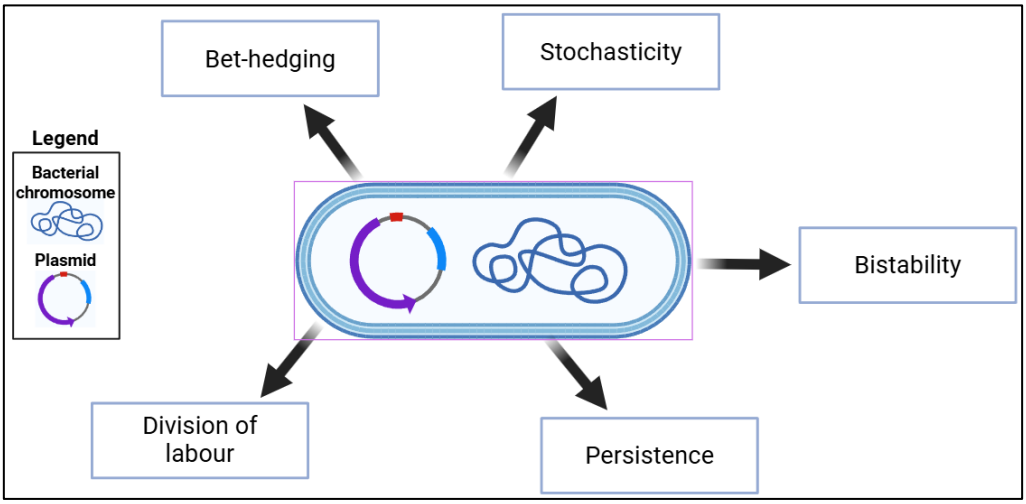

FIGURE 4: KEY MECHANISMS UNDERLYING PHENOTYPIC HETEROGENEITY IN MICROBIAL POPULATIONS.
Created with BioRender.com.

3.3.1 Noise in gene expression

Stochasticity, also known as noise in gene expression, is the major contributor to population heterogeneity[73,75]. It is typically divided into two classes: intrinsic noise and extrinsic noise[73,76,79]. Intrinsic noise refers to random fluctuations in gene expression caused by the limited number of reacting molecules, such as the transcription factors. This explains why two identical gene copies can behave differently within the same cell. Extrinsic noise, by contrast, results from variability in global factors such as growth rate, polymerase activity, or environmental fluctuations. These are often shaped by bioprocess design and operation[73].

High levels of noise are often observed in stress-related genes or those involved in energy and carbon metabolism, whereas essential genes, like those encoding DNA structural components, exhibit lower variability[73,80,81]. Moreover, expression systems using multiple operator sequences further amplify noise, as differences in operator strength modulates the transcriptional response among cells[73,82]. Stochasticity also extends to metabolic activity, driven by uneven distribution of key cellular resources such as cofactors, enzymes and ATP[75]. Furthermore, molecular crowding, which refers to the slow diffusion of reactants inside the cytoplasm, contributes to variability in biochemical reactions[75,83].

3.3.2 Bet-hedging

Bet-hedging is another major driver of phenotypic heterogeneity[73,84,85]. It enhances microbial survival under unpredictable environmental changes by stochastically generating a variety of phenotypes, shaped by the environment previously encountered[52,73,86]. For instance, phenotypic heterogeneity in metabolic functions enables a subpopulation to persist after a nutrient shift, as some cells can exploit the new resource[28,87]. In this way, bet-hedging allows cells to adopt phenotypes that may be disadvantageous in the current environment but beneficial under future conditions[28,73,88]. This strategy is particularly beneficial in fluctuating environments, as it maximises fitness in various conditions[73,89].

3.3.3 Bistability and persistence

Bistability and persistence are mechanisms linked to both noise and bet-hedging[73]. Bistability refers to the emergence of two distinct subpopulations of genetically identical cells under certain conditions, such as nutrient depletion. These subpopulations differ in term of their stress-specific protein contents, with one subpopulation having a high level of the trigger molecule (ON state), and the other a low level (OFF state)[73,76]. Cells stochastically switch between both states depending on the concentration of regulatory molecules[73,87]. This creates a cellular memory that improves response speed to recurrent stresses[76]. Persistence, often viewed as a form of bet-hedging, allows a fraction of cells to enter a slow-growing, stress-resistant state under stress conditions[28,73]. While persister cells may be less competitive under optimal conditions, they exhibit superior survival during stress. This trait is thought to result from pre-existing phenotypic heterogeneity, rather than being triggered directly by stress exposure[73,90].

3.3.4 Division of labour

Another manifestation of phenotypic heterogeneity is the division of labour within isogenic populations[91]. In this case, some cells with a specific phenotype specialise in tasks that compromise their own growth or survival but contribute to the overall fitness of the population[73,92]. The rest of the population, which maintains higher growth rates, naturally replenishes these sacrificial cells over time, allowing the division of labour to persist[73]. This strategy enables the coexistence of incompatible cellular processes across different individuals[28,73]. A well-studied example is the nitrogen fixation and photosynthesis in cyanobacteria: these processes cannot occur simultaneously in the same cell because the nitrogenase is damaged by the oxygen released by photosynthesis[28,93].

3.3.5 Bioreactor heterogeneities

Finally, bioreactor heterogeneities, such as gradients in pH, temperature, oxygen, and nutrient concentration, also induce phenotypic diversity[75,94–96]. Consequently, the residence time and spatial position of a cell within the bioreactor also contribute to population heterogeneity[76].

It is important to emphasise that, even in a clonal population of microbial cells, very different phenotypes leading to extreme heterogeneity can emerge[75]. While such heterogeneity usually aid population survival under stress, most sources of variability negatively impact bioprocess performance and must be carefully managed[75,76]. Given the wide range of mechanisms contributing to population heterogeneity, completely preventing it seems unrealistic. However, a deeper understanding combined with the use of advanced analytical tools could enable better management of this variability and potentially its exploitation to the advantage of bioprocesses.

4. Analysing and quantifying heterogeneity within cell populations

4.1. Automated flow cytometry for single-cell monitoring in bioprocessing

Flow cytometry (FC) is a high-throughput analytical technique that enables the rapid measurement of physical and physiological parameters at the single-cell level[97]. In this technique, cells are suspended in a fluid stream and aligned by a pressurized sheath fluid to pass one by one through a laser beam[98,99]. The light scattered by each cell is collected by optical detectors (typically photomultipliers), which convert the signal into electronic data (Figure 5). These measurements provide information on cell size (forward scatter, FSC), granularity (side scatter, SSC), and fluorescence intensity, especially from

reporter proteins such as GFP, which serve as proxies for gene expression, stress, or metabolic activity[97,100–103]. FC enables the analysis of thousands of cells per second and reveals variability in microbial populations with high precision[98].

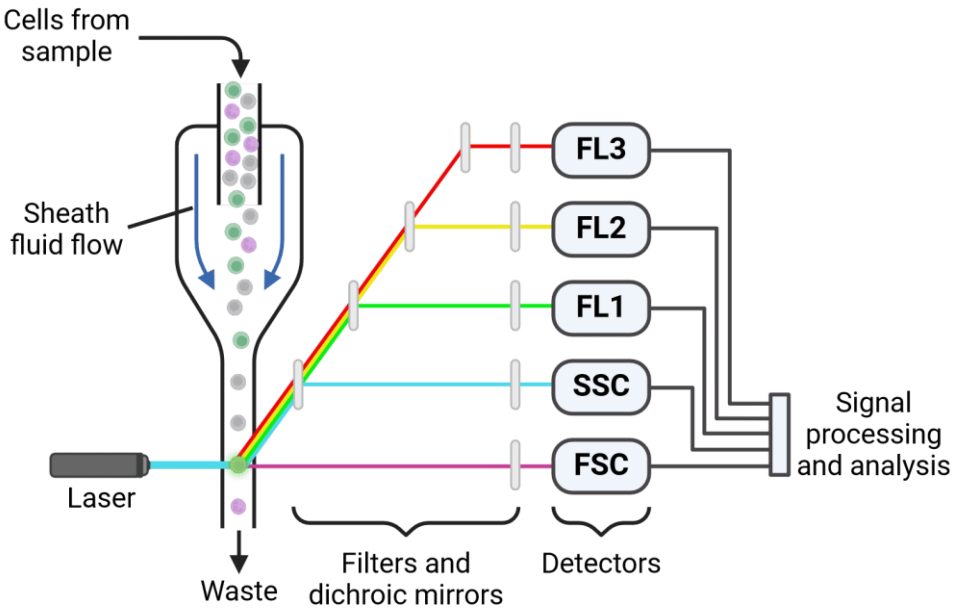

FIGURE 5: SCHEMATIC REPRESENTATION OF A FLOW CYTOMETER.
In a flow cytometer, cells are injected into a sheath fluid that confines them into a narrow, single-cell stream through hydrodynamic focusing. As individual cells pass through the laser beam, they scatter light, detected as forward scatter (FSC), indicative of cell size, and side scatter (SSC), reflecting the internal granularity. Simultaneously, fluorescence emissions from cellular components labelled with specific fluorophores are collected. These light signals are separated by dichroic mirrors and optical filters, then directed to corresponding detectors. The resulting data are electronically processed and analysed to quantify multiple cellular parameters[97–99]. Adapted from Antibodies.com[104].

In microbial bioprocessing, FC has become a valuable tool for monitoring phenotypic heterogeneity[76,105]. When coupled with automated sampling devices, automated real-time flow cytometry (ART-FCM) enables high-frequency acquisition of cytometric data directly from bioreactors[97]. This setup typically integrates online sampling, sample dilution and/or staining in a mixing micro-chamber, followed by direct injection into the cytometer[97]. Thanks to this configuration, ART-FCM can detect the appearance of subpopulations, such as low or high producers, that would remain invisible to bulk measurements[97,100,101,106]. Recent studies have shown its use in detecting bistable expression patterns or non-producing subpopulations during recombinant protein production in *E. coli* and *Pichia pastoris (P. pastoris)*[100,101].

ART-FCM offers several advantages for bioprocess monitoring. It enables the tracking of cellular dynamics in real time, an increased sampling frequency, the detection of subpopulations and reduces labour and manual handling compared to traditional off-line sampling[76,97,107].

Moreover, ART-FCM provides not only qualitative insights but also enables the quantitative analysis of population heterogeneity. Since each cell is measured individually, the resulting datasets reflect the phenotypic distribution of the population at any given time[108]. When compiled over time, these single-

cell datasets enable the quantification of heterogeneity based on the shape and spread of the dataset's distribution. Statistical tools such as Shannon entropy are increasingly used for this purpose, as discussed in the following section[109].

Finally, ART-FCM paves the way for feedback-control strategies in which cytometric data are used as inputs to adjust process parameters dynamically. Concepts such as the Cytostat and the Segregostat exploit these data to regulate inducer addition or nutrient feeding, with the goal of limiting unwanted diversification and improving process stability[97,110,111].

4.2. Shannon entropy as a proxy for population heterogeneity in continuous cultures

Shannon entropy is a mathematical concept from information theory that quantifies the uncertainty or diversity within a system[112]. In microbial systems and bioprocess engineering, it provides a valuable metric to assess the degree of heterogeneity within a cell population[109,113].

In this context, Shannon entropy is calculated based on the distribution of cells across distinct phenotypic states (e.g., gene expression levels or metabolic activity). Formally, it is defined as[112] :

$$H = -\sum_{i=1}^{n} p_i log_2(p_i)$$

where p_i is the proportion of cells in the i-th state and n is the total number of observed states. The entropy H, measured in bits, increases with the level of cell-to-cell heterogeneity in the population[114]. A value of $H = 0$ indicates a perfectly homogeneous population (i.e. all cells are in the same state), whereas higher values reflect increasing heterogeneity[115].

Unlike conventional measures of dispersion, such as standard deviation or the Fano factor, Shannon entropy does not rely on assumptions about the underlying distribution (e.g., normality), is not biased by the mean, and is robust to outliers. This makes it particularly suitable for biological systems, in which gene expression distributions are often skewed, bimodal, or non-Gaussian[109,114,115].

As previously explained, in continuous cultures such as chemostats, environmental conditions are kept constant, yet phenotypic diversification within population frequently arises over time. To reveal these hidden subpopulations, single-cell techniques such as FC are typically employed to generate datasets from which the Shannon entropy can be computed[109,114].

In practical applications, fluorescence intensity distributions obtained from FC (e.g., using GFP reporters) are binned to estimate the phenotype distributions (Figure 6). Entropy is then computed to quantify heterogeneity[109]. This approach allows the detection of emerging phenotypic subpopulations, the monitoring of population diversity dynamics over time, and the comparison of robustness or efficiency across different bioprocess conditions[109,115].

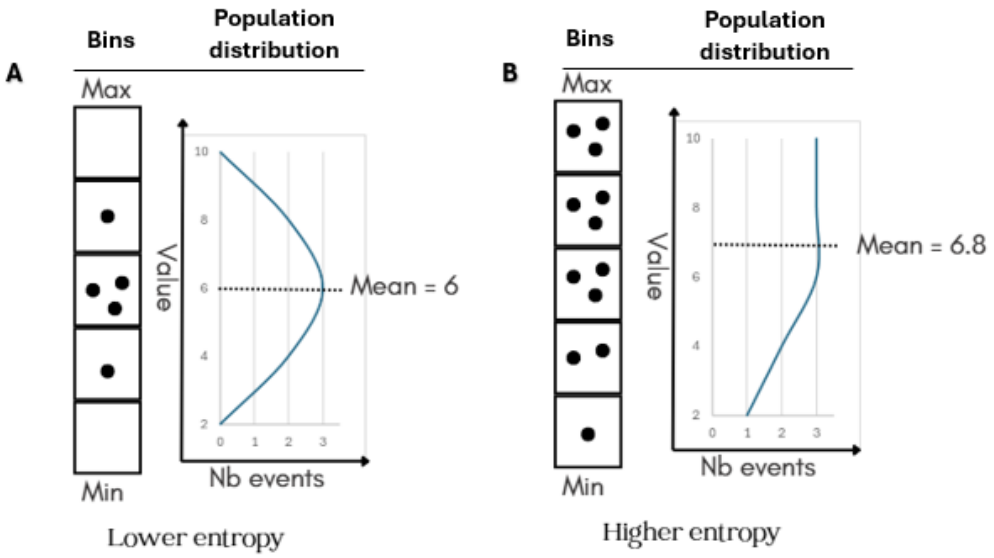

FIGURE 6: ILLUSTRATION OF ENTROPY WITHIN A CELL POPULATION.
(A) The values of a specific cellular characteristic (e.g., fluorescence intensity) in population A are distributed across three different bins, with one bin containing a higher number of events. This results in a low, but not minimal, entropy. (B) In contrast, the values in population B are spread across five bins, indicating a higher degree of dispersion and thus a higher entropy compared to population A. Although the mean value is similar in both populations, the figure highlights that the mean alone does not adequately reflect the variability within a population.

5. Controlling population heterogeneity in continuous cultures

Population heterogeneity, whether phenotypic or genotypic, often leads to a decline in production yield during continuous cultivation. This makes it a major obstacle to stable and efficient bioprocesses[75]. Therefore, developing strategies to control this variability is a central objective in microbial biotechnology.

In the present work, controllability is defined as the ability to maintain both a high production level, approximated here by fluorescence measurement obtained by online FC, and a low Shannon entropy, reflecting a more homogeneous population.

5.1. From automated monitoring to reactive control of microbial populations

Recent advances in ART-FCM have expanded the possibilities for monitoring and controlling continuous cultures[116]. As previously mentioned, ART-FCM enables the automated and real-time acquisition of population snapshots by connecting a flow cytometer directly to a cultivation device[97]. Reactive flow cytometry (RFC) builds on this principle but goes one step further by closing the loop between monitoring and control. In RFC, the data obtained by automated FC are processed in real time and used to trigger corrective actions, such as the pulsed addition of substrates or inducers, to synchronise phenotypic switching and reduce heterogeneity. In this way, RFC enables active population control[116].

Another promising approach is optogenetics, which uses light as a precise, rapid, and reversible signal to induce or repress gene expression[117,118]. Optogenetics has proven particularly effective in microfluidics platforms, where light can be finely controlled. Microfluidic devices are miniaturised cultivation systems that enable precise control and monitoring of individual cells. However, the use of optogenetics may be limiting in standard cultivation devices or during scale-up[116].

To further improve the effectiveness of RFC, engineered gene circuits such as the antithetic motif have been introduced[119,120]. This design relies on two molecules that neutralise each other upon binding, thereby creating a robust negative feedback loop that stabilises gene expression[116,119,121].

Taken together, these approaches illustrate the potential of RFC for population-level control. In the following section, one specific implementation of the RFC, known as the Segregostat, will be discussed as a concrete example of how RFC can be applied to continuous cultivation.

5.2. The Segregostat: real-time feedback control of cell populations

The Segregostat is a continuous cultivation system coupled with an online flow cytometer and automated feedback control. It uses single-cell fluorescence data from the flow cytometer to dynamically trigger inducer or feed pulses (Figure 7). Typically, cells are grown on a defined carbon source (e.g., glucose), and an inducer (e.g., lactose) is added when the proportion of induced cells falls below a defined threshold[109,122].

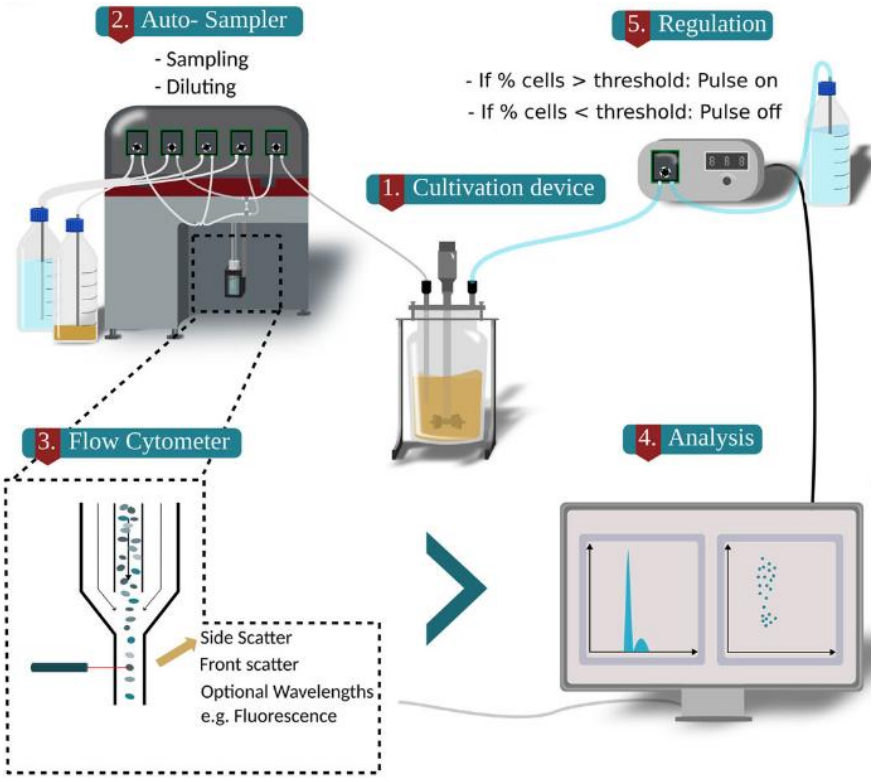

FIGURE 7: SCHEMATIC REPRESENTATION OF THE SEGREGOSTAT SET-UP.
The bioreactor (1), used for cultivation, is connected to an automated sampling device (2) via capillary tubing. Collected samples are diluting in a mixing chamber before being analysed by a flow cytometer (3). The flow cytometry data are processed (4) in real time using a custom Python script, which implement a feedback control loop. This loop regulates a pump to deliver pulses of inducer (5) depending on whether the measured population parameters meet a predefined setpoint. Extracted from Henrion et al. (2023)[109].

This approach was successfully applied to *E. coli* and *Pseudomonas putida* (*P. putida*) to regulate outer membrane permeability. By triggering glucose pulses when the fraction of permeabilized cells exceeded a set point, the system helped stabilise population dynamics[111]. Fluorescence measurements and Shannon entropy analyses demonstrated that the Segregostat enabled real-time monitoring and partial regulation of population diversification by adjusting culture conditions based on single-cell data[109].

A recent study by Henrion et al. (2024)[114] using the Segregostat with *E. coli* BL21 (DE3) and the T7 expression system showed that during induction phases (i.e. lactose addition), fluorescence increased and population entropy decreased, indicating a more homogeneous culture. In contrast, during relaxation phases (i.e. absence of inducer), fluorescence dropped, and entropy increased, revealing a re-diversification of the population. This was linked to a trade-off between gene expression and growth: highly induced cells grew slowly, while less induced cells grew faster and therefore reduce their GFP content more rapidly, thereby generating heterogeneity[114].

In other words, the study found that activating a burdensome gene usually leads to a reduction in growth rate. In continuous cultures such as chemostats, the growth rate of the population is constrained by the dilution rate, meaning that cells must grow at least as fast as they are being removed with the outflow to maintain themselves in the system. If gene expression slows cell growth below this required rate, the population is washed out. However, it was shown that this is avoided thanks to a phenomenon known as burden-entropy compensation: less induced cells, which grow faster, compensate for the burden of the others by outcompeting them, thereby sustaining the overall growth of the culture[114].

The authors hypothesised that increasing the frequency of induction pulses would stabilize the population in a high-expression and low-entropy state. However, over time, a new subpopulation with a reduced expression level emerged and took over the culture. Further investigation revealed this was a subpopulation of escape mutants with decreased induction strength, demonstrating a genetic adaptation in response to the high expression burden. Ultimately, the Segregostat was found to require the development of complementary control architectures or rules to fully prevent diversification during long-term cultivation[114].

5.3. Toward novel strategies to control heterogeneity in continuous cultures

Previous findings have highlighted the key role of the switching cost (i.e. the reduction in growth rate associated with the activation of a gene circuit) in shaping population dynamics. In the Segregostat experiment, for instance, escape variants emerged carrying mutations that reduced induction strength, thereby lowering the switching cost and allowing these cells to thrive under continuous cultivation conditions[114].

Despite advances in analytical tools such as online FC for monitoring microbial population heterogeneity in bioreactors, no robust strategy has yet been established to effectively control this heterogeneity during long-term continuous processes.

The present study aims to address this gap by further investigating population dynamics in prolonged chemostat cultures and by testing potential strategies with the goal of achieving high recombinant protein production (as reflected by high fluorescence) and low population entropy (as an indicator of high homogeneity).

Objectives

In continuous bioprocesses, maintaining long-term production stability is a major challenge, particularly when using synthetic expression systems such as the T7 system in *Escherichia coli*. These systems often impose a significant metabolic burden on the host cells, leading to both phenotypic and genotypic diversification within the cell population. This diversification can ultimately reduce production yields and compromise process predictability.

The present study aims to address this issue by investigating population dynamics in continuous cultures of *E. coli* expressing a fluorescent reporter protein (GFP) under the control of the T7 system. The main objective is to gain a deeper understanding of how population heterogeneity emerges and evolves in long-term continuous cultures using burdensome gene circuits, and to explore potential strategies for achieving a more stable and homogeneous production.

To this end, automated flow cytometry will be used to monitor gene expression at the single-cell level, while Shannon entropy will serve as a proxy for quantifying population heterogeneity over time. The first part of the study focuses on characterizing population dynamics over an extended cultivation period (150 hours). Based on this analysis, the second part of the study involves testing and evaluating different strategies of control. Specifically, two approaches will be explored: reducing the quality of the carbon source by switching to xylose, and lowering the cultivation temperature to 30°C instead of the standard 37°C. The goal is to limit population diversification and stabilize the production output, with GFP fluorescence used as a proxy for productivity.

Materials and methods

Details of my personal contributions to this master's thesis are provided in Appendix 1.

1. Strain, cultivation medium and precultures

The strain used in this study is *Escherichia coli* BL21 (DE3), harbouring the plasmid pET28::GFP (Addgene #60733), which expresses enhanced green fluorescent protein (EGFP) under the control of $P_{T7/lacO}$ promoter (Appendix 2). This strain was chosen as a model to investigate population dynamics during long-term continuous cultivation involving recombinant protein production using a burdensome gene circuit. Green fluorescent protein (GFP) expression serves as a proxy for heterologous protein production and can be easily quantified at the single-cell level using flow cytometry (FC).

All precultures and bioreactor cultivations were performed in a minimal mineral media (M9) containing the following salts (in g/L): K_2HPO_4 14.6, $NaH_2PO_4.2H_2O$ 3.6, Na_2SO_4 2, $(NH_4)_2SO_4$ 2.47, NH_4Cl 0.5, $(NH_4)_2$-H-citrate 1. The medium was autoclaved before being supplemented with a filtration-sterilised (0.2 µm, PTFE) mineral trace and thiamine solution composed of 3 mL/L of a trace elements solution, 3 mL/L of $FeCl_3.6H_2O$ (16.7 g/L), 3 mL/L of EDTA (20.1 g/L) and 2 mL/L of $MgSO_4$ (120g/L) and 1 g/L of thiamine. The trace element solution contained (in g/L): $CaCl_2.H_20$ 0.74, $ZnSO_4.7H_2O$ 0.18, $MnSO_4.H_20$ 0.1, $CuSO_4.5H_2O$ 0.1, $CoSO_4.7H_2O$ 0.21. Unless otherwise specified, glucose (5 g/L), autoclaved separately, was used as the carbon source. Kanamycin (50 mg/L), sterilized by filtration (0.2 µm, PTFE), was added to ensure plasmid maintenance.

Precultures were grown in 100 mL of medium in 1L baffle flasks, inoculated with 0.5 mL of a bacterial glycerol stock solution (25% glycerol, stored at -80°C) and incubated overnight at 37°C, 150 rpm.

2. Bioreactor cultivations

All continuous cultivations were conducted in a 1L Bionet F1 lab-scale bioreactor equipped with a dissolved oxygen (DO) probe (VisiFerm RS485-ECS 225 H0; Hamilton, Bonaduz, Switzerland), a biomass probe (Dencytee RS485 225; Hamilton, Bonaduz, Switzerland), and a pH probe (EasyFerm Bio PHI Arc 225), and connected to an automated flow cytometer (BD Accuri C6 Plus; BD Biosciences, USA) for online single-cell monitoring. The system included a feed tank and a waste tank, both connected to the bioreactor via peristaltic pumps (Figure 8). Prior to each experiment, the bioreactor was assembled and autoclaved together with the minimal mineral medium containing two drops per litre of antifoam KS911 (Evonik Operations GmbH, Essen, Germany). After sterilization, the medium was supplemented with the trace solution, kanamycin, and the appropriate carbon source, all sterilized separately as described previously (*see 1. Strain, cultivation medium and precultures*).

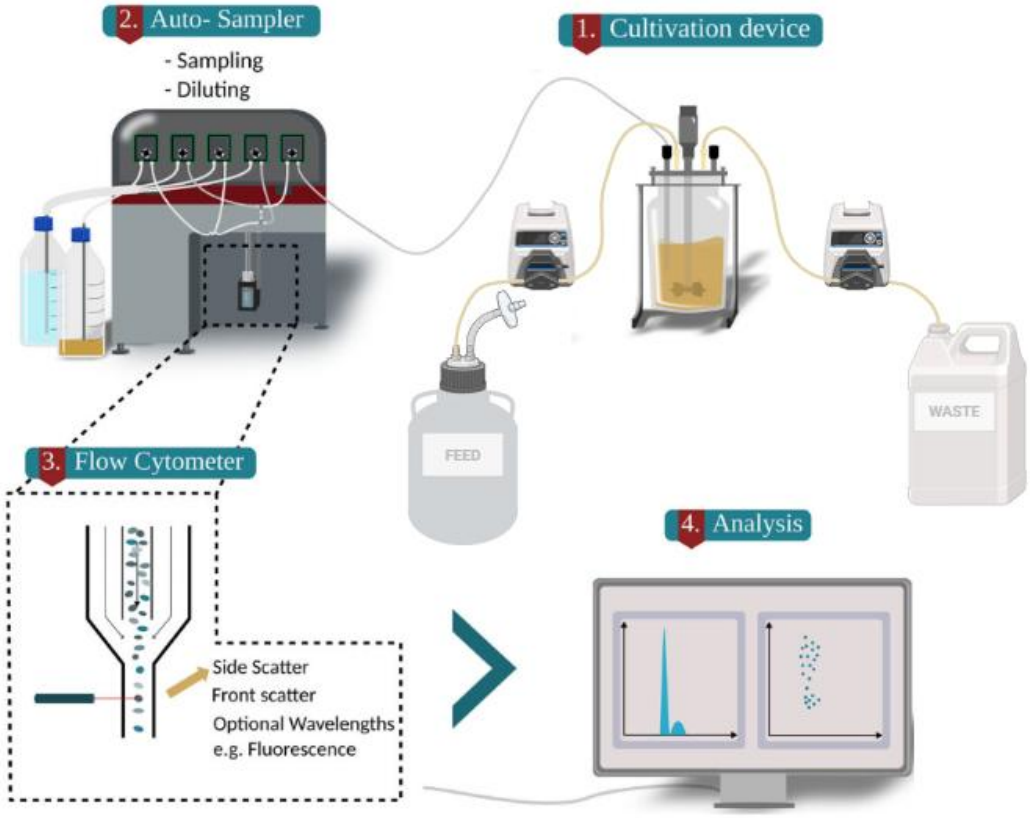

FIGURE 8: SCHEMATIC REPRESENTATION OF THE CHEMOSTAT SET-UP.

The cultivation device (1) consists of a bioreactor connected on one side to a feed tank, allowing continuous nutrients and inducer supply, and on the other side to a waste container, maintaining a constant volume via peristaltic pumps. For online sampling, the bioreactor is connected to an auto-sampler (2) through capillary tubing. Samples are diluted and then sent to the flow cytometer (3), where they pass through a laser beam. Data are collected and displayed in real time using the Cytometer software (4). Adapted from Henrion et al. (2023)[109], using BioRender.com.

Each culture began with a batch phase, during which cells grew on 5 g/L glucose unless otherwise specified. The transition to continuous mode (chemostat) was initiated once the DO concentration, monitored via the Bionet controller (Fermentation control unit with ROSITA 2.0 automation software, F1 Laboratory bioreactor in TWIN configuration, Bionet Ingeniería, Murcia, Spain) using the DO probe, sharply increased after a preceding drop, indicating the substrate depletion and the end of exponential growth (Figure 9). At this point, the peristaltic pumps were activated to start continuous feeding and effluent removal, maintaining a constant volume in the bioreactor. The feed medium was identical to the batch medium but also contained 1 g/L lactose as an inducer.

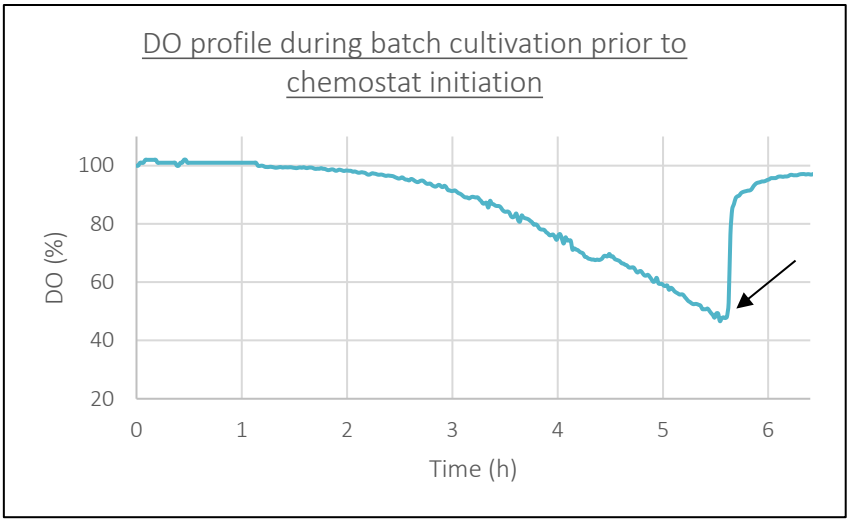

FIGURE 9: EVOLUTION OF DISSOLVED OXYGEN (DO) OVER TIME.
The black arrow indicates the sudden increase in DO following a prior decrease, marking the end of the exponential growth phase and so the onset of the stationary phase. This shift was used as an indicator to activate the peristaltic pumps and initiate chemostat cultivation.

Unless otherwise stated, cultures were operated under the following standard conditions : temperature of 37°C; stirring at 1000 rpm; pH 7; aeration at 1 VVM; initial optical density at 600 nm (OD600) of 0.3; glucose at 5 g/L as the carbon source; and a dilution rate of 0.45h^{-1}. Lactose, used as the inducer, was included in the feed and continuously supplied to the culture at a concentration of 1 g/L.

2.1. Experimental design

To investigate population dynamics and test strategies to control heterogeneity, different long-term continuous cultivations were conducted with varying conditions.

a) Glucose-based continuous culture at 37°C

This experiment, lasting 150 hours, served as a baseline to observe population dynamics under standard conditions. Glucose was used as the carbon source (5 g/L), and lactose (1 g/L) was continuously supplied to induce gene expression.

b) Xylose-based continuous culture at 37°C

Conducted over 110 hours, this experiment used xylose (5g/L) instead of glucose to explore whether this carbon source, by lowering the maximal growth rate, influenced the stability and heterogeneity of population during continuous induction.

c) Continuous cultivation at 30°C

This experiment aimed to evaluate the effect of reduced temperature on gene expression and diversification. It was conducted for 185 hours using glucose as the carbon source. Initially, the dilution rate was set at 0.45h^{-1}, but due to an absence of observable induction, it was lowered to 0.35 h^{-1} after 42 hours and further reduced to 0.30 h^{-1} after 43 hours (Table 2).

TABLE 2: SUMMARY OF APPLIED DILUTION RATES AND CORRESPONDING TIME INTERVALS DURING CONTINUOUS CULTURE AT 30°C.

Dilution rate (h^{-1})	Time (h)
0.45	T = 0 → T = 42
0.35	T = 42 → T = 138
0.35	T = 138 → T = 185

d) Continuous cultivation at 30°C with dilution rate screening.

In this 110-hour experiment, the temperature was again maintained at 30°C with glucose, but this time the dilution rate was gradually increased after at least five residence times at each condition. The specific dilution rates and their respective durations are provided in Table 3.

TABLE 3: SCREENING OF DILUTION RATES RANGING FROM 0.20 TO 0.45H^{-1} DURING CHEMOSTAT CULTIVATION AT 30°C.

Dilution rate (h^{-1})	Time (h)
0.20	T = 0 → T = 25
0.25	T = 25 → T = 45
0.30	T = 45 → T = 62
0.35	T = 62 → T = 90
0.40	T = 90 → T = 102.5
0.45	T = 102.5 → T = 110

2.2. Sampling and storage

For all chemostat experiments, offline samples were collected twice a day for cryopreservation. For each sample, 1 mL of culture was mixed with 1 mL of 50% (v/v) glycerol solution in cryovials and stored at -80°C for further analysis. OD600 was also measured using a spectrophotometer at the time of sampling. In addition, for the experiments conducted at 30°C, supernatant samples were collected twice per day. For this, 1 mL of culture was centrifuged at 12 000 rpm for one minute, and the cell-free supernatant was transferred into a new Eppendorf tube and stored at -20°C.

3. Automated flow cytometry and data treatment

An automated flow cytometer (BD Accuri C6 Plus; BD Biosciences, USA) was connected to the bioreactor to enable online monitoring of the culture at the single-cell level. This setup allows for real-time acquisition of GFP fluorescence, collected in the FL1-A channel of the flow cytometer, providing a precise proxy of gene expression distribution within the population.

Samples were automatically collected every 12 minutes using a capillary tube coupled to a peristaltic pump. The sample was introduced into an analysis chamber located within the cytometer. Based on the concentration measured during the previous acquisition (number of events per microliter), the sample was diluted using phosphate-buffered saline (PBS). A measurement of 40 000 events was then

performed, followed by a cleaning step in which the chamber was flushed several times with PBS before starting the next cycle.

PBS is composed of (in g/L): NaCl 8, KCl 0.2, Na_2PO_4 1.42, KH_2PO_4 0.24. Prior to use, PBS was sterilized by filtration through a 0.2 µm membrane filter (PTFE).

The resulting single-cell fluorescence data were further processed using Python scripts. In particular, Shannon entropy was computed over time to quantify population heterogeneity based on the distribution of fluorescence intensities. The complete set of scripts used in this study is accessible at https://gitlab.uliege.be/mipi/published-software/2025-master-thesis-alizee. Data processing and analysis were performed using the *mbiomass* library (https://gitlab.uliege.be/mipi/published-software/mbiomas-core) at commit *179357e26ab7ff8f2dee5813f9b4e1cb0abb6679*.

4. Maximum growth rate determination

To determine the maximal growth rate (μ_{max}) of the strain on glucose at 30°C, biomass data recorded by the online biomass probe installed on the Bionet F1 bioreactor during the batch phase were used. The exponential growth phase was identified using a Python script applied on the biomass signal over time, and μ_{max} was estimated by fitting a linear regression to the natural logarithm of biomass concentration as a function of time. The maximal growth rate on glucose at 37°C and on xylose at 37°C were obtained from Henrion et al. (2024)[114]. A summary of the maximal growth rates under the different conditions is provided in Appendix 3.

5. Isolation of clones and sample preparation for sequencing

To investigate the genotypic diversification occurring during long-term continuous cultivation of *E. coli* BL21 (DE3), samples were collected from a chemostat culture on glucose at 37°C. Three timepoints were selected for analysis: 24 hours, 115 hours, and 150 hours. From 10 isolated colonies of each sample, the genomic region corresponding to the lac promoter driving expression of the T7 RNA polymerase was sequenced. The complete procedure is described below, and the main steps are found in Figure 10.

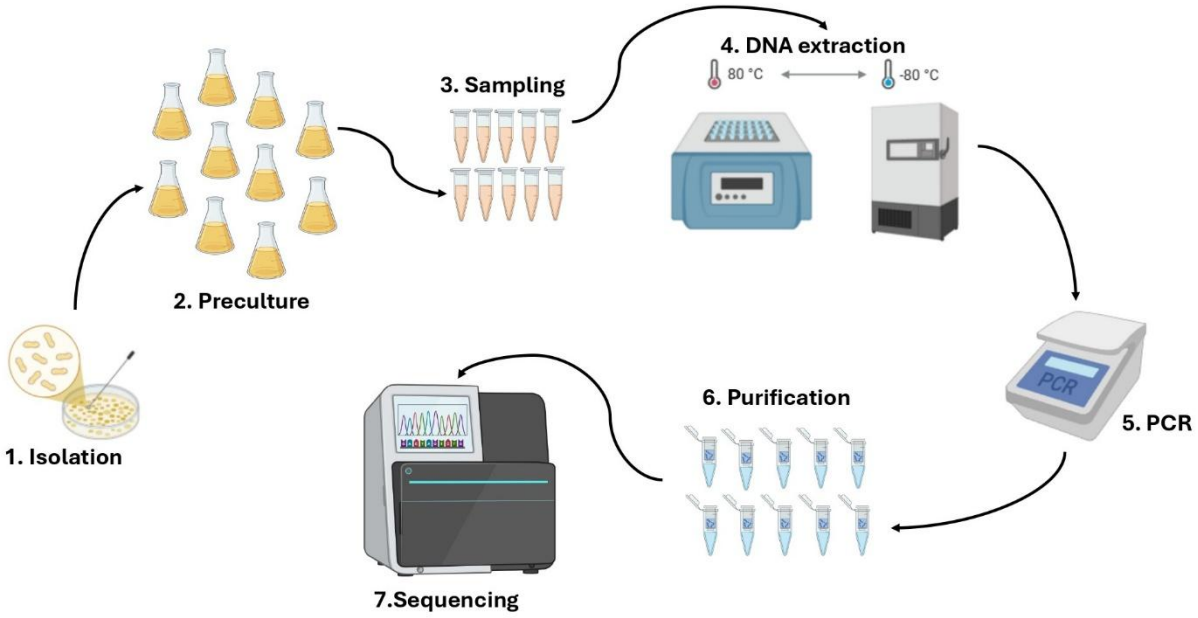

FIGURE 10: OVERVIEW OF THE MAIN STEPS FOR SEQUENCING BACTERIAL CHROMOSOMES FROM BIOREACTOR SAMPLES.
(1) The sample is plated on Lysogeny Broth (LB) agar supplemented with kanamycin (50 mg/L). After overnight incubation, 10 individual colonies are selected and cultured in LB medium containing kanamycin (50 mg/L) (2). After overnight growth, 1 mL of each preculture is collected for DNA extraction (3). A heat-freeze lysis method is applied in two cycles to release genomic DNA (4). The resulting supernatant is used as a template for PCR amplification (5). PCR products are purified using the NucleoSpin® Gel and PCR Clean-up Kit (Macherey-Nagel GmbH & Co. KG, Düren, Germany) (6), and the purified samples are then submitted for sequencing.

5.1. Preculture and clonal isolation

Frozen glycerol stocks (stored at -80°C) were thawed and streaked on Lysogeny Broth (LB) agar plates supplemented with kanamycin (50 mg/L). Plates were incubated overnight at 37°C. From each sample, 10 individual colonies were randomly picked and inoculated into 5 mL of LB medium (also containing kanamycin, 50 mg/L) in 50 mL baffled flasks. Cultures were grown overnight at 37°C with agitation at 150 rpm.

The LB medium used consisted of (in g/L): casein tryptone 10; yeast extract 5; and NaCl 10. For solid medium, 14g/L of agar were added to the LB. This nutrient-rich medium was used to promote rapid growth and achieve high biomass density.

5.2. DNA extraction and PCR amplification

Genomic DNA was extracted from each overnight culture using a heat-freeze lysis method. Briefly, 1 mL of each culture was centrifuged at 12 000 rpm for 2 minutes using a MiniSpin Plus centrifuge (Eppendorf, Hamburg, Germany). The supernatant was discarded, and the cell pellet was resuspended in 100 µL of milliQ water. Cells were lysed through two cycles of heat-shock: 1 minute at 80°C followed immediately by 1 minute at -80°C. After lysis, samples were centrifuged again (12 000 rpm, 2 minutes), and the supernatant, containing the genomic DNA, was used as the template for polymerase chain reaction (PCR).

The region containing the lacUV5 promoter upstream of the chromosomal T7 RNA polymerase gene was amplified using Q5® High-Fidelity DNA polymerase (New England Biolabs). PCR reactions were prepared according to the manufacturer's protocol (Table 4).

TABLE 4: PCR MIX USING Q5 DNA POLYMERASE.

Component	For 50 µl reaction
5x Q5 Reaction Buffer	10 µL
10 mM dNTPs	1 µL
10 µM Forward Prime	2.5 µL
10 µM Reverse Prime	2.5 µL
Template DNA	2 µL
Q5 High-Fidelity DNA polymerase	0.5 µL
Nuclease-Free Water	31.5 µL

The primers used were the followings:

Forward primer → CGCAACTCGTGAAAGGTAG

Reverse primer → CGTTTTGTGGCGTACCTTT

The program used in the Tprofessional Basic thermocycler (Biometra, Göttingen, Germany) to perform PCRs is provided in Table 5.

TABLE 5: THEMOCYCLING CONDITIONS.

	Steps	Temperature (°C)	Time (mm:ss)
	1	98	00:30
35x	2	98	00:10
	3	60	00:30
	4	72	01:45
	5	72	02:00

5.3. Sequencing preparation

PCR products were verified by agarose gel electrophoresis (1% agarose, TAE buffer). For this, 5µL of each reaction was loaded on the gel to confirm the expected amplicon size of approximately 2.8 kb. PCR products were then purified using the NucleoSpin® Gel and PCR Clean-up Kit (Macherey-Nagel GmbH & Co. KG, Düren, Germany) following the manufacturer's instructions.

Purified DNA was quantified and checked for purity using the NanoDrop 2000 spectrophotometer. Samples were then diluted to 10 ng/µl, as required by the sequencing laboratory, and submitted for sequencing (Sanger sequencing, Eurofins Genomics).

Results

1. Switching cost and the resulting cell population heterogeneity drive global bioprocess dynamics

As mentioned previously, continuous cultures such as chemostats, are widely used in microbial biotechnology due to their ability to maintain steady-state conditions over extended periods as well as their increased productivity (production/time)[11]. However, these systems are known to generate population instability over time, often leading to a progressive decline in productivity[3,17]. Such instability in population dynamics poses challenges for industrial bioprocesses relying on recombinant protein production.

Before examining the results in detail, it is essential to outline a concept that forms the basis of their interpretation. As shown in a previous study[109], burdensome gene circuits typically lead to increased phenotypic dispersion, which can be quantified using entropy as a metric. The gene of interest was fused to a fluorescent reporter, making it possible to monitor expression level through GFP fluorescence. In this context, entropy reflects population heterogeneity: higher entropy values indicate a broader distribution of gene expression levels across individual cells. A concrete illustration of this concept is provided by previously published data: *E. coli* P_{arab}::GFP, representing a system without switching cost (Figure 11A), and *S. cerevisiae* P_{glc3}::GFP, representing a system with switching cost (Figure 11B). Both were cultivated under chemostat conditions. As a reminder, the switching cost in this study is defined as the growth rate loss associated with gene expression. In Figure 11, it can be clearly seen that in the absence of a switching cost, fluorescence dispersion is low, corresponding to a low entropy. In contrast, in the system with a switching cost, fluorescence is more broadly distributed, indicating a higher entropy within the population.

In the present work, *E. coli* BL21 (DE3) harbouring the plasmid pET28::GFP was cultivated for 150 hours in a 1L bioreactor under chemostat conditions with glucose as the carbon source and lactose as the inducer. To monitor the dynamic of recombinant protein production at the single-cell level an automated flow cytometry system was implemented. This allowed for periodic sampling of the culture to quantify GFP fluorescence, used here as a proxy for recombinant protein expression. Since this strain utilizes the T7 expression system for GFP production, it is subject to a significant burden. However, the T7 system is commonly employed in industry due to its high expression strength[40].

Long-term continuous culture with this system offers an opportunity to gain insight into population dynamics associated with burdensome gene expression. The data presented in Figures 11C-F correspond to two independent biological replicates of this experiment.

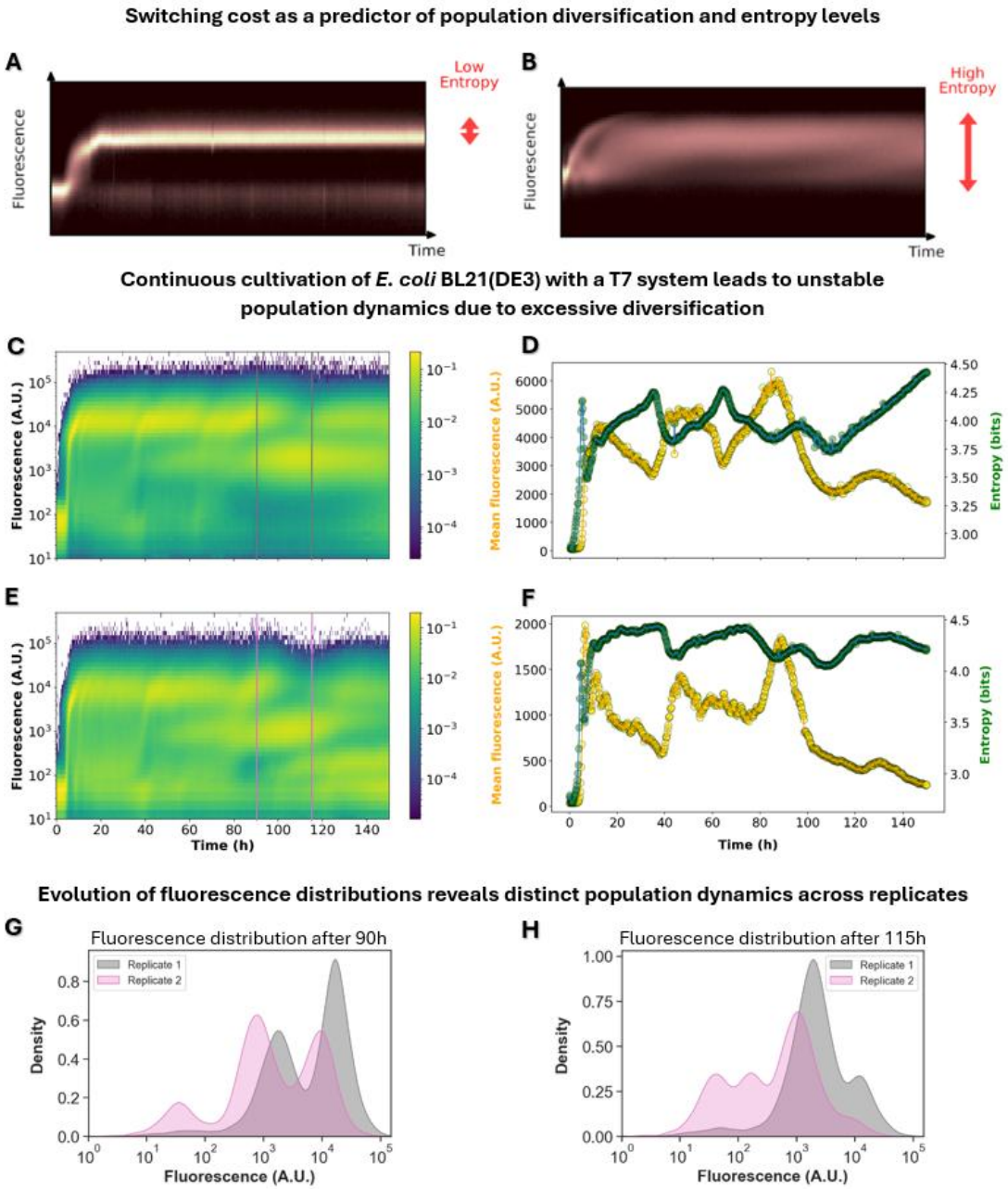

FIGURE 11: POPULATION HETEROGENEITY IN THE CONTEXT OF BURDENSOME GENE CIRCUITS.

A-B: *Single-cell fluorescence profiles over time, obtained via automated flow cytometry, illustrate population diversification in (A) E. coli P_{ara}::GFP and (B) S. cerevisiae P_{glc3}::GFP cultivated in bioreactors under chemostat conditions. Reporter gene induction occurred without an associated switching cost in (A), and with a switching cost in (B). Adapted from Delvenne et al. (2025)[123].* ***C-D:*** *First replicate of the long-term chemostat experiment using E. coli BL21 (DE3) pET28::GFP under lactose induction for 150h. (C) Single-cell fluorescence over time measured by automated flow cytometry. The colour bar represents the relative density of detected events: yellow indicates the highest density, while dark blue corresponds to regions with few events. The two grey lines correspond to the fluorescence distributions presented in panels G and H. (D) Entropy computed from the fluorescence distribution of the population; mean fluorescence values are plotted in yellow.* ***E-F:*** *Second biological replicate under identical conditions. (E) Single-cell fluorescence over time measured by automated flow cytometry (colour bar as in panel C). The two pink lines correspond to the fluorescence distributions presented in panels G and H. (F) Entropy and mean fluorescence dynamics of the second replicate.* ***G:*** *Zoom on the fluorescence profile after 90h in both replicates, highlighting the emergence of distinct subpopulations with different fluorescence intensities.* ***H:*** *Zoom on the fluorescence profile after 115h, illustrating distinct subpopulation dynamics in the two replicates.*

On the scatterplots showing the cells fluorescence across time a bursty diversification pattern is observed at the beginning of the induction (Figure 11C and E). This reflects the rapid activation of distinct fractions of the population in successive waves. Instead of a uniform response, cells activate in successive groups, indicating that induction occurs in an asynchronous way across the population. Following these waves of diversification, distinct groups of cells (i.e. subpopulations) with different fluorescence levels are observed as shown in Figures 11G and H, where each peak corresponds to a subpopulation.

To support the qualitative observations from Figure 11C and 11E, the mean fluorescence intensity and entropy were quantified over time. It is noticeable that higher entropy levels are correlated with lower mean fluorescence values (Figure 11D and 11F). This suggests that heterogeneity (i.e. high entropy levels) negatively impacts production.

While both experiments show similar overall patterns, the population dynamics are not exactly reproducible between the two replicates (Figures 11G and H). This show that long-term continuous cultivations under chemostat conditions present inherent instability and are unpredictable, even when performed with the exact same strain under similar conditions in the same equipment. Nevertheless, what can be observed in both case is the emergence of different subpopulations with distinct fluorescence levels over time, reflecting an increase in population heterogeneity through entropy rising.

2. Phenotypic and genotypic heterogeneity are involved in the diversification process during continuous culture

The burst-like diversification observed during the early phase of induction reflects phenotypic heterogeneity, with successive subpopulations activating recombinant protein expression one after the other. These waves of activation seem to be followed by washout events due to the metabolic burden associated with gene expression, and then by the emergence of new expressing subpopulations.

In parallel, genetic diversification was also monitored throughout the experiment. During the chemostat cultures, off-line samples were collected at different time points. From each sample, ten individual colonies were isolated and sequenced to identify potential genotypic changes. The results revealed the emergence of a genetic variant after approximately 115 hours, which progressively became dominant within the population. This mutant exhibits reduced GFP fluorescence, which can be explained by the specific mutations identified in its genome (Figure 12A).

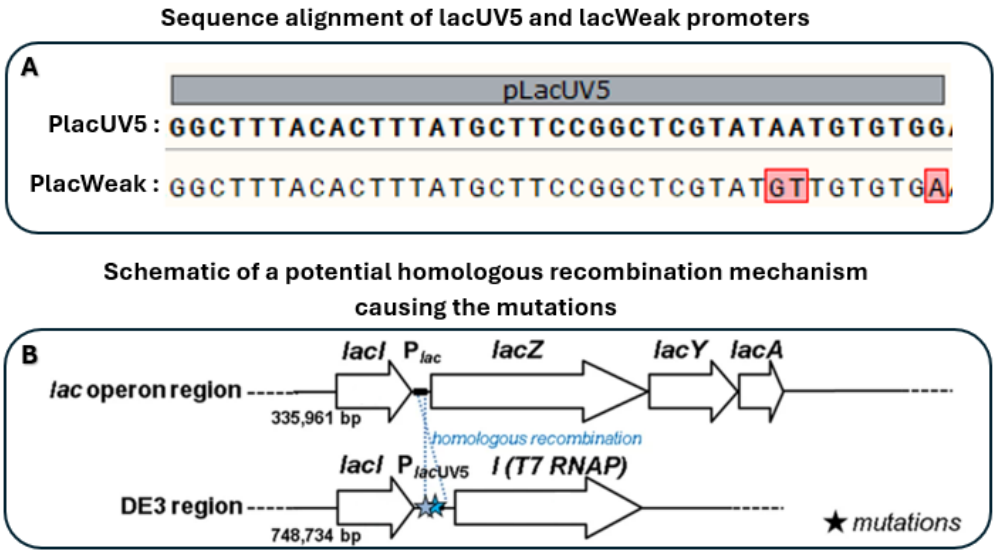

FIGURE 12: GENETIC ADAPTATION OVER TIME REVEALED BY THE EMERGENCE OF MUTATIONS IN CONTINUOUS CULTURE.
(A) Alignment of the lacUV5 promoter region (SnapGene) between the BL21 (DE3) strain and a mutant isolated after 115 hours in chemostat culture. (B) Schematic representation of the lac operon region and the DE3 prophage insertion in the E. coli BL21 (DE3) chromosome. Both regions contain related promoters controlling the chromosomal lac operon, and the PlacUV5 driving expression of the T7 RNA polymerase in the DE3 region. The high similarity between these promoters suggests a possible homologous recombination event (in blue) leading to the observed mutations. Adapted from Kwon et al. (2015)[124].

As described before, *E. coli* BL21 (DE3) expresses T7 RNA polymerase (T7 RNAP), which drives transcription from the T7 promoter present on the pET28 plasmid. T7 RNAP transcribes approximately eight times faster than the native *E. coli* RNA polymerase, enabling strong expression of recombinant proteins[39,124]. In this strain, the gene encoding T7 polymerase is integrated into the chromosome in the DE3 region and regulated by the lacUV5 promoter, a stronger variant of the wild-type *lac* promoter (PlacWeak)[124].

The mutant identified after 115 hours carried three point mutations (substitutions) in the lacUV5 promoter region (Figure 12A). These mutations likely result from homologous recombination between the lacUV5 promoter and the native *lac* operon promoter, which share high sequence similarity (Figure 12B)[124]. This region is considered a mutational hotspot, as such recombination events weaken the promoter, leading to lower T7 RNAP production and, consequently reduced expression of the recombinant protein. This alleviates the switching cost associated with recombinant protein production, favouring the persistence of such mutations in the population[114,124].

This mutation likely represents a genetic adaptation that allows cells to maintain growth under selective pressure by lowering expression levels of the burdensome gene circuit. Indeed, cells with weaker promoter activity are favoured as they achieve a better balance between growth and protein expression, illustrating the classic trade-off in recombinant protein production. This selective advantage promotes the emergence and eventual dominance of such mutants over time. Importantly, sequencing of colonies isolated at an earlier time point (24h) confirmed that the mutation was not pre-existing, supporting the hypothesis that it arose during the cultivation (Appendix 4).

These findings demonstrate that, beyond phenotypic diversification, prolonged recombinant protein expression from burdensome circuits can drive the selection of genetic variants that impact stability and productivity in continuous bioprocessing.

3. Reducing switching cost by providing a suboptimal carbon source to enhance population homogeneity during continuous cultivation

Considering the mutational escape observed in the previous section, it appears that the cell population tends to reduce the switching cost associated with recombinant protein expression. This phenomenon can be interpreted using the trade-off curve between growth and gene expression, which was previously established in a related study conducted by colleagues in our laboratory[114]. In that work, fluorescence decay during the relaxation phase (i.e. the decrease of fluorescence that follows an induction) was analysed across different cell percentiles (Figure 13). Because GFP is a highly soluble protein, its decrease over time primarily results from the dilution due to cell population growth. This property allowed for an indirect estimation of growth rates, and thus the construction of a trade-off curve linking fluorescence intensity (i.e. expression level) and growth rate (Figure 14A).

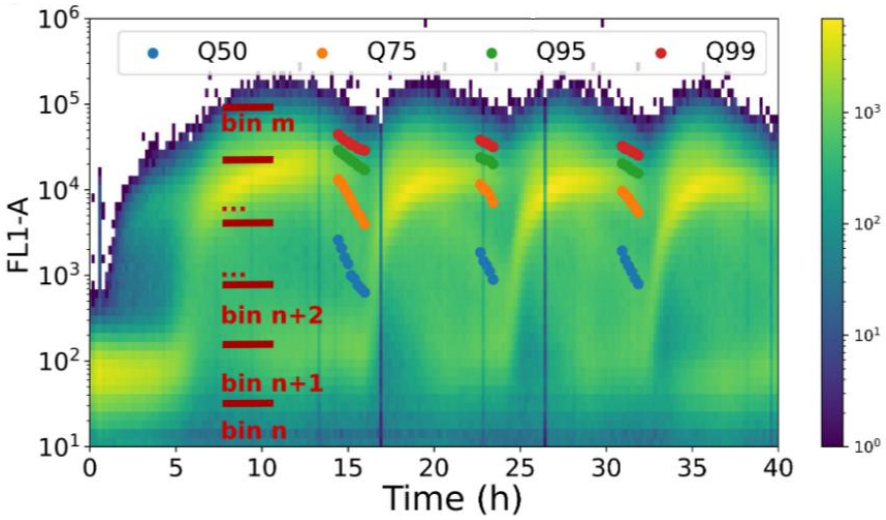

FIGURE 13: FLUORESCENCE RELAXATION ANALYSIS (FROM HENRION ET AL., 2024[114]).

The time density plot shows fluorescence intensity (FL1-A) on the y-axis and time on the x-axis. The colour bar represents the relative density of detected events: yellow indicates the highest density, while dark blue corresponds to regions with few events. The Q50, Q75, Q95, and Q99 values correspond to the 50th, 75th, 95th, and 99th percentiles of the fluorescence distribution at each time point. By analysing the decrease in these percentile values over time, fluorescence relaxation can be quantified. This relaxation serves as a proxy for growth rate, allowing the establishment of a relationship between growth rate and fluorescence intensity, forming the trade-off curve represented in Figure 14A.

This curve reveals that cells expressing higher levels of fluorescence suffer from a significantly reduced growth rate. Therefore, in the context of long-term cultivation, cells may adapt by reducing their fluorescence level to lower the switching cost, moving upward along the trade-off curve (Figure 14B). This adaptive strategy was concretely observed in the previous experiment, where mutations occurred in the lacUV5 promoter region after 115 hours of continuous cultivation. As shown in the previous section, this mutation resulted in a reduction of gene expression, consistent with the idea that cells tend to reduce their switching cost by lowering expression levels.

An alternative strategy to reduce this cost, without altering expression levels, is to lower the strain's maximal growth rate. This approach shifts the entire trade-off curve downward from the top (Figure 14C), reducing the fitness advantage of non-induced cells.

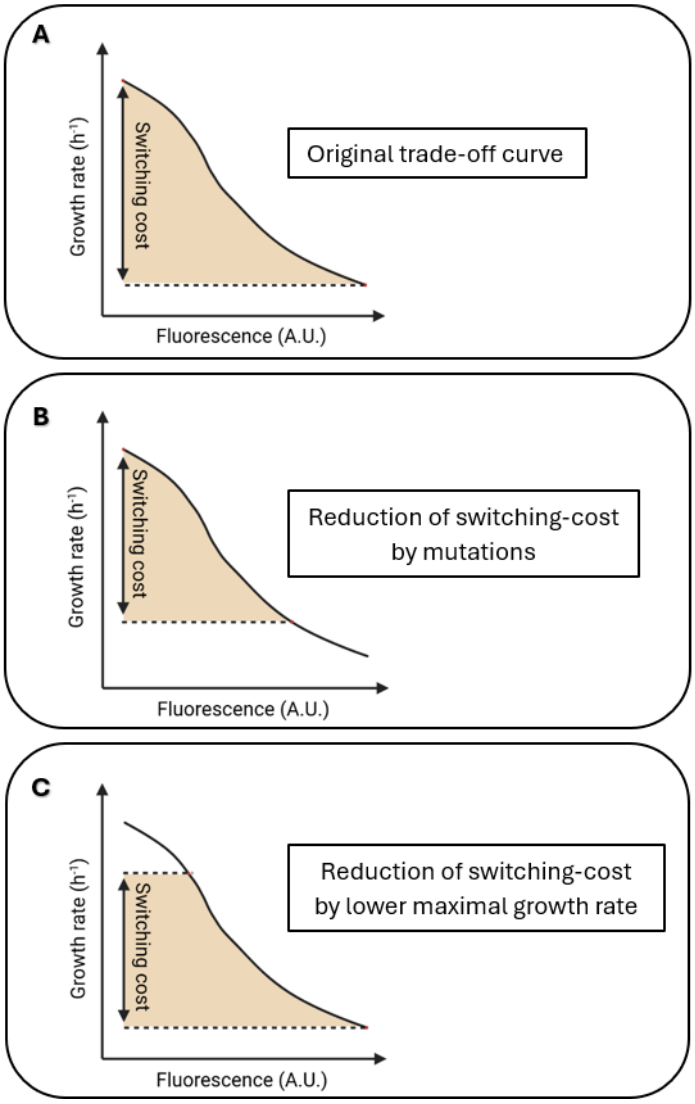

FIGURE 14: TRADE-OFF CURVE AND THE ASSOCIATED STRATEGIES FOR REDUCING SWITCHING COST.
(A) Trade-off curve previously established in our lab, showing the relationship between growth rate and expression level (fluorescence), where higher fluorescence corresponds to lower growth rates. (B) Strategy of reducing switching cost by lowering fluorescence levels, as naturally adopted by bacteria through mutations during long-term continuous cultures. (C) Strategy of reducing switching cost by decreasing the strain's maximal growth rate. Created with BioRender.com.

Based on this concept, we tested whether providing a less favourable carbon source than glucose, such as xylose, could improve population homogeneity by promoting a more uniform induction while maintaining elevated levels of recombinant protein production. Indeed, when grown on xylose, the strain exhibits a lower maximal growth rate ($0.55h^{-1}$ compared to $1.09h^{-1}$ on glucose), which, according to the trade-off model, effectively reduces the switching cost (Figure 14C).

A chemostat culture using xylose was performed under the same conditions as before, except for the carbon source. On figure 15A, cells appear to be successfully induced at the beginning of the chemostat, as shown by the initial increase in fluorescence. However, this is followed by a noisy, irregular signal. This noise can be explained by a rapid and drastic decrease in biomass (Figure 15B), combined with the automated dilution factor applied by the flow cytometer during sampling. At that point, nearly no events/µl were recorded, due to the high dilution factor applied (1:1024), indicating that the cytometer was essentially detecting noise rather than actual fluorescent events.

Later in the graph, an apparent increase in fluorescence can be observed, but this is in fact an artefact caused by a change in the cytometer's dilution settings (from 1:8 to 1:128). This change artificially amplifies the fluorescence signal without reflecting a real increase in biomass or protein expression. Altogether, these measurements indicate a complete washout of the population following induction under xylose conditions.

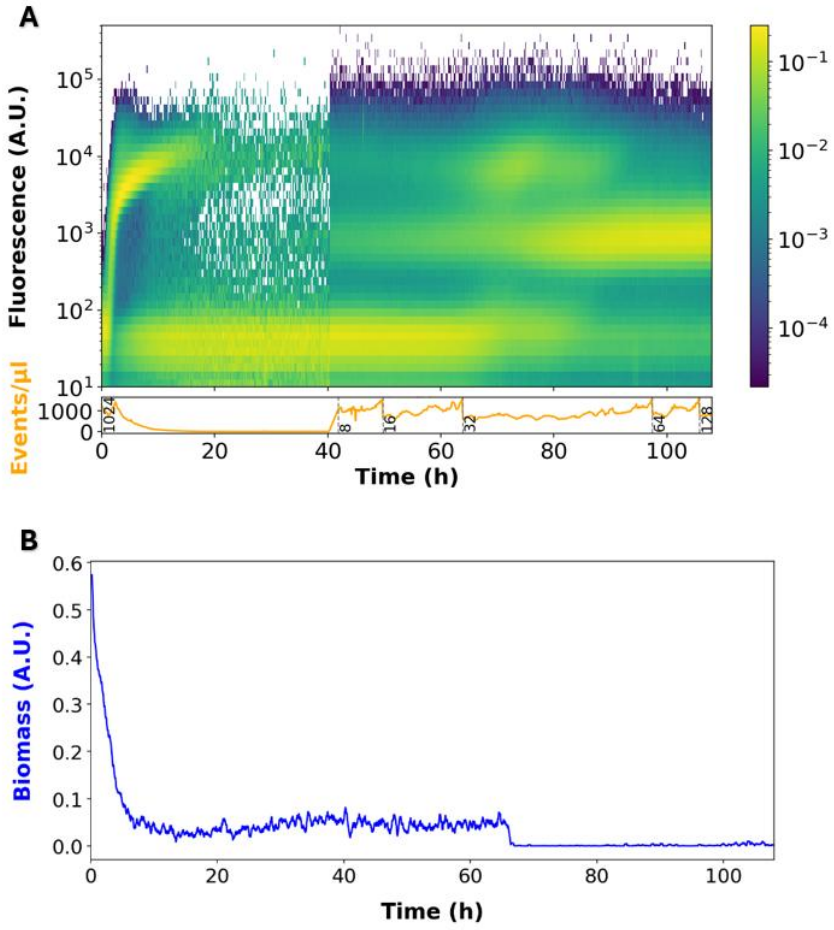

FIGURE 15: COLLAPSE OF E. COLI POPULATION UNDER XYLOSE-BASED CONTINUOUS CULTIVATION.
(A) Single-cell fluorescence over time measured by automated flow cytometry during a long-term chemostat cultivation of E. coli BL21 (DE3) pET28::GFP under lactose induction, with xylose as the carbon source. The colour bar represents the relative density of detected events: yellow indicates the highest density, while dark blue corresponds to regions with few events. The subplot below displays the corresponding events/µL recorded at each fluorescence measurement. A sharp drop in events/µL is observed between 20 h and 40 h, reaching zero, which explains the irregular and noisy signal in the fluorescence scatter plot. The numbers written vertically on the graph indicate the dilution factors applied by the flow cytometer during automated sampling. (B) Biomass over time, was monitored by the online biomass probe.

In contrast to what was observed in glucose cultures, where a subpopulation could survive and rescue the system, no fraction of the population under xylose succeeded in escaping the induction or stabilizing the culture. This suggest that the induction was uniformly experienced by all cells, leading to a collapse of the entire population.

An explanation for this phenomenon lies in the regulatory mechanism of sugar metabolism. As illustrated in Figure 16, the *lac* operon is tightly controlled and requires two conditions for activation. First, cyclic adenosine monophosphate (cAMP) molecules must form a complex with the catabolite activator protein (CAP), which then binds to the CAP-binding site near the *lac* promoter. This binding facilitates RNA polymerase recruitment and efficient transcription of the *lac* genes[125–129]. To achieve sufficient cAMP levels for the cAMP-CAP complex formation, glucose must be absent from the medium. Indeed, in presence of glucose, the glucose-specific Enzyme IIA ($EIIA^{Glc}$), which is part of the multi-phosphorylation cascade regulating glucose uptake and metabolism, remains unphosphorylated. Since adenylate cyclase activation, which synthesizes cAMP, depends on phosphorylated $EIIA^{Glc}$, the presence of glucose leads to low intracellular cAMP concentrations[130,131]. Furthermore, the process of inducer exclusion occurs, where unphosphorylated $EIIA^{Glc}$ inhibits the activity of certain sugar transporters such as the lactose permease, further reinforcing catabolite repression[131]. Second, the constitutive repressor LacI must be inactivated by allolactose, a derivative of lactose produced by beta-galactosidase. When allolactose binds LacI, it prevents LacI from binding to the operator region, allowing RNA polymerase to proceed with transcription[125,129]. Therefore, full activation of the lac operon requires both the absence of glucose and the presence of lactose.

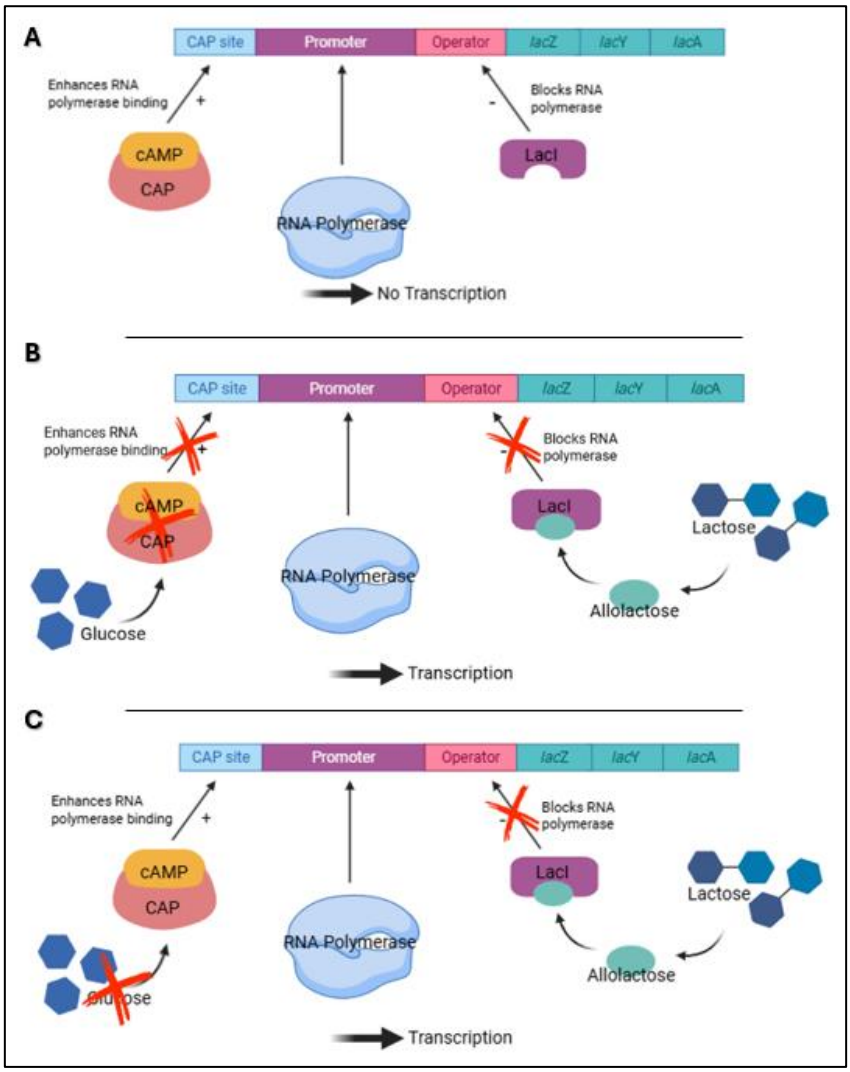

FIGURE 16: REGULATION OF THE LAC OPERON BY GLUCOSE THROUGH CATABOLITE REPRESSION MECHANISM.
(A) In the absence of lactose, the repressor protein LacI binds the operator region of the lac operon, preventing RNA polymerase from initiating transcription. (B) When glucose is present, intracellular cAMP levels remain low, preventing the formation of the cAMP-CAP complex. As a result, RNA polymerase binding to the lac promoter is inefficient. However, the presence of lactose leads to the production of allolactose, which binds to LacI and inhibits its ability to bind the operator, partially relieving repression. (C) In absence of glucose and in presence of lactose, cAMP levels increase, enabling the formation of the cAMP-CAP complex. This complex binds the CAP site, upstream of the promoter, facilitating efficient RNA polymerase binding. At the same time, allolactose (formed from lactose) binds to LacI, preventing it from blocking the operator. Together, these conditions fully activate transcription of the lac operon. Figure created with BioRender.com.

Additionally, the rapid population collapse can be further explained by the carbon source hierarchy. Indeed, it has been demonstrated that preferential use of certain carbon sources is partly regulated via cAMP levels, which inversely correlate with bacterial growth rate. A preferred carbon source that supports faster growth leads to lower intracellular cAMP levels. However, the metabolism of less preferred carbon sources requires higher cAMP levels because the cAMP receptor regulating these genes has lower sensitivity[131]. Since lactose is preferred over xylose, cAMP levels remain insufficient to activate xylose metabolism, further contributing to the inability of the population to adapt and survive.

With these regulatory mechanisms in mind, it becomes clear that in presence of glucose, catabolite repression limits lactose uptake in a subset of cells. This enables part of the population to escape induction, maintaining a higher growth rate, and sustain the culture. In contrast, when glucose is replaced by xylose, catabolite repression is lifted, and all cells are induced simultaneously. This effect is reinforced by the hierarchy of sugar utilization, where lactose is a more preferred carbon source than xylose. As a result, the entire population faces the metabolic burden of induction, with no subpopulation able to escape or compensate, explaining the complete washout observed under these conditions. This mechanism was previously described as environmental escape[123].

As shown in Figure 17A, in presence of glucose, cells segregate into two distinct phenotypic groups upon induction: one subpopulation exhibits high fluorescence, and so, a reduced growth rate, while the other maintains low fluorescence and a higher growth rate. This segregation increases population entropy, with the less fluorescent subpopulation supporting overall survival and preventing system washout. In contrast, when xylose replaces glucose, this phenotypic diversification is much less pronounced and is insufficient to maintain population viability, leading to washout (Figure 17B).

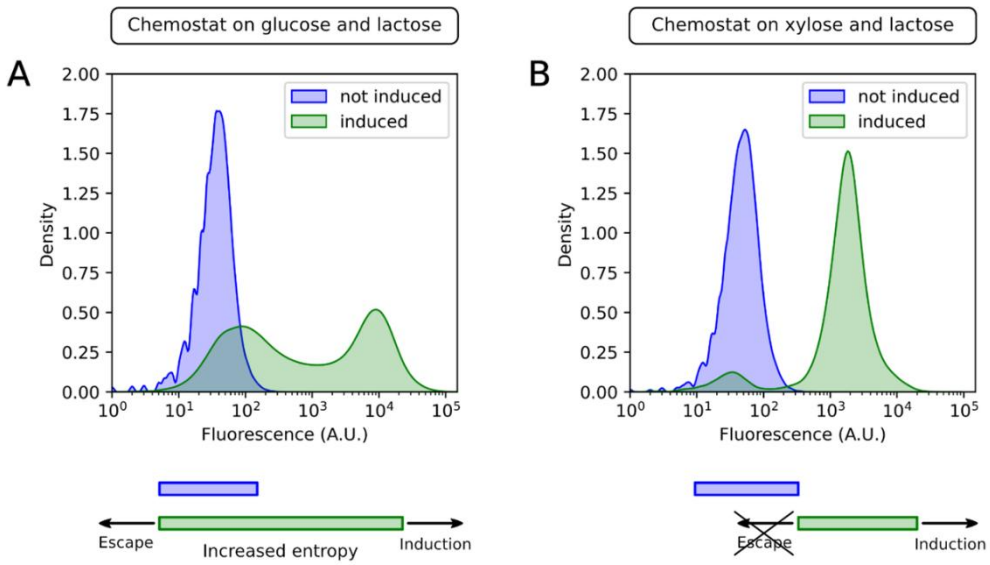

FIGURE 17: ENVIRONMENTAL ESCAPE MECHANISM ALLOWS POPULATION SURVIVAL UPON INDUCTION IN CONTINUOUS CULTURES.

(A) Fluorescence distribution in a glucose-lactose culture showing the emergence of two subpopulations during induction (green curve): one with high induction (high fluorescence level) associated with a slow-growing phenotype, and another with a lower expression level and a fast-growing phenotype. The blue curve represents the distribution prior to induction. (B) Fluorescence distribution in a xylose-lactose culture showing no segregation and nearly full induction of the population, indicating the absence of environmental escape. The blue curve represents the population before induction and the green curve during induction. Extracted from Delvenne et al. (2025)[123], based on experimental data obtained in the present work.

These results demonstrate that, in the absence of an adaptive potential via an escape route, the population face washout under continuous cultivation. This experiment also supports the hypothesis that population heterogeneity acts as an adaptive strategy to cope with burdensome expression system in continuous cultures. Moreover, it highlights that bioprocess heterogeneity arises not only from

genetic variation (as previously shown) but also from phenotypic variability, which may precede and potentially drive genetic adaptations.

4. Temperature reduction as an alternative strategy to lower switching cost and improve population homogeneity in continuous culture

Building on the results from the xylose strategy, which highlighted the importance of environmental escape for sustaining populations under burdensome recombinant protein production, we explored another approach. In this new strategy, glucose was retained as the carbon source to maintain the possibility of environmental escape, but the culture temperature was decreased from 37°C to 30°C. As in the previous chemostat experiments, all parameters were kept identical except for the carbon source and temperature. This approach aims to lower the switching cost by decreasing the strain's maximal growth rate, thereby reducing the fitness advantage of non-induced cells. In theory, this could promote a more homogeneous expression of the recombinant protein. The estimated growth rate at 30°C is provided in Appendix 3. Figure 18 shows the plots generated from collected data.

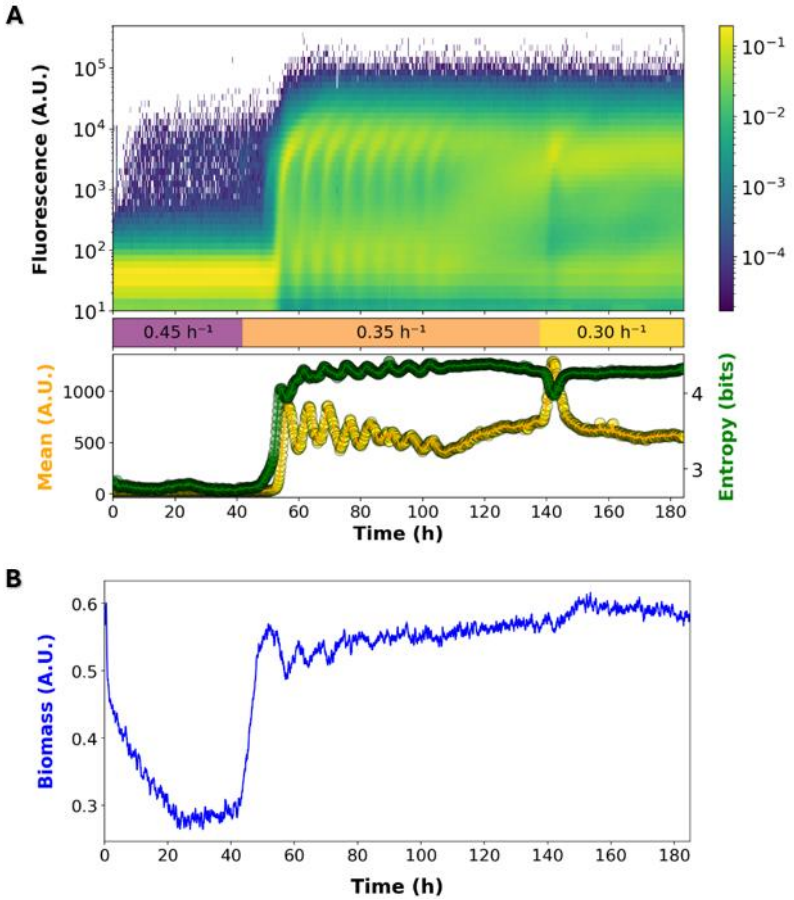

FIGURE 18: POPULATION HETEROGENEITY PERSISTS DESPITE REDUCED SWITCHING-COST UNDER LOW-TEMPERATURE INDUCTION IN CHEMOSTAT.

(A) Single-cell fluorescence dynamics monitored by automated flow cytometry during long-term chemostat cultivation of E. coli BL21 (DE3) pET28::GFP at 30°C under lactose induction, with glucose as the carbon source. The colour bar represents the relative density of detected events: yellow indicates the highest density, while dark blue corresponds to regions with few events. The top subplot displays changes in dilution rate over time. The bottom subplot quantifies mean fluorescence (in yellow) and entropy (in green) throughout the experiment, highlighting the relationship between expression levels and population heterogeneity. (B) Biomass evolution over time during the same chemostat cultivation.

Despite the reduced switching cost and the possibility of environmental escape, the population entropy remained high, indicating that production homogeneity was not achieved.

More specifically, at a dilution rate of 0.45h^{-1}, which was used at the start of the chemostat, no induction was observed, as no GFP fluorescence was detected. This is likely due to catabolite repression: with the lower growth rate, a small amount of glucose may remain in the medium, inhibiting lactose uptake and preventing induction. This is further supported by the observed sudden drop in biomass at the start of the chemostat, which remained relatively low compared to when a lower dilution rate was used (Figure 18B). Although samples were collected, measurements of sugar concentrations in the supernatant were not conducted due to time constraints. It would be useful to confirm this hypothesis by performing high-performance liquid chromatography (HPLC) analysis to assess the remaining sugar concentrations in the medium.

When the dilution rate was decreased to 0.35h^{-1}, induction began with a bursty behaviour, likely due to successive waves of induction in distinct fractions of the population. This was followed by a desynchronisation, leading to a diffuse "cloud" on the scatter plot (Figure 18A). This behaviour likely reflects the emergence of two subpopulations, producers and non-producers, whose relative dominance alternates over time. Such oscillations may be driven by the interplay between the metabolic burden associated with high expression levels and the environmental escape, which together drive the dynamic equilibrium between the two subpopulations. A similar phenomenon was observed at 37°C with a dilution rate of 0.45h^{-1}, suggesting that the population dynamics under both conditions were comparable.

At an even lower dilution rate of 0.30h^{-1}, the population appeared to segregate into two subpopulations, one exhibiting fluorescence and the other not, with some cells displaying intermediate fluorescence levels. However, throughout the experiment, the entropy level remained high, and no homogeneity was reached.

5. History-dependent population dynamics in continuous culture revealed by variation of dilution rates at 30°C

As the population dynamics were shown to vary significantly with the dilution rate in the previous experiment, we performed a screening with increasing dilution rates to assess whether a specific value would lead to greater population homogeneity, characterized by lower entropy and higher mean fluorescence. The same chemostat parameters were applied as before, except that dilution rates ranged from 0.20h^{-1} to 0.45h^{-1}, increasing by 0.05h^{-1} increments. Each condition was maintained for at least five residence times, in accordance with the standard practices in literature, where it is generally stated that between three and five residence times are sufficient for population to stabilise.

However, our results revealed that in the context of burdensome recombinant expression system, population stabilisation is not achieved within this timeframe. Despite screening a wide range of dilution rates, population entropy remained consistently high, and none of the tested conditions resulted in a homogeneous fluorescence profile (Figure 19). These findings suggest that, contrary to theoretical expectations, chemostat cultures involving burdensome gene expression may not reach steady state even after multiple residence times.

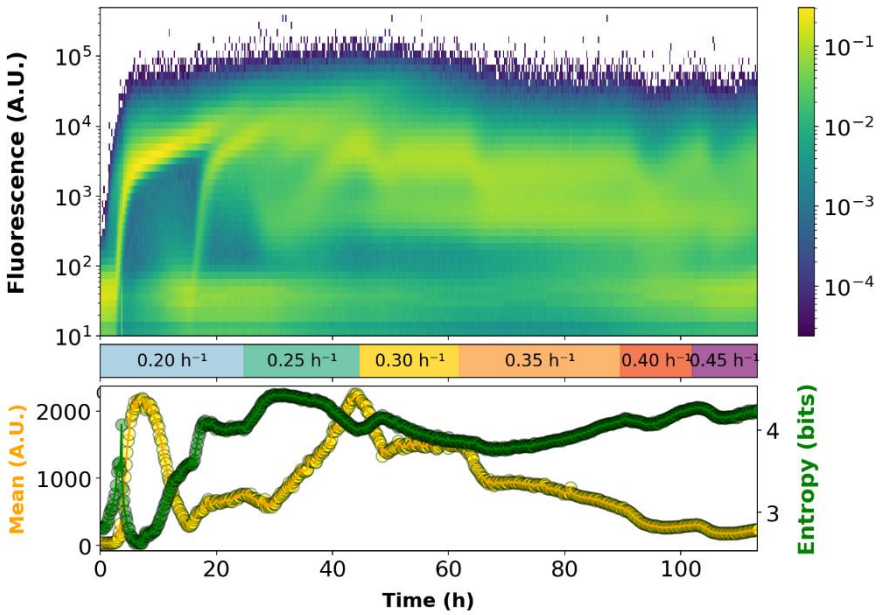

FIGURE 19: SCREENING OF DILUTION RATES UNDER REDUCED TEMPERATURE REVEALS PERSISTENT HETEROGENEITY IN CHEMOSTAT CULTURES.

Single-cell fluorescence was monitored over time by automated flow cytometry under the same conditions as in Figure 18 (30°C, glucose as the carbon source, induction with lactose). The colour bar represents the relative density of detected events: yellow indicates the highest density, while dark blue corresponds to regions with few events. This experiment involved a systematic screening of dilution rates, each maintained for at least five residence times as recommended in the literature to allow population stabilisation (stabilisation was not observed in this case). The top subplot displays the applied dilution rates over time, while the bottom subplot presents the evolution of mean fluorescence (in yellow) and population entropy (in green) throughout the experiment.

Interestingly, we also observed that population dynamics at a given dilution rate differed from those obtained in the previous experiment, despite identical dilution values. For instance, at $0.35h^{-1}$, the earlier experiment showed a burst-like induction pattern with successive waves of subpopulation activation (Figure 18), whereas in this case, a more diffuse, cloud-like distribution emerged (Figure 19). At $0.45h^{-1}$, no induction was previously observed, and similarly, here the fluorescence remained near zero, but entropy was higher, indicating persistent heterogeneity. These discrepancies indicate a clear history-dependence in population behaviour: the state of the system at a given point is shaped not only by current conditions, but also by the environmental trajectory leading up to them.

Contrary to our expectations, none of the tested dilution rates resulted in population homogenisation. Thus, the strategy of reducing the switching cost by lowering the temperature appears ineffective for achieving both high expression levels and population uniformity.

Discussion

Controlling population heterogeneity remains a major challenge in continuous bioprocesses, as it directly impacts both process stability and productivity. Gaining a deeper understanding of the origins and consequences of such variability is therefore essential for the design of robust and reliable long-term cultivation strategies.

To address this issue, this study investigated population dynamics during long-term continuous cultivation of *E. coli* BL21 (DE3) carrying the pET28::GFP plasmid, with the aim of identifying strategies to control population heterogeneity. Chemostat cultures of more than 100 hours were conducted, relying on the T7 expression system as a model for burdensome recombinant protein production. *E. coli* was chosen as the model strain because it is one of the most widely used host microorganisms for recombinant protein production, especially due to its rapid growth and well-characterised genome[38]. Moreover, the T7 RNA polymerase, known for its high transcriptional activity, imposes a considerable metabolic burden on cells[40], providing a relevant context to study the impact of burdensome expression in continuous culture. The use of green fluorescent protein (GFP) as a reporter further enabled single-cell monitoring by flow cytometry (FC), offering a reliable proxy for recombinant protein production and population heterogeneity.

1. Population dynamics reveal the absence of steady state in chemostat cultivation

Chemostats are traditionally described as stable systems capable of maintaining steady-state conditions over long periods[19,132]. However, the experiments conducted in this study revealed that, in the context of recombinant protein production with a burdensome gene circuit, chemostats do not reach a true steady state. At the macroscopic level, parameters such as biomass (Figure 20B) and dissolved oxygen (DO) (Figure 20C) appeared stable, which could lead to the assumption of a steady state. These bulk parameters do not capture variability between individual cells. Yet, single-cell analysis by FC demonstrated a dynamic population heterogeneity (Figure 20A), highlighting the importance of monitoring cultures at the cellular level to detect fluctuations that remain hidden when relying solely on macroscopic parameters. This is in line with previous reports showing that continuous cultures often harbour significant phenotypic heterogeneity despite apparently stable bulk parameters[76,133]. For example, Nikolic et al. (2017)[134] reported that clonal cells in carbon-limited chemostats growing in the presence of two sugars exhibited variation in carbon assimilation rates, and consequently in their growth rates.

The results of the present study indicate that heterogeneity is particularly pronounced in the context of burdensome gene circuits. However, in less burdensome expression systems, chemostats have been shown to maintain a much more homogeneous single-cell distribution, with reduced variability in gene expression. For instance, Henrion et al. (2023) by using an arabinose-inducible system demonstrated that *E. coli* populations cultivated in chemostats exhibited stable and relatively uniform expression profiles, indicating that in the absence of strong metabolic burden, cellular heterogeneity can be minimised (Figure 11A)[109].

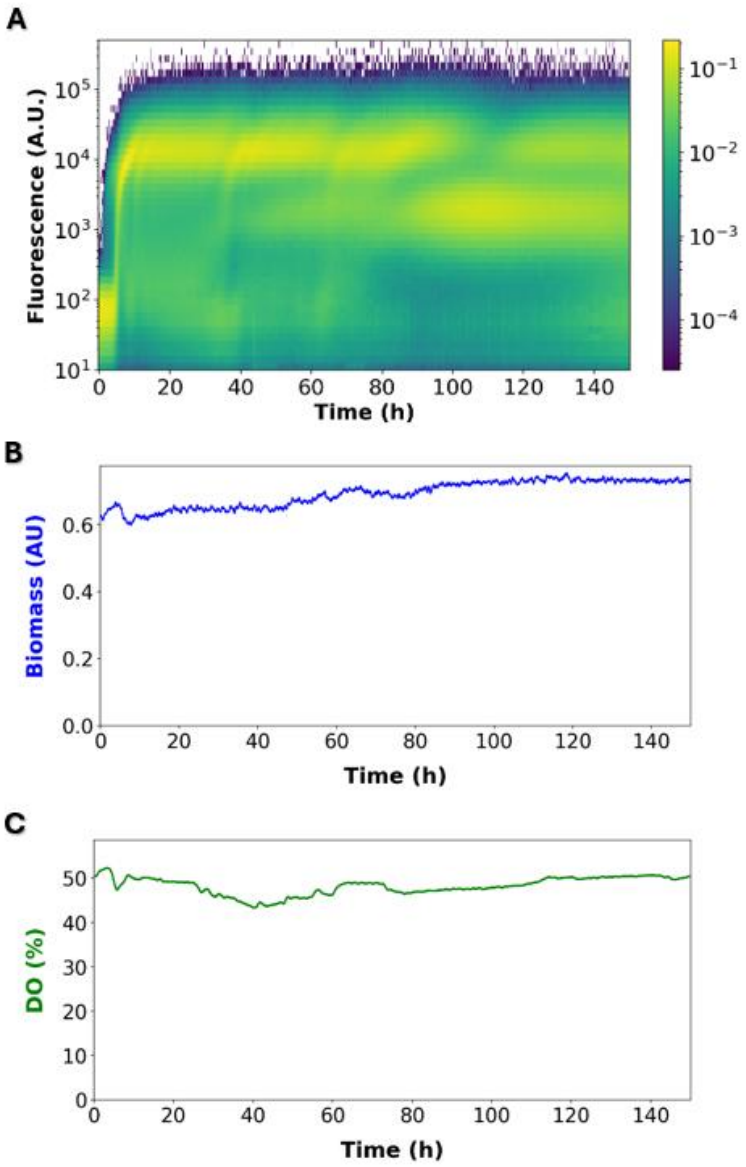

FIGURE 20: HETEROGENEITY OF POPULATION DESPITE A CONSTANT BIOMASS AND DISSOLVED OXYGEN LEVEL (SUPPLEMENTARY INFORMATION FROM FIGURE 11).

Evolution of fluorescence (A), biomass (B), and dissolved oxygen (B) over time during a glucose-limited chemostat culture at 37°C.

One clear illustration of the hidden heterogeneity is the burst-like activation pattern observed during induction in glucose-fed chemostats at 37°C (Figure 20A). Instead of showing uniform induction, fractions of the population activated sequentially, producing waves of expression that could lead to the washout of induced fractions. This dynamic likely originate from stochastic differences in gene expression or in inducer uptake pathways across cells. Indeed, Choi et al. (2008) demonstrated that in the lactose operon of *E. coli*, random fluctuations in the abundance of permease molecules could trigger heterogeneous induction events in isogenic populations, resulting in asynchronous activation[135].

The bursts observed in this study can also be explained by the fact that induced cells carried a significant metabolic burden, which reduced their growth rate compared to non-induced cells and increased their likelihood of being washed out. As a result, new waves of induction emerged from the remaining population, illustrating how phenotypic heterogeneity can spontaneously arise in continuous cultures

under burdensome expression and shape population dynamics. Such diversification events have also been observed under similar chemostat conditions by Henrion et al. (2023), who reported that in continuous *E. coli* cultures using the T7 system induced with lactose, the population profiles revealed recurrent bursts of diversification[109].

Phenotypic heterogeneity not only influenced short-term population dynamics but also appeared to pave the way for longer-term genetic diversification. Sequencing analyses revealed the emergence of mutations in the lacUV5 promoter region after approximately 115 hours (Figure 12A). These mutations likely resulted from homologous recombination events between similar promoter sequences, as suggested by Kwon et al. (2015)[124]. By reducing promoter strength and thus limiting T7 RNA polymerase activation, the variants lowered the metabolic burden and gained a selective advantage under chemostat conditions. Such findings are consistent with previous observation that continuous cultures exert strong selective pressure leading to adaptive mutations. For example, Notley-McRobb and Ferenci (1999) reported that mutations improving nutrient uptake conferred a selective advantage in glucose-limited *E.coli* chemostats[136]. Similarly, Frumkin et al. (2017) showed that gene architectures minimising metabolic cost, such as weaker promoters or optimised translation strategies, improved cellular fitness by alleviating resource consumption[137]. Importantly, Henrion et al. (2024) also reported the same lacUV5 mutation[114], supporting the idea that promoter-weakening mutations represent a convergent evolutionary solution to mitigate expression burden in continuous cultures. The recurrence of this mutation in independent experiments indicates that it is a reproducible adaptive response rather than a random mutation. These findings illustrate that, in addition to phenotypic heterogeneity, genotypic diversification can also arise in chemostat culture, reinforcing the dynamic behaviour of continuous cultures under strong expression burden.

An additional factor likely contributing to the persistence of heterogeneity is the variation in the ratio of available carbon sources during cultivation. The coexistence of both induced and non-induced fractions of cells may alter nutrient availability, creating transient advantages for specific subpopulations. For instance, highly expressing cells typically grow more slowly and consume less glucose, thereby leaving more substrate available for non-induced cells. In line with this hypothesis, Li and Rinas (2020) reported that upon induction of recombinant protein production in *E. coli* BL21 (DE3), most cells exhibited a reduced growth rate due to the switching cost of T7 activation, which led to glucose accumulation in the medium[138]. Thus, a possible hypothesis for the sustained coexistence of induced and non-induced cells is that temporal shifts in glucose and lactose concentrations create alternating selective advantages for different subpopulations. Such oscillations in resource distribution could sustain the coexistence of multiple phenotypic states, preventing homogenisation of the population even after many residence times. To clarify this phenomenon, monitoring glucose and lactose concentrations throughout cultivation would be valuable to determine whether such substrate shifts indeed occur.

Importantly, the results also indicate that the classical rule of five residence times is not sufficient to ensure stability in burdensome chemostat cultures. According to the literature, chemostat cultures are generally assumed to reach steady-state conditions after approximately three to five residence times[139-143]. However, under the tested conditions involving a burdensome gene circuit, this assumption did not hold true. Although cultivations extended well beyond five residence times, single-cell analyses

revealed persistent heterogeneity and dynamic fluctuations in fluorescence and entropy, indicating that the population had not reached a true steady state. In the last experiment, which involved screening different dilution rates, each rate was maintained for at least five residence times, in accordance with the conventional criterion. Nevertheless, neither fluorescence nor entropy measurements showed signs of stabilisation (Figure 19). Moreover, scatter plots demonstrated that fluorescence intensity within the population remained heterogeneous regardless of the dilution rate applied (Figure 19). These findings suggest that the strong metabolic burden imposed by recombinant protein production continuously drives the strain to adapt to alleviate this cost, which may explain why a true steady state was not reached in this context.

Overall, the results demonstrate that burdensome gene circuits inherently promote diversification in continuous cultures, corroborating previous studies linking highly burdensome expression systems to instability in such conditions[109,114,144]. The results of this work highlight the intrinsic trade-off between growth and recombinant protein production. Strong expression systems like T7 impose a high switching cost, leading either to reduced expression through genetic adaptation or to segregation into heterogeneous subpopulations. While such diversification allows survival under selective pressure[145,146], it comes at the expense of stability and productivity, as mean expression levels decline over time. Thus, although chemostats may appear stable when evaluated through macroscopic parameters, they remain highly dynamic at the cellular level, emphasizing the need for careful monitoring and control strategies to ensure stable yields over extended cultivation periods.

2. History dependence as a driver of heterogeneity and adaptation in continuous culture

By analysing the two chemostat cultures conducted at 30°C, it can be observed that, for the same dilution rate, population dynamics differed considerably. A burst-like phenomenon was observed in the first experiment at 0.35 h^{-1} (Figure 18A), whereas no bursts were detected in the second experiment at the same dilution rate (Figure 19). Similarly, at 0.45h^{-1}, one culture showed no induction (Figure 21A), while in the other a small, induced subpopulation coexisted with a non-induced one (Figure 21B). These results strongly suggest that in chemostat cultures, population dynamics are influenced not only by the current operating conditions but also by the environmental history of the cells. In other words, population behaviour is shaped by both the present conditions and the sequence of conditions previously experienced.

Although such history-dependent effects have not often been discussed explicitly in the context of chemostats, related concepts have been described in fluctuating microbial systems. For instance, Nguyen et al. (2021) showed that environmental fluctuations shape microbial behaviour and evolution, while Vermeersch et al. (2022) described history-dependent behaviour (HDB) in which prior exposure to a substrate changes how cells respond to it later[147,148]. For example, cells previously exposed to a nutrient can resume growth faster (i.e. have a shorter lag phase) when they encounter it again[148]. In the present case, history-dependent effects do not refer to re-exposure to a past environment, but rather to the influence of previous conditions on current population dynamics. Consequently, two cultures exposed to different past environments may behave differently, even when placed under the same chemostat conditions afterwards.

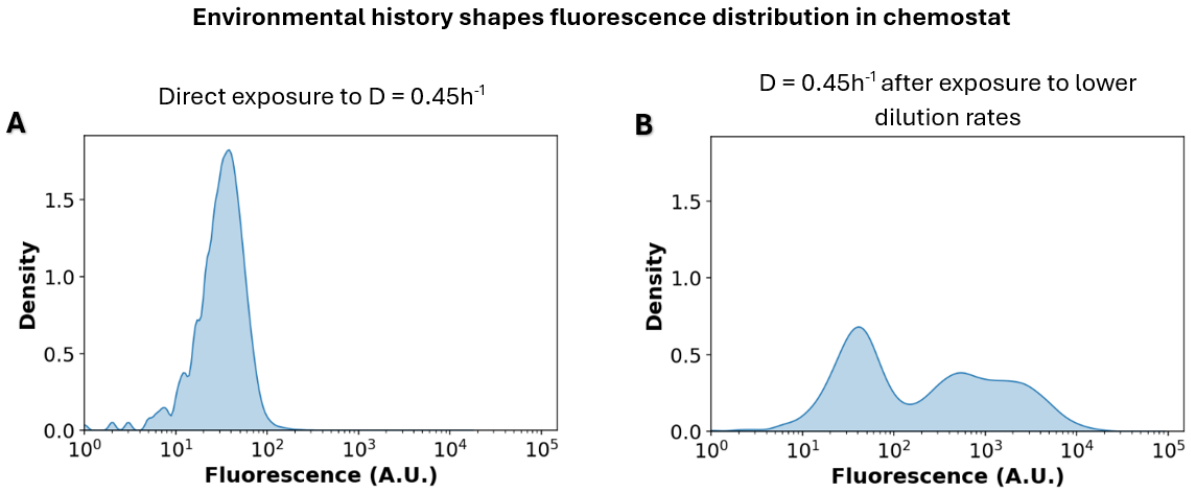

FIGURE 21: EFFECT OF ENVIRONMENTAL HISTORY ON FLUORESCENCE DISTRIBUTION AT A DILUTION RATE OF 0.45H^{-1} (SUPPLEMENTARY INFORMATION FROM FIGURES 18 AND 19).

(A) Representative fluorescence distribution from the chemostat culture at 30°C. When 0.45h^{-1} is applied as the initial dilution rate, the population remains homogeneous but without GFP expression. (B) Representative fluorescence distribution from the chemostat culture at 30°C subjected to sequential exposure to different dilution rates. When 0.45h^{-1} follows a sequence of lower dilution rates, two subpopulations emerge: one expressing GFP and one remaining uninduced.

This history dependence may result from the high rate of phenotypic and genotypic diversification occurring under the selective pressure of chemostat cultivation. As discussed in the introduction, phenotypic heterogeneity itself can be shaped by previous environments[28,73]. Over longer timescales, genetic diversification may further contribute to population heterogeneity, as adaptive mutants selected under past conditions may persist and influence future dynamics. This provides a possible explanation for why two cultures with different environmental histories can exhibit distinct behaviours under identical conditions.

In the case of varying dilution rates, the sequence in which dilution rates are applied plays a critical role in shaping population dynamics. When the dilution rate is gradually increased (e.g., from 0.20 to 0.45h^{-1} in 0.05h^{-1} increments), cells initially face long residence times at low dilution rates, providing greater opportunity for adaptation through evolutionary diversification. At the same time, the low substrate availability under these conditions imposes starvation stress, further promoting heterogeneity. In contrast, when the dilution rate decreases (starting at 0.45h^{-1} to 0.30h^{-1}), cells first experience high dilution rates, where survival depends on rapid growth to avoid washout. Although nutrients are more abundant under these conditions, the demand for fast growth imposes a distinct physiological stress[19,149]. Thus, reaching the same dilution rate (e.g., 0.35h^{-1}) through increasing or decreasing sequences can result in very different dynamics, reinforcing the influence of past conditions on present population behaviour.

The importance of culture history may extend even to preculture conditions, which can strongly influence subsequent dynamics. For example, differences in the carbon source used during the preculture stage could alter metabolic states at inoculation, potentially leading to distinct population behaviours in chemostat. Hoang et al. (2023) demonstrated that the choice of medium during

preculture significantly influences the degree of population heterogeneity in later stages of the bioprocess[150].

Building on these findings, the implications for designing continuous bioprocesses at the industrial scale are considerable. History-dependent effects have important implications: two chemostats operated under identical conditions may still exhibit different productivity and stability due to differences in their prior culture history. To ensure robust and reproducible production, bioprocess design should therefore account for the influence of environmental history on population dynamics. This requires that each step of the cultivation process should be carefully regulated and standardised, to avoid unintended differences in conditions perceived by the cells during continuous cultivation.

3. Lowering the switching cost by reducing the quality of the carbon source using xylose fails to homogenise continuous culture

The analysis of population dynamics in *E. coli* BL21 (DE3) cultivated under standard conditions (i.e. with glucose at 37°C) revealed a clear link between the switching cost and population behaviour. During long-term cultivation with a burdensome gene circuit, the observed mutations indicate that bacteria naturally evolve to reduce the switching cost, notably by weakening the strength of the T7 RNAP promoter and thereby lowering recombinant gene expression[114,124]. This reduction in GFP expression reduces the switching cost, as reflected in the trade-off curve (Figure 14), and alleviates the metabolic burden. Such observations suggest that a potential strategy to control population dynamics and promote homogeneity in continuous cultures is to reduce the switching cost not by lowering gene expression, as bacteria do, but by decreasing the maximal growth rate of the strain. This approach decreases the growth-rate gap between induced and non-induced cells while preserving strong promoter activity.

A recent study conducted by Henrion et al. (2024)[114], proposed using xylose as the carbon source to achieve this effect. Their results showed that replacing glucose with xylose lowered population entropy while increasing the level of induction of the T7 system compared with glucose-fed cultures (Figure 22A). However, the results of the present work contradict these findings. When xylose was used directly as the main carbon source, the system underwent complete washout, demonstrating that this approach is not effective in homogenising the population. As shown in Figure 22B, the evolution of entropy and mean fluorescence in the experiment of this study diverges considerably from the patterns reported by Henrion et al. (2024)[114].

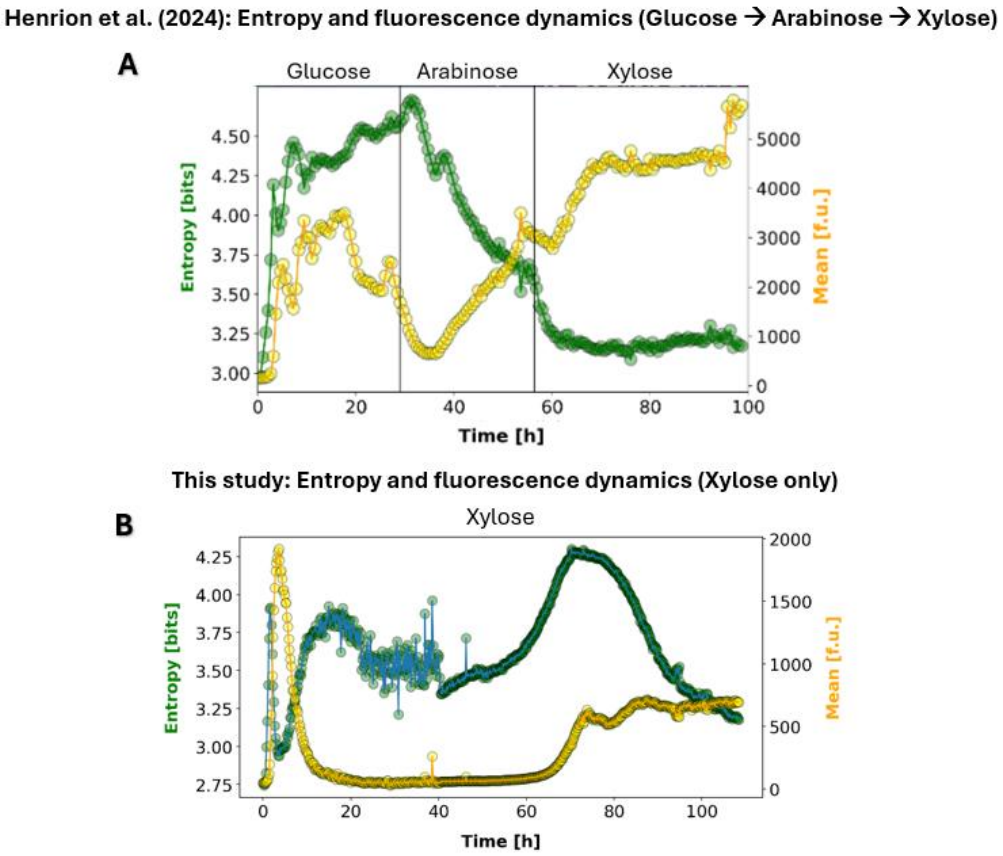

FIGURE 22: COMPARISON OF RESULTS BETWEEN THIS STUDY AND HENRION ET AL. (2024)[114] (SUPPLEMENTARY DATA RELATED TO FIGURE 15).

(A) Data from Henrion et al. (2024), showing population entropy (in green) and mean fluorescence (in yellow) during sequential cultivation on glucose, arabinose, and xylose. (B) Results of this study, in which xylose was provided as the sole carbon source throughout cultivation. While Henrion et al. (2024) reported a decrease in entropy and an increase in fluorescence during the transition to xylose, the present experiment shows that direct growth on xylose leads instead to a different dynamic. The apparent increase in fluorescence observed at the end of the experiment conducted in this study is in fact an artefact. It was caused by a change in the cytometer dilution factor, which resulted from the sharp drop in biomass, meaning the fluorescence was in reality nearly absent (see Figure 15).

The divergence with the findings of Henrion et al. (2024)[114], can likely be explained by differences in the previous environmental conditions encountered by cells, and thus by the previously mentioned history-dependent effect. Indeed, in their study, xylose was introduced only after initial growth phases on glucose and arabinose[114]. As highlighted earlier, history dependence plays a decisive role in shaping population dynamics. Microbial memory has been reported to often rely on semi-stable epigenetic changes such as chromatin remodelling, as well as protein inheritance and the persistence of specific metabolic states, allowing cells to respond more rapidly to recurring or related conditions[148]. In particular, exposure to arabinose before xylose could act as a preconditioning step, since arabinose is generally considered a preferred carbon source for *E. coli* compared to xylose[128,131]. Indeed, growth on arabinose leads to elevated intracellular levels of cAMP molecules (unlike growth on glucose), which may provide a metabolic advantage when shifting to xylose. Since xylose uptake requires higher cAMP levels, this prior induction could shorten the lag phase and reduce the stress response compared to a direct transition from glucose in the preculture to xylose in the chemostat[131,151]. This reduced stress and

pre-adaptation could explain why different population dynamics are observed *in E. coli* chemostats using xylose between the two studies.

It is also plausible that the sequential use of glucose and arabinose allowed bacteria to adapt, potentially through beneficial mutations enhancing growth rate or optimising carbon uptake pathways, thereby facilitating subsequent survival on xylose. For example, mutations leading to the overexpression of the transcriptional regulator XylR have been shown to reduce the lag phase during the transition to xylose by accelerating the induction of xylose metabolic genes[152].

In contrast, in the present study, cultures were grown directly on xylose without such prior possible adaptation. Under these conditions, the metabolic burden imposed by strong expression was too high to sustain growth, leading to washout. These findings reinforce the importance of considering cultivation history when designing strategies aimed at reducing the switching cost and homogenising population dynamics in continuous cultures.

4. Environmental escape of cells from unfit phenotypic states drives a Fitness-Entropy compensation effect in continuous culture

The comparison between glucose- and xylose-fed chemostat cultures using lactose as the inducer highlights the significant role of environmental escape in sustaining cell populations under burdensome recombinant expression. When *E. coli* BL21 (DE3) was grown on glucose, the population was maintained in the bioreactor despite the growth reduction caused by recombinant gene activation. In theory, if all cells had been induced simultaneously by lactose, their growth rate would have dropped below the dilution rate imposed by the chemostat, leading to complete washout. However, this was not the case. Instead, induction occurred progressively and heterogeneously: fractions of the population became induced in a burst-like manner and were likely washed out due to their lower growth rate, while other fractions remained non-induced or only weakly induced. These non-induced cells ensured the maintenance of the overall biomass in the bioreactor, preventing population collapse.

In contrast, when xylose was used directly as the main carbon source, the population dynamic was clearly different. Under these conditions, cells were almost uniformly induced, and the entire system underwent washout. As discussed earlier, this difference can be explained by the absence of catabolite repression in the xylose condition combined with the hierarchy of carbon source utilisation[129–131]. Because lactose is preferentially consumed over xylose, the addition of lactose forced all cells into induction, eliminating the possibility for a subpopulation to remain uninduced. Without this environmental escape (Figure 17B), no mechanism compensated for the reduced growth rate of induced cells, and the population collapsed[123].

With glucose the dynamic is different mainly because an environmental escape is possible (Figure 17A). Two mechanisms appear to contribute to this process. First, noise in gene expression, particularly in the regulation of carbon uptake pathways, can cause some cells to be induced earlier than others, making them better suited to lactose consumption while other cells remain uninduced[73,153,154]. Second, induced cells, expressing the recombinant protein, grow more slowly due to the metabolic burden, which reduces their consumption of glucose. This slowdown leads to an accumulation of glucose in the medium, providing a resource for the faster-growing, non-induced cells[123,138]. These non-induced cells can thrive on the available glucose while avoiding induction thanks to catabolite repression. The

alternation between induced and non-induced cells generates oscillations in the ratio of glucose to lactose within the culture medium. These fluctuations in substrate availability continuously reshape the environment, reinforcing the heterogeneity in the population. This phenomenon, in which a cell population modifies its environment and is subsequently influenced by the resulting environmental changes, is referred to as environmental feedback[123].

Through this process, environmental feedback permits what is termed environmental escape: the possibility for a fraction of the population to avoid induction and maintain growth, even under strong selective pressure for expression. This escape prevents the collapse that would otherwise occur if all cells were induced simultaneously. The consequence of this mechanism is a fitness-entropy compensation effect, in which the reduced fitness of induced cells is counterbalanced by the survival and proliferation of non-induced cells. In practice, cells compensate for the fitness loss associated with recombinant protein production by generating entropy, that is, by diversifying into distinct subpopulations whose coexistence ensure population persistence (Figure 17A)[114,123]. Taken together, these results show that environmental feedback, by enabling environmental escape, emerges as a key driver of this fitness-entropy compensation mechanism, maintaining the viability of the culture under burdensome gene expression.

These findings highlight the importance of allowing a degree of environmental escape within the system to achieve better control over the population. Without such escape, the culture undergoes washout, making further regulation impossible. While heterogeneity is often perceived as detrimental in bioprocessing, the present results suggest that such diversity is not always negative. On the contrary, it can be strategically leveraged to sustain the population under burdensome recombinant protein production, as exemplified in this study.

5. Implications of the interactions between the cellular host, gene circuits and environmental conditions for the design of continuous bioprocesses

The chemostat culture conducted on glucose at 37°C provides clear evidence of the necessity to control population dynamics in systems employing burdensome gene circuits for recombinant protein production, as illustrated with *E. coli* BL21 (DE3). Such control is critical to ensure high and stable yields.

The results obtained in this study suggest that population dynamics emerge from the combined effects of the genetic circuit, the host population, and the surrounding environment. According to the theory of switching cost, the host's genetic circuits directly shape population dynamics through the metabolic burden they impose on individual cells. Indeed, non-burdensome gene circuits tend to generate more homogeneous expression patterns, whereas burdensome gene circuits result in heterogeneous recombinant protein production[109]. In turn, the cell population both influences and is influenced by the environment through environmental feedback, which can drive environmental escape. The environment also acts on the genetic circuits through history-dependent effects and environmental feedback, further modulating expression and population dynamics over time (Figure 23).

These interactions highlight how continuous cultures can be influenced by multiple interconnected factors, including switching cost, history dependence, and environmental escape. Considering these parameters together may offer valuable insights into the mechanisms underlying heterogeneity in such systems and help identify approaches that could improve long-term stability and productivity.

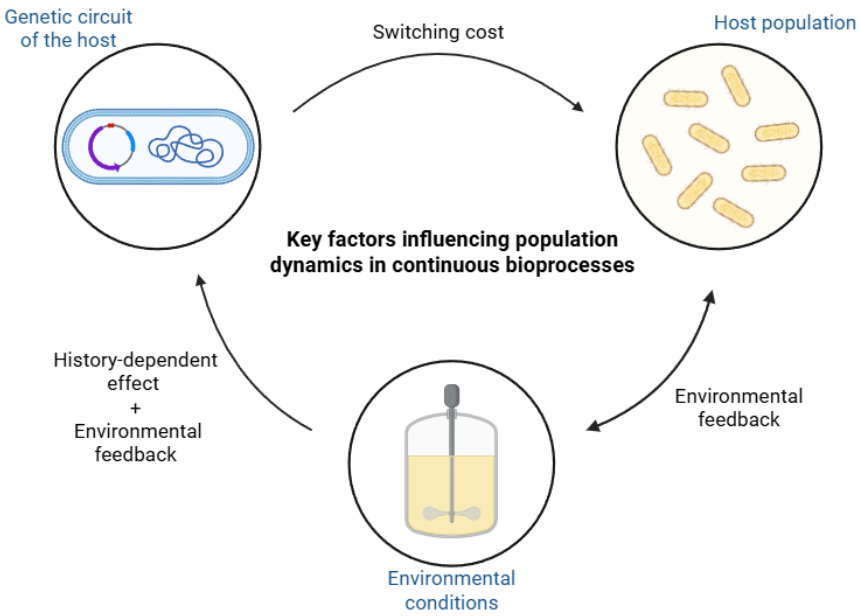

FIGURE 23: ILLUSTRATION OF THE INTERPLAY BETWEEN GENETIC CIRCUIT, HOST POPULATION, AND ENVIRONMENTAL CONDITIONS SHAPING THE STABILITY AND PERFORMANCE OF CONTINUOUS CULTURES.

Switching cost, environmental feedback, and history dependent effects form a dynamic feedback loop that governs population dynamics and culture stability.

Conclusion and perspectives

In conclusion, this work assessed the population dynamics of *E. coli* BL21 (DE3) carrying a burdensome T7-based recombinant expression system during long-term chemostat cultivations. The population dynamics were monitored using an automated flow cytometry to assess phenotypic heterogeneity at the single-cell level under different environmental conditions. The control strategies tested here were based on the assumption that decreasing the strain's maximal growth rate, either by modifying the carbon source or by lowering the temperature, would reduce the switching cost and promote population homogenisation. However, the results obtained indicate that this approach alone was insufficient to achieve the desired effect in continuous culture.

The observations made throughout this study highlight that switching cost, although an important parameter as described by Henrion et al. (2024), is not the only factor to consider when designing control strategies for continuous bioprocesses. Additional components, such as culture history and the potential for environmental escape enabling fitness-entropy compensation, appear to play a decisive role. These mechanisms underlying cell population diversification have fundamental implications for the experimental set-up. While five residence times are typically considered sufficient to reach steady state in chemostat cultures, our results indicate that this assumption does not hold for burdensome expression systems. Without adequate control strategies, population stability may never be achieved, which challenges the general applicability of this rule in the context of recombinant protein production.

The interplay between genetic circuit, host physiology, and environment creates a feedback loop that shapes population dynamics and underscores the need to reconsider how continuous cultures are designed and controlled. Particular attention should be given to the key parameters identified in this study, including switching cost, history dependence, and environmental escape. Understanding and managing these interactions is critical for designing robust bioprocesses capable of maintaining high productivity and stability over extended cultivation periods.

From an industrial perspective, process design strategies could be strengthened by complementing traditional process engineering parameters, such as dilution rates and bioreactor volume, with dynamic control approaches. These approaches should account for host-circuit-environment interactions and be supported by real-time cell monitoring.

The findings of this study open up several directions for future research. Regarding the system itself, the T5 promoter system could be considered as an alternative expression system to the T7 RNAP. Indeed, the T5 system retains high expression efficiency while imposing a lower metabolic burden which could potentially reduce selective pressure and promote better population homogenisation. Another option would be to consider dynamic and adaptive control methods, such as adaptive laboratory evolution (ALE), starting from pre-adapted mutant populations, which could help cultures self-adjust to environmental pressure and improve long-term stability. Such strategies may allow the selection of mutants with enhanced robustness while maintaining productivity.

In addition, the role of environmental escape also requires close attention. In this study, lactose was used as the inducer, allowing a fraction of the population to evade induction, partly due to catabolite repression. Testing a non-metabolizable inducer (other than IPTG, which presents previously discussed

limitations), such as the methyl-β-D-thiogalactopyranoside (TMG), could provide a clearer understanding of the mechanisms conditioning environmental escape. This may reduce or eliminate escape routes and offer insight into how changes in induction affect population dynamics, stability, and productivity. Additionally, identifying carbon sources that enable a controlled degree of environmental escape while lowering the switching cost could provide a balance between flexibility and robustness in long-term production.

Finally, applying these experimental approaches to the production of more complex and industrially relevant proteins, such as proinsulin, would help determine whether the key parameters identified here remain critical in systems with greater folding, processing, and metabolic requirements. Comparing the population dynamics and stability between GFP and such complex products would help assess the generality of the present findings and refine control strategies for real industrial applications.

This work highlights the multifactorial nature of population heterogeneity in continuous cultures employing burdensome gene circuits. Moving towards integrated, systemic, and dynamically managed strategies will be essential to unlock the full potential of continuous recombinant protein production. Coupled with real-time single-cell monitoring, such approaches could enable the rational design of continuous processes that remain both productive and stable over extended periods, thereby enhancing their industrial applicability.

Bibliography

(1) Medeiros Garcia Alcântara, J.; Sponchioni, M. Chapter One - Evolution and Design of Continuous Bioreactors for the Production of Biological Products. In *Advances in Chemical Engineering*; Moscatelli, D., Sponchioni, M., Eds.; Process Intensification in the Manufacturing of Biotherapeutics; Academic Press, 2022; Vol. 59, pp 1–26. https://doi.org/10.1016/bs.ache.2022.03.001.

(2) Choi, J. H.; Keum, K. C.; Lee, S. Y. Production of Recombinant Proteins by High Cell Density Culture of *Escherichia Coli*. *Chem. Eng. Sci.* 2006, *61* (3), 876–885. https://doi.org/10.1016/j.ces.2005.03.031.

(3) Xie, D. Continuous Biomanufacturing with Microbes — Upstream Progresses and Challenges. *Curr. Opin. Biotechnol.* 2022, *78*, 102793. https://doi.org/10.1016/j.copbio.2022.102793.

(4) Jayakrishnan, A.; Wan Rosli, W. R.; Tahir, A. R. M.; Razak, F. S. A.; Kee, P. E.; Ng, H. S.; Chew, Y.-L.; Lee, S.-K.; Ramasamy, M.; Tan, C. S.; Liew, K. B. Evolving Paradigms of Recombinant Protein Production in Pharmaceutical Industry: A Rigorous Review. *Sci* 2024, *6* (1), 9. https://doi.org/10.3390/sci6010009.

(5) Johnson, I. S. Human Insulin from Recombinant DNA Technology. *Science* 1983, *219* (4585), 632–637. https://doi.org/10.1126/science.6337396.

(6) Demain, A. L.; Vaishnav, P. Production of Recombinant Proteins by Microbes and Higher Organisms. *Biotechnol. Adv.* 2009, *27* (3), 297–306. https://doi.org/10.1016/j.biotechadv.2009.01.008.

(7) Silva, A. C. General Concepts. In *Biotechnology for Pharmaceutical Sciences: Concepts and Applications*; Silva, A. C., Ed.; Springer Nature Switzerland: Cham, 2024; pp 1–5. https://doi.org/10.1007/978-3-031-60061-6_1.

(8) Sanchez-Garcia, L.; Martín, L.; Mangues, R.; Ferrer-Miralles, N.; Vázquez, E.; Villaverde, A. Recombinant Pharmaceuticals from Microbial Cells: A 2015 Update. *Microb. Cell Factories* 2016, *15* (1), 33. https://doi.org/10.1186/s12934-016-0437-3.

(9) Süntar, I.; Çetinkaya, S.; Haydaroğlu, Ü. S.; Habtemariam, S. Bioproduction Process of Natural Products and Biopharmaceuticals: Biotechnological Aspects. *Biotechnol. Adv.* 2021, *50*, 107768. https://doi.org/10.1016/j.biotechadv.2021.107768.

(10) Graumann, K.; Premstaller, A. Manufacturing of Recombinant Therapeutic Proteins in Microbial Systems. *Biotechnol. J.* 2006, *1* (2), 164–186. https://doi.org/10.1002/biot.200500051.

(11) Matanguihan, C.; Wu, P. Upstream Continuous Processing: Recent Advances in Production of Biopharmaceuticals and Challenges in Manufacturing. *Curr. Opin. Biotechnol.* 2022, *78*, 102828. https://doi.org/10.1016/j.copbio.2022.102828.

(12) Kager, J.; Bartlechner, J.; Herwig, C.; Jakubek, S. Direct Control of Recombinant Protein Production Rates in *E. Coli* Fed-Batch Processes by Nonlinear Feedback Linearization. *Chem. Eng. Res. Des.* 2022, *182*, 290–304. https://doi.org/10.1016/j.cherd.2022.03.043.

(13) Dewasme, L.; Coutinho, D.; Wouwer, A. V. Adaptive and Robust Linearizing Control Strategies for Fed-Batch Cultures of Microorganisms Exhibiting Overflow Metabolism. In *Informatics in Control, Automation and Robotics*; Cetto, J. A., Ferrier, J.-L., Filipe, J., Eds.; Springer: Berlin, Heidelberg, 2011; pp 283–305. https://doi.org/10.1007/978-3-642-19539-6_19.

(14) Kopp, J.; Slouka, C.; Spadiut, O.; Herwig, C. The Rocky Road From Fed-Batch to Continuous Processing With *E. Coli. Front. Bioeng. Biotechnol.* 2019, *7*. https://doi.org/10.3389/fbioe.2019.00328.

(15) Kaki, S. B.; Naga Prasad, A.; Chintagunta, A. D.; Dirisala, V. R.; Sampath Kumar, N. S.; Naidu, S. J. K.; Ramesh, B. Industrial Scale Production of Recombinant Human Insulin Using *Escherichia Coli* BL-21. *Iran. J. Sci. Technol. Trans. Sci.* 2022, *46* (2), 373–383. https://doi.org/10.1007/s40995-022-01269-7.

(16) Drobnjakovic, M.; Hart, R.; Kulvatunyou, B. (Serm); Ivezic, N.; Srinivasan, V. Current Challenges and Recent Advances on the Path towards Continuous Biomanufacturing. *Biotechnol. Prog.* 2023, *39* (6), e3378. https://doi.org/10.1002/btpr.3378.

(17) Kopp, J.; Kittler, S.; Slouka, C.; Herwig, C.; Spadiut, O.; Wurm, D. J. Repetitive Fed-Batch: A Promising Process Mode for Biomanufacturing With *E. Coli. Front. Bioeng. Biotechnol.* 2020, *8*. https://doi.org/10.3389/fbioe.2020.573607.

(18) Slouka, C.; Kopp, J.; Hutwimmer, S.; Strahammer, M.; Strohmer, D.; Eitenberger, E.; Schwaighofer, A.; Herwig, C. Custom Made Inclusion Bodies: Impact of Classical Process Parameters and Physiological Parameters on Inclusion Body Quality Attributes. *Microb. Cell Factories* 2018, *17* (1), 148. https://doi.org/10.1186/s12934-018-0997-5.

(19) Gresham, D.; Hong, J. The Functional Basis of Adaptive Evolution in Chemostats. *FEMS Microbiol. Rev.* 2015, *39* (1), 2–16. https://doi.org/10.1111/1574-6976.12082.

(20) Kittler, S.; Slouka, C.; Pell, A.; Lamplot, R.; Besleaga, M.; Ablasser, S.; Herwig, C.; Spadiut, O.; Kopp, J. Cascaded Processing Enables Continuous Upstream Processing with *E. Coli* BL21(DE3). *Sci. Rep.* 2021, *11* (1), 11477. https://doi.org/10.1038/s41598-021-90899-9.

(21) Niazi, S. K. Continuous Manufacturing of Recombinant Drugs: Comprehensive Analysis of Cost Reduction Strategies, Regulatory Pathways, and Global Implementation. *Pharmaceuticals* 2025, *18* (8), 1157. https://doi.org/10.3390/ph18081157.

(22) Glaser, J. A. Continuous Chemical Production Processes. *Clean Technol. Environ. Policy* 2015, *17* (2), 309–316. https://doi.org/10.1007/s10098-015-0903-3.

(23) Kralisch, D.; Hessler, N.; Klemm, D.; Erdmann, R.; Schmidt, W. White Biotechnology for Cellulose Manufacturing—The HoLiR Concept. *Biotechnol. Bioeng.* 2010, *105* (4), 740–747. https://doi.org/10.1002/bit.22579.

(24) Luttmann, R.; Borchert, S.-O.; Mueller, C.; Loegering, K.; Aupert, F.; Weyand, S.; Kober, C.; Faber, B.; Cornelissen, G. Sequential/Parallel Production of Potential Malaria Vaccines – A Direct Way from Single Batch to Quasi-Continuous Integrated Production. *J. Biotechnol.* 2015, *213*, 83–96. https://doi.org/10.1016/j.jbiotec.2015.02.022.

(25) Khanal, O.; and Lenhoff, A. M. Developments and Opportunities in Continuous Biopharmaceutical Manufacturing. *mAbs* 2021, *13* (1), 1903664. https://doi.org/10.1080/19420862.2021.1903664.

(26) Snoeck, S.; Guidi, C.; De Mey, M. "Metabolic Burden" Explained: Stress Symptoms and Its Related Responses Induced by (over)Expression of (Heterologous) Proteins in *Escherichia Coli. Microb. Cell Factories* 2024, *23* (1), 96. https://doi.org/10.1186/s12934-024-02370-9.

(27) Rugbjerg, P.; Sommer, M. O. A. Overcoming Genetic Heterogeneity in Industrial Fermentations. *Nat. Biotechnol.* 2019, *37* (8), 869–876. https://doi.org/10.1038/s41587-019-0171-6.

(28) Ackermann, M. A Functional Perspective on Phenotypic Heterogeneity in Microorganisms. *Nat. Rev. Microbiol.* 2015, *13* (8), 497–508. https://doi.org/10.1038/nrmicro3491.

(29) Glick, B. R. Metabolic Load and Heterologous Gene Expression. *Biotechnol. Adv.* 1995, *13* (2), 247–261. https://doi.org/10.1016/0734-9750(95)00004-A.

(30) Wu, G.; Yan, Q.; Jones, J. A.; Tang, Y. J.; Fong, S. S.; Koffas, M. A. G. Metabolic Burden: Cornerstones in Synthetic Biology and Metabolic Engineering Applications. *Trends Biotechnol.* 2016, *34* (8), 652–664. https://doi.org/10.1016/j.tibtech.2016.02.010.

(31) Mao, J.; Zhang, H.; Chen, Y.; Wei, L.; Liu, J.; Nielsen, J.; Chen, Y.; Xu, N. Relieving Metabolic Burden to Improve Robustness and Bioproduction by Industrial Microorganisms. *Biotechnol. Adv.* 2024, *74*, 108401. https://doi.org/10.1016/j.biotechadv.2024.108401.

(32) Dana, A.; Tuller, T. The Effect of tRNA Levels on Decoding Times of mRNA Codons. *Nucleic Acids Res.* 2014, *42* (14), 9171–9181. https://doi.org/10.1093/nar/gku646.

(33) Borkowski, O.; Ceroni, F.; Stan, G.-B.; Ellis, T. Overloaded and Stressed: Whole-Cell Considerations for Bacterial Synthetic Biology. *Curr. Opin. Microbiol.* 2016, *33*, 123–130. https://doi.org/10.1016/j.mib.2016.07.009.

(34) Kurland, C.; Gallant, J. Errors of Heterologous Protein Expression. *Curr. Opin. Biotechnol.* 1996, *7* (5), 489–493. https://doi.org/10.1016/S0958-1669(96)80050-4.

(35) Wagner, S.; Baars, L.; Ytterberg, A. J.; Klussmeier, A.; Wagner, C. S.; Nord, O.; Nygren, P.-Å.; Wijk, K. J. van; Gier, J.-W. de. Consequences of Membrane Protein Overexpression in *Escherichia Coli**. *Mol. Cell. Proteomics* 2007, *6* (9), 1527–1550. https://doi.org/10.1074/mcp.M600431-MCP200.

(36) Kittler, S.; Kopp, J.; Veelenturf, P. G.; Spadiut, O.; Delvigne, F.; Herwig, C.; Slouka, C. The Lazarus *Escherichia Coli* Effect: Recovery of Productivity on Glycerol/Lactose Mixed Feed in Continuous Biomanufacturing. *Front. Bioeng. Biotechnol.* 2020, *8*. https://doi.org/10.3389/fbioe.2020.00993.

(37) Peebo, K.; Neubauer, P. Application of Continuous Culture Methods to Recombinant Protein Production in Microorganisms. *Microorganisms* 2018, *6* (3), 56. https://doi.org/10.3390/microorganisms6030056.

(38) Zhang, Z.-X.; Nong, F.-T.; Wang, Y.-Z.; Yan, C.-X.; Gu, Y.; Song, P.; Sun, X.-M. Strategies for Efficient Production of Recombinant Proteins in *Escherichia Coli*: Alleviating the Host Burden and Enhancing Protein Activity. *Microb. Cell Factories* 2022, *21* (1), 191. https://doi.org/10.1186/s12934-022-01917-y.

(39) Wagner, S.; Klepsch, M. M.; Schlegel, S.; Appel, A.; Draheim, R.; Tarry, M.; Högbom, M.; van Wijk, K. J.; Slotboom, D. J.; Persson, J. O.; de Gier, J.-W. Tuning *Escherichia Coli* for Membrane Protein Overexpression. *Proc. Natl. Acad. Sci.* 2008, *105* (38), 14371–14376. https://doi.org/10.1073/pnas.0804090105.

(40) Du, F.; Liu, Y.-Q.; Xu, Y.-S.; Li, Z.-J.; Wang, Y.-Z.; Zhang, Z.-X.; Sun, X.-M. Regulating the T7 RNA Polymerase Expression in *E. Coli* BL21 (DE3) to Provide More Host Options for Recombinant Protein Production. *Microb. Cell Factories* 2021, *20* (1), 189. https://doi.org/10.1186/s12934-021-01680-6.

(41) Tan, S.-I.; Ng, I.-S. New Insight into Plasmid-Driven T7 RNA Polymerase in *Escherichia Coli* and Use as a Genetic Amplifier for a Biosensor. *ACS Synth. Biol.* 2020, *9* (3), 613–622. https://doi.org/10.1021/acssynbio.9b00466.

(42) Jeong, H.; Barbe, V.; Lee, C. H.; Vallenet, D.; Yu, D. S.; Choi, S.-H.; Couloux, A.; Lee, S.-W.; Yoon, S. H.; Cattolico, L.; Hur, C.-G.; Park, H.-S.; Ségurens, B.; Kim, S. C.; Oh, T. K.; Lenski, R. E.; Studier, F. W.; Daegelen, P.; Kim, J. F. Genome Sequences of *Escherichia Coli* B Strains REL606 and BL21(DE3). *J. Mol. Biol.* 2009, *394* (4), 644–652. https://doi.org/10.1016/j.jmb.2009.09.052.

(43) Hausjell, J.; Weissensteiner, J.; Molitor, C.; Halbwirth, H.; Spadiut, O. *E. Coli* HMS174(DE3) Is a Sustainable Alternative to BL21(DE3). *Microb. Cell Factories* 2018, *17* (1), 169. https://doi.org/10.1186/s12934-018-1016-6.

(44) Wurm, D. J.; Veiter, L.; Ulonska, S.; Eggenreich, B.; Herwig, C.; Spadiut, O. The *E. Coli* pET Expression System Revisited—Mechanistic Correlation between Glucose and Lactose Uptake. *Appl. Microbiol. Biotechnol.* 2016, *100* (20), 8721–8729. https://doi.org/10.1007/s00253-016-7620-7.

(45) Dvorak, P.; Chrast, L.; Nikel, P. I.; Fedr, R.; Soucek, K.; Sedlackova, M.; Chaloupkova, R.; de Lorenzo, V.; Prokop, Z.; Damborsky, J. Exacerbation of Substrate Toxicity by IPTG in *Escherichia Coli* BL21(DE3) Carrying a Synthetic Metabolic Pathway. *Microb. Cell Factories* 2015, *14* (1), 201. https://doi.org/10.1186/s12934-015-0393-3.

(46) Briand, L.; Marcion, G.; Kriznik, A.; Heydel, J. M.; Artur, Y.; Garrido, C.; Seigneuric, R.; Neiers, F. A Self-Inducible Heterologous Protein Expression System in *Escherichia Coli*. *Sci. Rep.* 2016, *6* (1), 33037. https://doi.org/10.1038/srep33037.

(47) Novagen. pET System Manual, 2003. https://kirschner.med.harvard.edu/files/protocols/Novagen_petsystem.pdf (accessed 2025-07-24).

(48) Beselin, A. Optimization of Lipase Production in Burkholderia Glumae, Ruhr-Universität Bochum, Faculty of Biology, International Graduate School of Biosciences, 2005. https://www.researchgate.net/publication/40536223_Optimization_of_lipase_production_in_Burkholderia_glumae (accessed 2025-07-24).

(49) Studier, F. W.; Moffatt, B. A. Use of Bacteriophage T7 RNA Polymerase to Direct Selective High-Level Expression of Cloned Genes. *J. Mol. Biol.* 1986, *189* (1), 113–130. https://doi.org/10.1016/0022-2836(86)90385-2.

(50) Schuster, L. A.; Reisch, C. R. Plasmids for Controlled and Tunable High-Level Expression in *E. Coli.* *Appl. Environ. Microbiol.* 2022, *88* (22), e00939-22. https://doi.org/10.1128/aem.00939-22.

(51) Vethanayagam, J. G.; Flower, A. M. Decreased Gene Expression from T7 Promoters May Be Due to Impaired Production of Active T7 RNA Polymerase. *Microb. Cell Factories* 2005, *4* (1), 1–7. https://doi.org/10.1186/1475-2859-4-3.

(52) Ryall, B.; Eydallin, G.; Ferenci, T. Culture History and Population Heterogeneity as Determinants of Bacterial Adaptation: The Adaptomics of a Single Environmental Transition. *Microbiol. Mol. Biol. Rev.* 2012, *76* (3), 597–625. https://doi.org/10.1128/mmbr.05028-11.

(53) Drake, J. W.; Charlesworth, B.; Charlesworth, D.; Crow, J. F. Rates of Spontaneous Mutation. *Genetics* 1998, *148* (4), 1667–1686. https://doi.org/10.1093/genetics/148.4.1667.

(54) Imhof, M.; Schlötterer, C. Fitness Effects of Advantageous Mutations in Evolving *Escherichia Coli* Populations. *Proc. Natl. Acad. Sci.* 2001, *98* (3), 1113–1117. https://doi.org/10.1073/pnas.98.3.1113.

(55) Perfeito, L.; Fernandes, L.; Mota, C.; Gordo, I. Adaptive Mutations in Bacteria: High Rate and Small Effects. *Science* 2007, *317* (5839), 813–815. https://doi.org/10.1126/science.1142284.

(56) Hastings, P. J. Adaptive Amplification. *Crit. Rev. Biochem. Mol. Biol.* 2007, *42* (4), 271–283. https://doi.org/10.1080/10409230701507757.

(57) Sandegren, L.; Andersson, D. I. Bacterial Gene Amplification: Implications for the Evolution of Antibiotic Resistance. *Nat. Rev. Microbiol.* 2009, *7* (8), 578–588. https://doi.org/10.1038/nrmicro2174.

(58) Moxon, R.; Bayliss, C.; Hood, D. Bacterial Contingency Loci: The Role of Simple Sequence DNA Repeats in Bacterial Adaptation. *Annu. Rev. Genet.* 2006, *40* (Volume 40, 2006), 307–333. https://doi.org/10.1146/annurev.genet.40.110405.090442.

(59) Chen, F.; Liu, W.-Q.; Liu, Z.-H.; Zou, Q.-H.; Wang, Y.; Li, Y.-G.; Zhou, J.; Eisenstark, A.; Johnston, R. N.; Liu, G.-R.; Yang, B.-F.; Liu, S.-L. mutL as a Genetic Switch of Bacterial Mutability: Turned on or off through Repeat Copy Number Changes. *FEMS Microbiol. Lett.* 2010, *312* (2), 126–132. https://doi.org/10.1111/j.1574-6968.2010.02107.x.

(60) Mahillon, J.; Chandler, M. Insertion Sequences. *Microbiol. Mol. Biol. Rev.* 1998, *62* (3), 725–774. https://doi.org/10.1128/mmbr.62.3.725-774.1998.

(61) Gaffé, J.; McKenzie, C.; Maharjan, R. P.; Coursange, E.; Ferenci, T.; Schneider, D. Insertion Sequence-Driven Evolution of *Escherichia Coli* in Chemostats. *J. Mol. Evol.* 2011, *72* (4), 398–412. https://doi.org/10.1007/s00239-011-9439-2.

(62) Zhang, Z.; Saier Jr, M. H. A Mechanism of Transposon-Mediated Directed Mutation. *Mol. Microbiol.* 2009, *74* (1), 29–43. https://doi.org/10.1111/j.1365-2958.2009.06831.x.

(63) Notley-McRobb, L.; Seeto, S.; Ferenci, T. Enrichment and Elimination of mutY Mutators in *Escherichia Coli* Populations. *Genetics* 2002, *162* (3), 1055–1062. https://doi.org/10.1093/genetics/162.3.1055.

(64) Miller, J. H.; Suthar, A.; Tai, J.; Yeung, A.; Truong, C.; Stewart, J. L. Direct Selection for Mutators in *Escherichia Coli*. *J. Bacteriol.* 1999, *181* (5), 1576–1584. https://doi.org/10.1128/jb.181.5.1576-1584.1999.

(65) Matic, I.; Rayssiguier, C.; Radman, M. Interspecies Gene Exchange in Bacteria: The Role of SOS and Mismatch Repair Systems in Evolution of Species. *Cell* 1995, *80* (3), 507–515. https://doi.org/10.1016/0092-8674(95)90501-4.

(66) Foster, P. L. Stress-Induced Mutagenesis in Bacteria. *Crit. Rev. Biochem. Mol. Biol.* 2007, *42* (5), 373–397. https://doi.org/10.1080/10409230701648494.

(67) Bjedov, I.; Tenaillon, O.; Gérard, B.; Souza, V.; Denamur, E.; Radman, M.; Taddei, F.; Matic, I. Stress-Induced Mutagenesis in Bacteria. *Science* 2003, *300* (5624), 1404–1409. https://doi.org/10.1126/science.1082240.

(68) Zhaxybayeva, O.; Doolittle, W. F. Lateral Gene Transfer. *Curr. Biol.* 2011, *21* (7), R242–R246. https://doi.org/10.1016/j.cub.2011.01.045.

(69) Wegrzyn, G.; Wegrzyn, A. Stress Responses and Replication of Plasmids in Bacterial Cells. *Microb. Cell Factories* 2002, *1* (1), 2. https://doi.org/10.1186/1475-2859-1-2.

(70) Rokney, A.; Kobiler, O.; Amir, A.; Court, D. L.; Stavans, J.; Adhya, S.; Oppenheim, A. B. Host Responses Influence on the Induction of Lambda Prophage. *Mol. Microbiol.* 2008, *68* (1), 29–36. https://doi.org/10.1111/j.1365-2958.2008.06119.x.

(71) Le Gac, M.; Brazas, M. D.; Bertrand, M.; Tyerman, J. G.; Spencer, C. C.; Hancock, R. E. W.; Doebeli, M. Metabolic Changes Associated With Adaptive Diversification in *Escherichia Coli*. *Genetics* 2008, *178* (2), 1049–1060. https://doi.org/10.1534/genetics.107.082040.

(72) Gudelj, I.; Weitz, J. S.; Ferenci, T.; Claire Horner-Devine, M.; Marx, C. J.; Meyer, J. R.; Forde, S. E. An Integrative Approach to Understanding Microbial Diversity: From Intracellular Mechanisms to Community Structure. *Ecol. Lett.* 2010, *13* (9), 1073–1084. https://doi.org/10.1111/j.1461-0248.2010.01507.x.

(73) Heins, A.-L.; Weuster-Botz, D. Population Heterogeneity in Microbial Bioprocesses: Origin, Analysis, Mechanisms, and Future Perspectives. *Bioprocess Biosyst. Eng.* 2018, *41* (7), 889–916. https://doi.org/10.1007/s00449-018-1922-3.

(74) Schlüter, J.-P.; Czuppon, P.; Schauer, O.; Pfaffelhuber, P.; McIntosh, M.; Becker, A. Classification of Phenotypic Subpopulations in Isogenic Bacterial Cultures by Triple Promoter Probing at Single Cell Level. *J. Biotechnol.* 2015, *198*, 3–14. https://doi.org/10.1016/j.jbiotec.2015.01.021.

(75) Delvigne, F.; Zune, Q.; Lara, A. R.; Al-Soud, W.; Sørensen, S. J. Metabolic Variability in Bioprocessing: Implications of Microbial Phenotypic Heterogeneity. *Trends Biotechnol.* 2014, *32* (12), 608–616. https://doi.org/10.1016/j.tibtech.2014.10.002.

(76) Delvigne, F.; Goffin, P. Microbial Heterogeneity Affects Bioprocess Robustness: Dynamic Single-Cell Analysis Contributes to Understanding of Microbial Populations. *Biotechnol. J.* 2014, *9* (1), 61–72. https://doi.org/10.1002/biot.201300119.

(77) David, F.; Berger, A.; Hänsch, R.; Rohde, M.; Franco-Lara, E. Single Cell Analysis Applied to Antibody Fragment Production with *Bacillus Megaterium*: Development of Advanced Physiology and Bioprocess State Estimation Tools. *Microb. Cell Factories* 2011, *10* (1), 23. https://doi.org/10.1186/1475-2859-10-23.

(78) Xiao, Y.; Bowen, C. H.; Liu, D.; Zhang, F. Exploiting Nongenetic Cell-to-Cell Variation for Enhanced Biosynthesis. *Nat. Chem. Biol.* 2016, *12* (5), 339–344. https://doi.org/10.1038/nchembio.2046.

(79) Bandiera, L.; Furini, S.; Giordano, E. Phenotypic Variability in Synthetic Biology Applications: Dealing with Noise in Microbial Gene Expression. *Front. Microbiol.* 2016, *7*. https://doi.org/10.3389/fmicb.2016.00479.

(80) Liu, J.; François, J.-M.; Capp, J.-P. Use of Noise in Gene Expression as an Experimental Parameter to Test Phenotypic Effects. *Yeast* 2016, *33* (6), 209–216. https://doi.org/10.1002/yea.3152.

(81) Silander, O. K.; Nikolic, N.; Zaslaver, A.; Bren, A.; Kikoin, I.; Alon, U.; Ackermann, M. A Genome-Wide Analysis of Promoter-Mediated Phenotypic Noise in *Escherichia Coli*. *PLOS Genet.* 2012, *8* (1), e1002443. https://doi.org/10.1371/journal.pgen.1002443.

(82) Delvigne, F.; Baert, J.; Sassi, H.; Fickers, P.; Grünberger, A.; Dusny, C. Taking Control over Microbial Populations: Current Approaches for Exploiting Biological Noise in Bioprocesses. *Biotechnol. J.* 2017, *12* (7), 1600549. https://doi.org/10.1002/biot.201600549.

(83) Klumpp, S.; Scott, M.; Pedersen, S.; Hwa, T. Molecular Crowding Limits Translation and Cell Growth. *Proc. Natl. Acad. Sci.* 2013, *110* (42), 16754–16759. https://doi.org/10.1073/pnas.1310377110.

(84) Levy, S. F. Cellular Heterogeneity: Benefits Besides Bet-Hedging. *Curr. Biol.* 2016, *26* (9), R355–R357. https://doi.org/10.1016/j.cub.2016.03.034.

(85) de Jong, I. G.; Haccou, P.; Kuipers, O. P. Bet Hedging or Not? A Guide to Proper Classification of Microbial Survival Strategies. *BioEssays* 2011, *33* (3), 215–223. https://doi.org/10.1002/bies.201000127.

(86) Sánchez-Romero, M. A.; Casadesús, J. Contribution of Phenotypic Heterogeneity to Adaptive Antibiotic Resistance. *Proc. Natl. Acad. Sci.* 2014, *111* (1), 355–360. https://doi.org/10.1073/pnas.1316084111.

(87) Acar, M.; Mettetal, J. T.; van Oudenaarden, A. Stochastic Switching as a Survival Strategy in Fluctuating Environments. *Nat. Genet.* 2008, *40* (4), 471–475. https://doi.org/10.1038/ng.110.

(88) Davidson, F. A.; Seon-Yi, C.; Stanley-Wall, N. R. Selective Heterogeneity in Exoprotease Production by *Bacillus Subtilis*. *PLOS ONE* **2012**, *7* (6), e38574. https://doi.org/10.1371/journal.pone.0038574.

(89) Grimbergen, A. J.; Siebring, J.; Solopova, A.; Kuipers, O. P. Microbial Bet-Hedging: The Power of Being Different. *Curr. Opin. Microbiol.* **2015**, *25*, 67–72. https://doi.org/10.1016/j.mib.2015.04.008.

(90) Amato, S. M.; Brynildsen, M. P. Persister Heterogeneity Arising from a Single Metabolic Stress. *Curr. Biol.* **2015**, *25* (16), 2090–2098. https://doi.org/10.1016/j.cub.2015.06.034.

(91) Reuven, P.; Eldar, A. Macromotives and Microbehaviors: The Social Dimension of Bacterial Phenotypic Variability. *Curr. Opin. Genet. Dev.* **2011**, *21* (6), 759–767. https://doi.org/10.1016/j.gde.2011.09.011.

(92) Wang, X.; Kang, Y.; Luo, C.; Zhao, T.; Liu, L.; Jiang, X.; Fu, R.; An, S.; Chen, J.; Jiang, N.; Ren, L.; Wang, Q.; Baillie, J. K.; Gao, Z.; Yu, J. Heteroresistance at the Single-Cell Level: Adapting to Antibiotic Stress through a Population-Based Strategy and Growth-Controlled Interphenotypic Coordination. *mBio* **2014**, *5* (1), 10.1128/mbio.00942-13. https://doi.org/10.1128/mbio.00942-13.

(93) Adams, D. G. Heterocyst Formation in Cyanobacteria. *Curr. Opin. Microbiol.* **2000**, *3* (6), 618–624. https://doi.org/10.1016/S1369-5274(00)00150-8.

(94) Müller, S.; Harms, H.; Bley, T. Origin and Analysis of Microbial Population Heterogeneity in Bioprocesses. *Curr. Opin. Biotechnol.* **2010**, *21* (1), 100–113. https://doi.org/10.1016/j.copbio.2010.01.002.

(95) Lara, A. R.; Galindo, E.; Ramírez, O. T.; Palomares, L. A. Living with Heterogeneities in Bioreactors: Understanding the Effects of Environmental Gradients on Cells. *Mol. Biotechnol.* **2006**, *34* (3), 355–381. https://doi.org/10.1385/MB:34:3:355.

(96) Becker, L.; Sturm, J.; Eiden, F.; Holtmann, D. Analyzing and Understanding the Robustness of Bioprocesses. *Trends Biotechnol.* **2023**, *41* (8), 1013–1026. https://doi.org/10.1016/j.tibtech.2023.03.002.

(97) Heins, A.-L.; Hoang, M. D.; Weuster-Botz, D. Advances in Automated Real-Time Flow Cytometry for Monitoring of Bioreactor Processes. *Eng. Life Sci.* **2022**, *22* (3–4), 260–278. https://doi.org/10.1002/elsc.202100082.

(98) Adan, A.; Alizada, G.; Kiraz, Y.; Baran, Y.; Nalbant, A. Flow Cytometry: Basic Principles and Applications. *Crit. Rev. Biotechnol.* **2017**, *37* (2), 163–176. https://doi.org/10.3109/07388551.2015.1128876.

(99) Austin Suthanthiraraj, P. P.; Graves, S. W. Fluidics. *Curr. Protoc. Cytom.* **2013**, *65* (1), 1.2.1-1.2.14. https://doi.org/10.1002/0471142956.cy0102s65.

(100) Broger, T.; Odermatt, R. P.; Huber, P.; Sonnleitner, B. Real-Time on-Line Flow Cytometry for Bioprocess Monitoring. *J. Biotechnol.* **2011**, *154* (4), 240–247. https://doi.org/10.1016/j.jbiotec.2011.05.003.

(101) Zhao, R.; Natarajan, A.; Srienc, F. A Flow Injection Flow Cytometry System for On-Line Monitoring of Bioreactors. *Biotechnol. Bioeng.* 1999, *62* (5), 609–617. https://doi.org/10.1002/(SICI)1097-0290(19990305)62:5<609::AID-BIT13>3.0.CO;2-C.

(102) Rieseberg, M.; Kasper, C.; Reardon, K. F.; Scheper, T. Flow Cytometry in Biotechnology. *Appl. Microbiol. Biotechnol.* 2001, *56* (3), 350–360. https://doi.org/10.1007/s002530100673.

(103) McKinnon, K. M. Flow Cytometry: An Overview. *Curr. Protoc. Immunol.* 2018, *120*, 5.1.1-5.1.11. https://doi.org/10.1002/cpim.40.

(104) Hamnett, R. *The Complete Flow Cytometry & FACS Technique Guide.* https://www.antibodies.com/applications/flow-cytometry (accessed 2025-07-25).

(105) Brognaux, A.; Han, S.; Sørensen, S. J.; Lebeau, F.; Thonart, P.; Delvigne, F. A Low-Cost, Multiplexable, Automated Flow Cytometry Procedure for the Characterization of Microbial Stress Dynamics in Bioreactors. *Microb. Cell Factories* 2013, *12*, 100. https://doi.org/10.1186/1475-2859-12-100.

(106) Heins, A.-L.; Johanson, T.; Han, S.; Lundin, L.; Carlquist, M.; Gernaey, K. V.; Sørensen, S. J.; Eliasson Lantz, A. Quantitative Flow Cytometry to Understand Population Heterogeneity in Response to Changes in Substrate Availability in *Escherichia Coli* and *Saccharomyces Cerevisiae* Chemostats. *Front. Bioeng. Biotechnol.* 2019, *7*. https://doi.org/10.3389/fbioe.2019.00187.

(107) Arnoldini, M.; Heck, T.; Blanco-Fernández, A.; Hammes, F. Monitoring of Dynamic Microbiological Processes Using Real-Time Flow Cytometry. *PLOS ONE* 2013, *8* (11), e80117. https://doi.org/10.1371/journal.pone.0080117.

(108) Buysschaert, B.; Kerckhof, F.-M.; Vandamme, P.; De Baets, B.; Boon, N. Flow Cytometric Fingerprinting for Microbial Strain Discrimination and Physiological Characterization. *Cytometry A* 2018, *93* (2), 201–212. https://doi.org/10.1002/cyto.a.23302.

(109) Henrion, L.; Martinez, J. A.; Vandenbroucke, V.; Delvenne, M.; Telek, S.; Zicler, A.; Grünberger, A.; Delvigne, F. Fitness Cost Associated with Cell Phenotypic Switching Drives Population Diversification Dynamics and Controllability. *Nat. Commun.* 2023, *14* (1), 6128. https://doi.org/10.1038/s41467-023-41917-z.

(110) Kacmar, J.; Gilbert, A.; Cockrell, J.; Srienc, F. The Cytostat: A New Way to Study Cell Physiology in a Precisely Defined Environment. *J. Biotechnol.* 2006, *126* (2), 163–172. https://doi.org/10.1016/j.jbiotec.2006.04.015.

(111) Sassi, H.; Nguyen, T. M.; Telek, S.; Gosset, G.; Grünberger, A.; Delvigne, F. Segregostat: A Novel Concept to Control Phenotypic Diversification Dynamics on the Example of Gram-Negative Bacteria. *Microb. Biotechnol.* 2019, *12* (5), 1064–1075. https://doi.org/10.1111/1751-7915.13442.

(112) Shannon, C. E. A Mathematical Theory of Communication. *Bell Syst. Tech. J.* 1948, *27* (3), 379–423. https://doi.org/10.1002/j.1538-7305.1948.tb01338.x.

(113) Bowsher, C. G.; Swain, P. S. Environmental Sensing, Information Transfer, and Cellular Decision-Making. *Curr. Opin. Biotechnol.* 2014, *28*, 149–155. https://doi.org/10.1016/j.copbio.2014.04.010.

(114) Henrion, L.; Vandenbroucke, V.; Martinez, J. A.; Kopp, J.; Telek, S.; Zicler, A.; Delvigne, F. Lowering the Switching Cost Related to the Activation of Burdensome Gene Circuits Promotes Cell Population Homogeneity and Productivity. bioRxiv October 16, 2024, p 2024.10.14.618176. https://doi.org/10.1101/2024.10.14.618176.

(115) Eigenfeld, M.; Schwaminger, S. P. Cellular Variability as a Driver for Bioprocess Innovation and Optimization. *Biotechnol. Adv.* 2025, *79*, 108528. https://doi.org/10.1016/j.biotechadv.2025.108528.

(116) Delvigne, F.; Martinez, J. A. Advances in Automated and Reactive Flow Cytometry for Synthetic Biotechnology. *Curr. Opin. Biotechnol.* 2023, *83*, 102974. https://doi.org/10.1016/j.copbio.2023.102974.

(117) Rullan, M.; Benzinger, D.; Schmidt, G. W.; Milias-Argeitis, A.; Khammash, M. An Optogenetic Platform for Real-Time, Single-Cell Interrogation of Stochastic Transcriptional Regulation. *Mol. Cell* 2018, *70* (4), 745-756.e6. https://doi.org/10.1016/j.molcel.2018.04.012.

(118) Milias-Argeitis, A.; Rullan, M.; Aoki, S. K.; Buchmann, P.; Khammash, M. Automated Optogenetic Feedback Control for Precise and Robust Regulation of Gene Expression and Cell Growth. *Nat. Commun.* 2016, *7* (1), 12546. https://doi.org/10.1038/ncomms12546.

(119) Aoki, S. K.; Lillacci, G.; Gupta, A.; Baumschlager, A.; Schweingruber, D.; Khammash, M. A Universal Biomolecular Integral Feedback Controller for Robust Perfect Adaptation. *Nature* 2019, *570* (7762), 533–537. https://doi.org/10.1038/s41586-019-1321-1.

(120) Briat, C.; Khammash, M. Perfect Adaptation and Optimal Equilibrium Productivity in a Simple Microbial Biofuel Metabolic Pathway Using Dynamic Integral Control. *ACS Synth. Biol.* 2018, *7* (2), 419–431. https://doi.org/10.1021/acssynbio.7b00188.

(121) Briat, C.; Gupta, A.; Khammash, M. Antithetic Proportional-Integral Feedback for Reduced Variance and Improved Control Performance of Stochastic Reaction Networks. *J. R. Soc. Interface* 2018, *15* (143), 20180079. https://doi.org/10.1098/rsif.2018.0079.

(122) Nguyen, T. M.; Telek, S.; Zicler, A.; Martinez, J. A.; Zacchetti, B.; Kopp, J.; Slouka, C.; Herwig, C.; Grünberger, A.; Delvigne, F. Reducing Phenotypic Instabilities of Microbial Population during Continuous Cultivation Based on Cell Switching Dynamics. bioRxiv March 9, 2021, p 2021.01.13.426484. https://doi.org/10.1101/2021.01.13.426484.

(123) Delvenne, M.; Vandenbroucke, V.; Henrion, L.; Sehrt, M.; Martinez, J. A.; Sloodts, A.; Telek, S.; Zicler, A.; Delvigne, F. A Fitness-Entropy Compensation Effect Set the Trade-off between Growth and Gene Expression in Cell Populations. 2025.

(124) Kwon, S.-K.; Kim, S. K.; Lee, D.-H.; Kim, J. F. Comparative Genomics and Experimental Evolution of *Escherichia Coli* BL21(DE3) Strains Reveal the Landscape of Toxicity Escape from Membrane Protein Overproduction. *Sci. Rep.* 2015, *5* (1), 1–13. https://doi.org/10.1038/srep16076.

(125) *Catabolite Repression | cAMP, CAP, Glucose and Lac Operon.*; 2022. https://www.youtube.com/watch?v=cq4LrT_R3kU (accessed 2025-06-24).

(126) *Lac Operon & Catabolite Repression*; 2023. https://www.youtube.com/watch?v=bibDhYVPiIc (accessed 2025-06-24).

(127) Deutscher, J. The Mechanisms of Carbon Catabolite Repression in Bacteria. *Curr. Opin. Microbiol.* 2008, *11* (2), 87–93. https://doi.org/10.1016/j.mib.2008.02.007.

(128) Desai, T. A.; Rao, C. V. Regulation of Arabinose and Xylose Metabolism in *Escherichia Coli*. *Appl. Environ. Microbiol.* 2010, *76* (5), 1524–1532. https://doi.org/10.1128/AEM.01970-09.

(129) Santillán, M.; Mackey, M. C. Influence of Catabolite Repression and Inducer Exclusion on the Bistable Behavior of the Lac Operon. *Biophys. J.* 2004, *86* (3), 1282–1292. https://doi.org/10.1016/S0006-3495(04)74202-2.

(130) Stülke, J.; Hillen, W. Carbon Catabolite Repression in Bacteria. *Curr. Opin. Microbiol.* 1999, *2* (2), 195–201. https://doi.org/10.1016/S1369-5274(99)80034-4.

(131) Ammar, E. M.; Wang, X.; Rao, C. V. Regulation of Metabolism in *Escherichia Coli* during Growth on Mixtures of the Non-Glucose Sugars: Arabinose, Lactose, and Xylose. *Sci. Rep.* 2018, *8*, 609. https://doi.org/10.1038/s41598-017-18704-0.

(132) Ziv, N.; Brandt, N. J.; Gresham, D. The Use of Chemostats in Microbial Systems Biology. *J. Vis. Exp. JoVE* 2013, No. 80, 50168. https://doi.org/10.3791/50168.

(133) Wright, N. R.; Rønnest, N. P.; Sonnenschein, N. Single-Cell Technologies to Understand the Mechanisms of Cellular Adaptation in Chemostats. *Front. Bioeng. Biotechnol.* 2020, *8*. https://doi.org/10.3389/fbioe.2020.579841.

(134) Nikolic, N.; Schreiber, F.; Co, A. D.; Kiviet, D. J.; Bergmiller, T.; Littmann, S.; Kuypers, M. M. M.; Ackermann, M. Cell-to-Cell Variation and Specialization in Sugar Metabolism in Clonal Bacterial Populations. *PLOS Genet.* 2017, *13* (12), e1007122. https://doi.org/10.1371/journal.pgen.1007122.

(135) Choi, P. J.; Cai, L.; Frieda, K.; Xie, X. S. A Stochastic Single-Molecule Event Triggers Phenotype Switching of a Bacterial Cell. *Science* 2008, *322* (5900), 442–446. https://doi.org/10.1126/science.1161427.

(136) Notley-McRobb, L.; Ferenci, T. Adaptive Mgl-Regulatory Mutations and Genetic Diversity Evolving in Glucose-Limited *Escherichia Coli* Populations. *Environ. Microbiol.* 1999, *1* (1), 33–43. https://doi.org/10.1046/j.1462-2920.1999.00002.x.

(137) Frumkin, I.; Schirman, D.; Rotman, A.; Li, F.; Zahavi, L.; Mordret, E.; Asraf, O.; Wu, S.; Levy, S. F.; Pilpel, Y. Gene Architectures That Minimize Cost of Gene Expression. *Mol. Cell* 2017, *65* (1), 142–153. https://doi.org/10.1016/j.molcel.2016.11.007.

(138) Li, Z.; Rinas, U. Recombinant Protein Production-Associated Metabolic Burden Reflects Anabolic Constraints and Reveals Similarities to a Carbon Overfeeding Response. *Biotechnol. Bioeng.* 2021, *118* (1), 94–105. https://doi.org/10.1002/bit.27553.

(139) Tamires Moreira Melo, N.; Pontes, G. C.; Procópio, D. P.; de Gois e Cunha, G. C.; Eliodório, K. P.; Costa Paes, H.; Basso, T. O.; Parachin, N. S. Evaluation of Product Distribution in Chemostat and Batch Fermentation in Lactic Acid-Producing *Komagataella Phaffii* Strains Utilizing Glycerol as Substrate. *Microorganisms* 2020, *8* (5), 781. https://doi.org/10.3390/microorganisms8050781.

(140) Minden, S.; Aniolek, M.; Noorman, H.; Takors, R. Mimicked Mixing-Induced Heterogeneities of Industrial Bioreactors Stimulate Long-Lasting Adaption Programs in Ethanol-Producing Yeasts. *Genes* 2023, *14* (5), 997. https://doi.org/10.3390/genes14050997.

(141) Glauche, F.; Glazyrina, J.; Cruz Bournazou, M. N.; Kiesewetter, G.; Cuda, F.; Goelling, D.; Raab, A.; Lang, C.; Neubauer, P. Detection of Growth Rate-dependent Product Formation in Miniaturized Parallel Fed-batch Cultivations. *Eng. Life Sci.* 2017, *17* (11), 1215–1220. https://doi.org/10.1002/elsc.201600029.

(142) Mitchell, A. M.; Gogulancea, V.; Smith, W.; Wipat, A.; Ofiţeru, I. D. Recombinant Protein Production with *Escherichia Coli* in Glucose and Glycerol Limited Chemostats. *Appl. Microbiol.* 2021, *1* (2), 239–254. https://doi.org/10.3390/applmicrobiol1020018.

(143) Heins, A.-L.; Johanson, T.; Han, S.; Lundin, L.; Carlquist, M.; Gernaey, K. V.; Sørensen, S. J.; Eliasson Lantz, A. Quantitative Flow Cytometry to Understand Population Heterogeneity in Response to Changes in Substrate Availability in *Escherichia Coli* and *Saccharomyces Cerevisiae* Chemostats. *Front. Bioeng. Biotechnol.* 2019, *7*. https://doi.org/10.3389/fbioe.2019.00187.

(144) Vethanayagam, J. G.; Flower, A. M. Decreased Gene Expression from T7 Promoters May Be Due to Impaired Production of Active T7 RNA Polymerase. *Microb. Cell Factories* 2005, *4* (1), 3. https://doi.org/10.1186/1475-2859-4-3.

(145) Moreno-Gámez, S.; Kiviet, D. J.; Vulin, C.; Schlegel, S.; Schlegel, K.; van Doorn, G. S.; Ackermann, M. Wide Lag Time Distributions Break a Trade-off between Reproduction and Survival in Bacteria. *Proc. Natl. Acad. Sci.* 2020, *117* (31), 18729–18736. https://doi.org/10.1073/pnas.2003331117.

(146) Sánchez-Romero, M. A.; Casadesús, J. Contribution of Phenotypic Heterogeneity to Adaptive Antibiotic Resistance. *Proc. Natl. Acad. Sci.* 2014, *111* (1), 355–360. https://doi.org/10.1073/pnas.1316084111.

(147) Nguyen, J.; Fernandez, V.; Pontrelli, S.; Sauer, U.; Ackermann, M.; Stocker, R. A Distinct Growth Physiology Enhances Bacterial Growth under Rapid Nutrient Fluctuations. *Nat. Commun.* 2021, *12*, 3662. https://doi.org/10.1038/s41467-021-23439-8.

(148) Vermeersch, L.; Cool, L.; Gorkovskiy, A.; Voordeckers, K.; Wenseleers, T.; Verstrepen, K. J. Do Microbes Have a Memory? History-Dependent Behavior in the Adaptation to Variable Environments. *Front. Microbiol.* 2022, *13*. https://doi.org/10.3389/fmicb.2022.1004488.

(149) Peoples, L. M.; Isanta-Navarro, J.; Bras, B.; Hand, B. K.; Rosenzweig, F.; Elser, J. J.; Church, M. J. Physiology, Fast and Slow: Bacterial Response to Variable Resource Stoichiometry and Dilution Rate. *mSystems* 2024, *9* (8), e00770-24. https://doi.org/10.1128/msystems.00770-24.

(150) Hoang, M. D.; Riessner, S.; Oropeza Vargas, J. E.; von den Eichen, N.; Heins, A.-L. Influence of Varying Pre-Culture Conditions on the Level of Population Heterogeneity in Batch Cultures with an *Escherichia Coli* Triple Reporter Strain. *Microorganisms* 2023, *11* (7), 1763. https://doi.org/10.3390/microorganisms11071763.

(151) Watanabe, S.; Fukumori, F.; Nishiwaki, H.; Sakurai, Y.; Tajima, K.; Watanabe, Y. Novel Non-Phosphorylative Pathway of Pentose Metabolism from Bacteria. *Sci. Rep.* 2019, *9*, 155. https://doi.org/10.1038/s41598-018-36774-6.

(152) Barthe, M.; Tchouanti, J.; Gomes, P. H.; Bideaux, C.; Lestrade, D.; Graham, C.; Steyer, J.-P.; Meleard, S.; Harmand, J.; Gorret, N.; Cocaign-Bousquet, M.; Enjalbert, B. Availability of the Molecular Switch XylR Controls Phenotypic Heterogeneity and Lag Duration during *Escherichia Coli* Adaptation from Glucose to Xylose. *mBio* 2020, *11* (6), 10.1128/mbio.02938-20. https://doi.org/10.1128/mbio.02938-20.

(153) Bi, S.; Kargeti, M.; Colin, R.; Farke, N.; Link, H.; Sourjik, V. Dynamic Fluctuations in a Bacterial Metabolic Network. *Nat. Commun.* 2023, *14* (1), 2173. https://doi.org/10.1038/s41467-023-37957-0.

(154) Schmutzer, M.; Wagner, A. Gene Expression Noise Can Promote the Fixation of Beneficial Mutations in Fluctuating Environments. *PLoS Comput. Biol.* 2020, *16* (10), e1007727. https://doi.org/10.1371/journal.pcbi.1007727.

Appendix

Appendix 1

PERSONAL CONTRIBUTION

All experimental work presented in this thesis was performed by myself. Following initial training provided by the laboratory technician, I independently set up and operated the bioreactor cultures, including both batch and long-term chemostat experiments.

Data analyses were performed using Python scripts based on the *mbiomass* library developed within the team. While the core code was pre-existing, I adapted and refined it to adjust the graphs and visual outputs to the specific needs of this study.

The experimental design combined elements from prior work with my own contributions: while changing the carbon source to lower the switching cost followed the study of Henrion et al. (2024), the reduced-temperature cultivation strategy and the screening of dilution rates were my own proposal.

The entire manuscript was written by me, with constructive feedback and revisions provided by my supervisor, Professor Delvigne, and other team members. These exchanges contributed to refining both the scientific content and the clarity of presentation.

Regarding visual material, some figures were adapted or extracted from existing literature, while others were fully conceived and designed by me using BioRender to clearly communicate the experimental workflow and key concepts.

Appendix 2

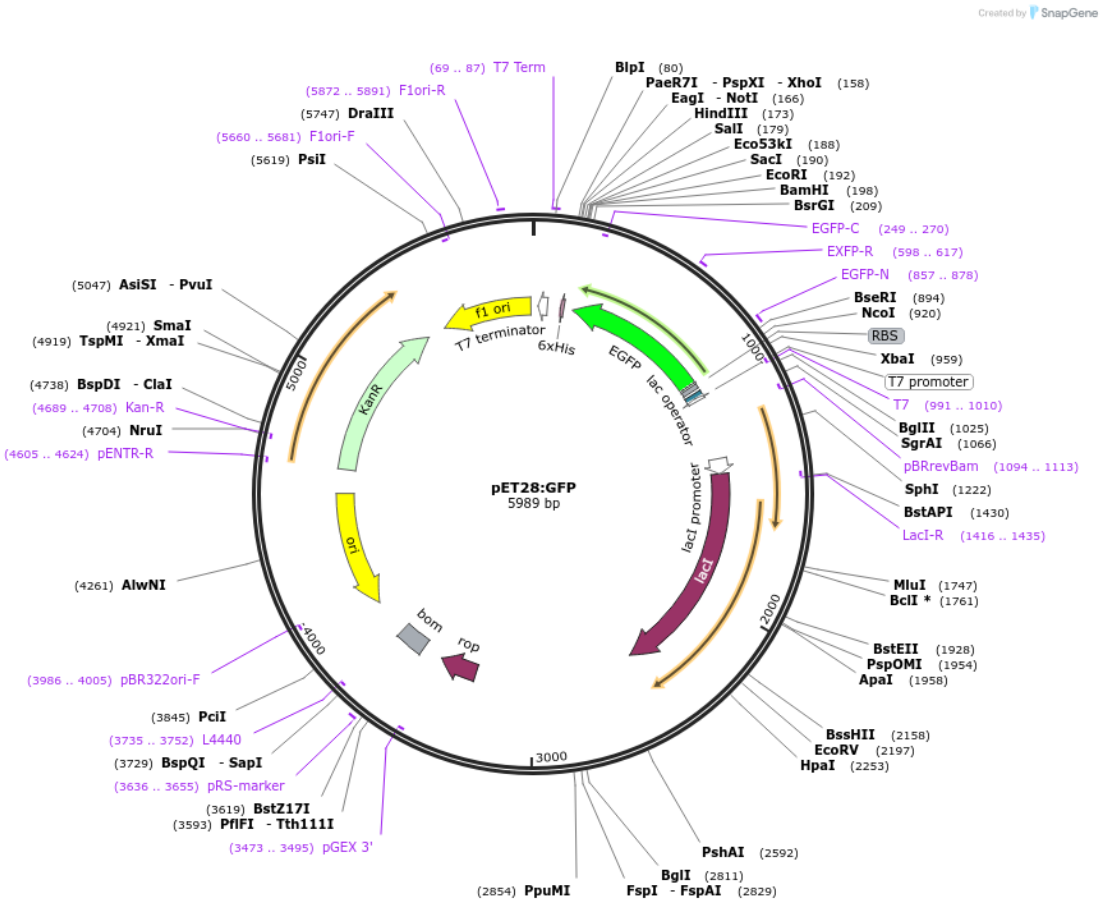

***Appendix 2**: Plasmid map of pET28::GFP. Created by SnapGene.*

Appendix 3

***Appendix 3:** Maximal growth rates of E. coli BL21 (DE3) under different cultivation conditions.*

Conditions	Maximal growth rate (h^{-1})	Source
Glucose 37°C	1.09	Henrion et al., 2024[114]
Xylose 37°C	0.55	Henrion et al., 2024[114]
Glucose 30°C	0.41	This study, from batch measurements

It should be noted that the measured growth rate for glucose at 30°C (0.41h^{-1}) likely underestimates the true maximal value, as the precultures were performed at 37°C and required an adaptation phase upon transfer to 30°C. This effect reduced the apparent maximal growth rate. However, the fact that the culture did not wash out at a dilution rate of 0.45h^{-1} in chemostat indicates that the actual maximal growth rate at 30°C exceeds this value.

Appendix 4

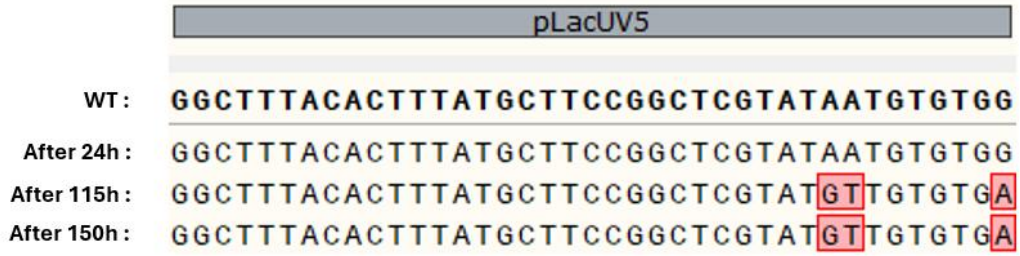

***Appendix 4**: Representative alignment of lacUV5 promoter sequences at different time points during continuous cultivation. Sequences are aligned to the wild type (WT) lacUV5 promoter. Mutations relative to the WT are highlighted in red. Each sequence represents one colony and is representative of the 10 colonies analysed at each time point. Alignment created with SnapGene.*